Beyond oxygen and nutrients: Regulatory roles of vascular endothelial cells for

normal retinal neurogenesis in zebrafish embryos

A Dissertation

Presented in Partial Fulfillment of the Requirements for the

Degree of Doctor of Philosophy

with a

Major in Neuroscience

in the

College of Graduate Studies

University of Idaho

by

Susov Dhakal

Major Professor: Deborah L. Stenkamp, Ph.D.

Committee members: Peter G. Fuerst, Ph.D.; Barrie Robison, Ph.D.;

Eric Shelden, Ph.D.

Department Administrator: James J. Nagler, Ph.D.

July 2015

Authorization to Submit Dissertation

This dissertation of Susov Dhakal, submitted for the degree of Doctor of Philosophy with a Major in Neuroscience and titled "**Beyond oxygen and nutrients: Regulatory roles of vascular endothelial cells for normal retinal neurogenesis in zebrafish embryos**," has been reviewed in final form. Permission, as indicated by the signatures and dates below, is now granted to submit final copies to the College of Graduate Studies for approval**.**

Major professor: _____ Date:_____
                                         Deborah L. Stenkamp, Ph.D.

Committee members: _____ Date:_____
                                         Peter G. Fuerst, Ph.D.

                                         _____ Date:_____
                                         Barrie Robison, Ph.D.

                                         _____ Date:_____
                                         Eric Shelden, Ph.D.

Department
Administrator: _____ Date:_____
                                         James J. Nagler, Ph.D

Abstract

Vertebrate retina is one of the most metabolically active tissues in the body and is extremely vascularized to ensure constant supply of oxygen (Alvarez et al. 2007; Wangsa-Wirawan & Linsenmeier 2003). Numerous studies have been conducted to understand the interactions between blood vessels of the eye and different retinal pathologies associated with ocular vasculature. However, interactions between the endothelial cells of early ocular vasculature and developing neural retina have not been studied in detail and remain unknown. Known roles of early ocular vasculature in developing retina is limited to supply of oxygen and nutrients (Geudens & Gerhardt 2011). Therefore, in order to contribute to our further understanding of the regulatory roles of endothelial cells in developing retina, I present the findings of my studies in this dissertation.

First, I characterized the retinal phenotype of *cloche* zebrafish mutants which have extremely reduced endothelial and hematopoietic cells resulting in absence of vasculature and circulation throughout their body (Stainier et al. 1995; Sumanas et al. 2005; Weinstein et al. 1996; Xiong et al. 2008). In *cloche* mutants, the eyes are microphthalmic and extremely disorganized at 72 hours post fertilization (hpf) *Cloche* mutants also have defects in differentiation of both neuronal and non-neuronal cells in their retina. My analyses also show that *cloche* mutants have defects in cell proliferation and increased cell death.

Second, in order to identify specific roles of systemic factors versus circulating factors during retinal neurogenesis, I characterized retinal phenotypes of zebrafish

embryos after selectively disrupting their vascular endothelial cells and of zebrafish

mutants that lack circulation or circulating red blood cells. Absence of endothelial

cells affected normal retinal development in zebrafish embryos whereas absence of

circulation or circulating red blood cells did not affect retinal neurogenesis. My results

suggest that vascular endothelial cells regulate retinal neurogenesis in zebrafish

embryos and endothelial cells are required for cell proliferation, cell survival and cell

differentiation in developing retina. Identification of regulatory targets from

vasculature to control retinal neurogenesis can potentially provide new directions to

treat retinal pathologies resulting from abnormal vasculature as well as retinal

regeneration in humans.

Acknowledgements

First of all, I would like to thank my advisor Dr. Deborah L. Stenkamp for her constant guidance and feedback throughout the course of my doctoral degree. In addition, I would also like to thank my committee members Dr. Peter Fuerst, Dr. Barrie Robison and Dr. Eric Shelden for their invaluable suggestions to help me during my research.

Additionally, I would also like to thank Ms. Ruth Frey, the scientific aide, in our laboratory for her technical assistance throughout my research. I would like to thank Dr. Eric Shelden (Washington State University) again for hsp27 antibody and hypoxic samples, Dr. Jesus Torres Vazquez (NYU School of Medicine) for *Tg(cdh5:GAL4ff)* fish and Dr. Jeffery Essner (University of Iowa) for *silent heart* mutant adult zebrafish, Dr. James Fadool (Florida State University) for 1D1 antibody, Dr. Michael J Redd (University of Utah) for L-plastin antibody and Ann Norton from optical imaging core at the University of Idaho for her technical assistance with imaging.

Table of contents

List of figures

List of abbreviations

ath 5 = atonal homologue-5

ANOVA = analysis of variation

BCIP = 5-bromo-4-chloro-3-indolyl-phosphate

BDNF = brain derived neurotropic factors

CC3 = cleaved caspase-3

cdh5 = cadherin-5

CGZ = circumferential germinal zone

clo = cloche

CNS = central nervous system

crx = cone-rod homeobox

dpf = days post fertilization

drv = dorsal retinal vessels

DTA = diphtheria toxin A

FGF = fibroblast growth factor

GFP = green fluorescent protein

hpf = hours post fertilization

IGF = insulin like growth factor

INL = inner nuclear layer

IPL = inner plexiform layer

kdrl = kinase insert domain receptor like

lycat = lysocardiolipin

Met = metronidazole

MO = morpholino

NBT = nitro blue tetrazolium

NeuroD = neurogenic differentiation

nrv = nasal retinal vessels

ONL = outer nuclear layer

OPL = outer plexiform layer

pax6 = paired homeobox-6

PH3 = phosphohistone-3

PKC = protein kinase C

PTU = phenylthiourea

RGC = retinal ganglion cells

ROP = retinopathy of prematurity

RPE = retinal pigmented epithelium

rx1 = retinal homeobox-1

sih = silent heart

SV2 = synaptic vesicle-2

tnnt2 = troponin-2

UAS = upstream activator sequence

VEGF = vascular endothelial growth factor

VEGFR-2 = vascular endothelial growth factor receptor-2

vlt = vlad tepes

vrv = ventral retinal vessels

WMD = wet macular degeneration

ZIRC = zebrafish international resource center

Chapter 1. Introduction

<u>Specific aims:</u>

The importance of circulation and vasculature from a metabolic standpoint during development of an organism has been very well studied (Lutty & McLeod 2003; Cringle et al. 2006). However, no studies have been performed to identify non-metabolic roles of vasculature and circulation during development, especially during retinal development. The eye is an extremely vascularized organ because of its very high metabolic demand (Alvarez et al. 2007; Wangsa-Wirawan & Linsenmeier 2003). *In vitro* and *in vivo* studies have also shown that endothelial cells of the vasculature are able to influence neuronal cell proliferation (Aizawa & Shoichet 2012; Faigle & Song 2012; Palmer et al. 2000). Unfortunately, little is known about relationship between vasculature and retinal neurogenesis. Understanding regulatory relationship between the vascular endothelial cells and developing neurons in the retina is extremely important to develop novel treatment approaches against retinal pathologies and the information derived from such interactions can be potentially applied to develop regeneration strategies of mammalian retina.

I proposed the following three specific aims in order to better understand the regulatory relationship between endothelial cells of the vasculature and developing retinal neurons Figure (1.1).

Specific aim I: Characterize retinal phenotype of *cloche* zebrafish mutants.

Specific aim II: Characterize retinal phenotype of zebrafish embryos after selectively ablating vascular endothelial cells.

Specific aim III: Characterize retinal phenotype of zebrafish embryos lacking total circulation and lacking circulating red blood cells.

Significance:

Access to blood supply has been identified as one of the crucial requirements during organogenesis and any deficiency in the formation of blood vessels have been shown to impact normal development and eventual death of the organism (Geudens & Gerhardt 2011). However, roles of early ocular vasculature in regulating the activities of retinal progenitor cells remain unknown. Vasculature has been thought to simply supply chemical factors and oxygen to developing organs including the retina (Haigh 2008). The explicit nature of factors supplied by the vasculature to the developing retina has not been identified and explored yet. *In vitro* studies have shown that endothelial cells secrete factors that stimulate neuroepithelial cells to proliferate (Shen et al., 2004). Similarly, neurogenesis in mice brain occurs within a microenvironment rich with vascular supply (Palmer et al. 2000; Shen et al. 2009) indicating the existence of a relationship between the two components. Studies have also been performed to determine the role of vascular factors in neurogenesis in the brain (Stainier et al. 1996; Aizawa & Shoichet 2012). *In vivo* studies have also shown that optic fissure closure is affected by abnormal vasculature in zebrafish *lmo2* mutants (Weiss et al. 2012). Therefore, vasculature seems to be more than a conduit for oxygen and other chemical factors in regulating neurogenesis.

Diseases like wet macular degeneration (WMD), which is the leading cause of vision loss among adult humans, are associated with excessive blood vessel growth

in the eye (Ferris et al. 1984; Ferrara 2010). Similarly, other ocular diseases like diabetic retinopathy and retinopathy of prematurity are also caused by abnormal vascular growth, which ultimately leads to blindness (Kahn & Hiller 1974; Gibson et al. 1990). Therefore, understanding the roles of vasculature in early retinal development is critical as it will provide information regarding the interactions between vasculature and retinal stem cells and it could have immense impacts in the treatment of retinal disorders.

<u>The vertebrate eye:</u>

The vertebrate eye is a part of central nervous system (CNS) and develops from neural tube and cells from the ectoderm of gastrula. Vertebrate eye is initially formed by an evagination of diencephalon, which results in formation of optic vesicle (Chow & Lang 2001; Gilbert 2000). Optic vesicle extends towards surface ectoderm to induce formation of lens placode which eventually develops into lens and other parts of the eye (Chow & Lang 2001; Gilbert 2000). Then, the optic vesicle invaginates to form a two layered cup and is called optic cup (Chow & Lang 2001). Neural retina and nonpigmented layer of optic cup develops from inner optic cup layer whereas retinal pigmented epithelium (RPE) develops from outer optic cup layer (Hilfer 1983).

The retina is a multilayered tissue composed of neuronal and non-neuronal cells and is the innermost layer of the eye (Figure 1.2). The outermost layer of the retina or the outer nuclear layer (ONL) consists of rod and cone photoreceptor cells. Rods help mediate vision in scotopic conditions whereas cones are involved more

during photopic conditions. Next to ONL lies the outer plexiform layer (OPL) where axons of rod and cone photoreceptors form synapses with the dendrites of bipolar and horizontal cells. The cell bodies of bipolar, horizontal and amacrine cells are located in the inner nuclear layer (INL). Dendrites of horizontal cells are limited to OPL and they do not project any processes to the inner plexiform layer (IPL). The bipolar cell axon and amacrine cell dendrites form synapses with dendrites of the retinal ganglion cells (RGC) at IPL. Amacrine cell processes are limited to INL and do not project any neurons towards OPL. Finally, the innermost layer of the retina comprises cell bodies of ganglion cells and displaced amacrine cells. The axons of RGCs leave the retina through optic disk, travel through the optic nerve and transmit their signals to the visual cortex in thalamus and midbrain. Rods, cones, bipolar cells, horizontal cells, amacrine cells and ganglion cells are the neuronal cells present in a vertebrate retina and are involved in transmission of visual signals. Müller glia, microglia and astroglia are principle non-neuronal cells present in vertebrate retina. Cell bodies of Müller glia are present in the INL and their endfeet extend to the inner and outer limiting membranes of retina (Bringmann et al. 2006). Therefore, Müller cells are the primary cells involved in structural support of the retina. Besides structural support, Müller cells are involved in multiple other functions in the retina such as maintaining retinal homeostasis, response to retinal injury, regulate synaptic activity by up taking excess glutamate, among others (Newman & Reichenbach 1996; Reichenbach & Bringmann 2013). Astrocytes are closely associated with retinal vasculature and they help in patterning of retinal vasculature during mammalian eye development (Fruttiger 2007). In case of teleost fish like zebrafish,

the function of retinal astrocytes remains unexplored (Gestri et al. 2012). Lastly, microglia are the leukocytes of CNS including the retina and are involved in phagocytosis of dying neurons (Neumann et al. 2009). Therefore, presence of many different cell types in the retina indicates that it is extremely complex but highly organized tissue.

The process of conversion of energy from photons into visual signals via release of neurotransmitters is called phototransduction and this process takes place in the photoreceptors of the retina. The simplest path of transmission of electrical signal in the retina is from photoreceptors to bipolar cells to the RGCs. Horizontal and amacrine cells are interneurons of the retina and are also involved in electric signal transmission. The horizontal cells are involved in contrast sensitivity and edge detection (Barlow & Levick 1965; Baylor et al. 1971). Amacrine cells are involved in perceiving changes in illumination and generating responses to moving objects.

The zebrafish as an animal model:

The zebrafish (*Danio rerio*) is a tropical freshwater vertebrate which is native to northern India, northern Pakistan, Nepal, Bhutan and South Asia. An adult captive zebrafish is about 2-3 inches long and its average life span is about 2-3 years.

Zebrafish has rapidly developed into an exceptionally useful animal model for research in developmental biology, genetics, and regeneration. Zebrafish has following advantages as an animal model: (i) high degree of homology to human genome, (ii) external and rapid development (A zebrafish is sexually mature within 3-4 months after fertilization), (iii) extremely high fecundity and fertility rates yielding

higher sample size for the experiments leading to increased power of statistical analyses, (iv) ability to maintain transparent embryos, (v) non-invasive visualization of different cellular behaviors such as angiogenesis, retinal neurogenesis, during development, (vi) availability of diverse genetic tools, and (vii) ability to regenerate multiple tissues including the retina post injury (This feature helps us understand the process of retinal regeneration and can have implications in treating human retinal pathologies).

Zebrafish embryos have additional advantage over mammalian animal models to conduct this study because zebrafish embryos do not need active circulation of oxygen until at least 5 dpf in order to survive (Pelster & Burggren 1996; Jacob et al. 2002). Lack of tissue oxygenation will lead to death if mammalian models are used for this study. Availability of transgenic zebrafish that express green fluorescent protein (GFP) under the regulatory elements of *kdrl* gene (VEGFR2 receptor), *Tg(kdrl:GFP)*, in all their vascular endothelial cells also makes analysis of vasculature easier (Jin et al. 2005).

Ocular vasculature development in zebrafish embryos:

In zebrafish, blood vessels are formed by two processes- vasculogenesis and angiogenesis (Risau 1997; Vailhé et al. 2001; Saint-Geniez & D'Amore 2004). Vasculogenesis is a process in which blood vessels are synthesized *de novo* from assembly of precursor molecules (Eilken & Adams 2010; Saint-Geniez & D'Amore 2004). Blood vessels and vascular plexus are formed through vasculogenesis initially. Angiogenesis is the process of formation of new blood vessels from pre-

existing vessels (Iruela-Arispe 2005; Saint-Geniez & D'Amore 2004). Ocular

vasculature in zebrafish embryos develops through the process of angiogenesis.

Embryonic zebrafish retina is supplied by three primary blood vessels: hyaloid

vessels, superficial ring vessels and choroidal vessels (Kitambi et al. 2009; Alvarez et

al. 2007; Hartsock et al. 2014). Hyaloid vessels and superficial ring vessels are

referred to as hyaloid system. The hyaloid system eventually reorganizes itself to

retinal vessels in adult zebrafish retina, which supplies blood and nutrients to the

inner retina (Alvarez et al. 2007; Saint-Geniez & D'Amore 2004). Hyaloid vessels

invade retina through optic disc and form a network like structure under the lens

(Kitambi et al. 2009). First evidence of hyaloid vessels is present around 18-20 hpf

behind the lens in zebrafish embryos (Hartsock et al. 2014). A circular superficial ring

vessel surrounding the lens is established by 48 hpf (Kitambi et al. 2009; Alvarez et

al. 2007; Hartsock et al. 2014). Starting around 60 hpf, the hyaloid vessels start

forming a network behind the lens and start engulfing the lens from behind by

progressing towards lens equator and by 5 dpf, hyaloid vessels completely cover the

lens and form a network surrounding the lens (Alvarez et al. 2007). Three radial

vessels, dorsal, ventral and nasal radial vessels are formed between 48 hpf and 72

hpf and they connect with superficial ring vessel surrounding the lens (Kitambi et al.

2009). Blood enters through nasal radial vessel (nrv) and exits through dorsal radial

vessel (drv) and ventral radial vessel (vrv) (Kitambi et al. 2009). Hyaloid and

superficial ring vessels are composed of single layered endothelial cells in zebrafish

embryos, which eventually become the innermost cellular layer of adult blood

vessels. Hyaloid and retinal vasculature starts supplying blood and other factors to

the developing lens and inner retina around 24 hpf (Paik & Zon 2010) although zebrafish embryo heart starts beating around 22 hpf (Stainier et al. 1993). Studies have shown that blood vessel development is strictly regulated by vascular endothelial growth factor (VEGF) (Mackenzie & Ruhrberg 2012; Liang et al. 2001; Li et al. 2013; Haigh 2008; Nasevicius et al. 2000). Choroid vessels are present outside the retina and they supply blood to the retinal pigmented epithelium and the photoreceptors (Saint-Geniez & D'Amore 2004). Details of development of choroid vasculature have not been studied yet in the zebrafish.

Zebrafish as a model for studying relationship between early ocular vasculature and retinal neurogenesis:

Embryonic zebrafish retina consists of 6 different types of neurons and 3 different types of non-neuronal cells by the time retinal neurogenesis is completed at 72 hpf (Stenkamp 2007). These cells develop at different developmental time points and they develop layer by layer from outside to the inside relative to apical surface of the retina. Retinal ganglion cells are the first cell type to exit cell cycle and undergo terminal mitosis in zebrafish embryo and they undergo through this process between 24-36 hpf. Cells of the INL, bipolar, amacrine and horizontal cells, undergo terminal mitosis between 36-48 hpf. Cone photoreceptors undergo terminal mitosis between 48 hpf and 60 hpf whereas rod photoreceptors are formed between 55-72 hpf.

As retinal neurogenesis and ocular vascular development start simultaneously in zebrafish embryos, they serve as an excellent animal model to study the

developmental relationship between early ocular vasculature and retinal

neurogenesis (Figure 1.3).

Vasculature related ocular pathologies:

Several retinal pathologies such as retinopathy of prematurity (ROP), diabetic

retinopathy, wet form of age related macular degeneration (AMD), persistent fetal

vasculature, macular telangiectasia and Norrie disease are associated with vascular

abnormalities. Neovasculaization of the retina is the major cause of blindness in such

pathologies. Vasculature related retinal abnormalities affect both adults as well

children. For example, diabetic retinopathy is of one of the leading causes of

blindness in adults suffering from diabetes. Diabetic retinopathy starts with formation

of microaneurysms, small swellings in the retinal blood vessels. As the disease

progresses, retinal blood vessels start getting blocked causing hypoxia in the retina.

In response to hypoxic conditions in the retina, new blood vessels are formed to

maintain the oxygen and nutrition requirements in the eye. Uncontrolled growth of

new and fragile blood vessels eventually causes the fluids to leak in the center of the

eye affecting the vision (Ciulla et al. 2003; Kempen et al. 2004). During the

progression of diabetic retinopathy, neurons start degenerating from very early stage

and neuronal cell death in the retina keeps increasing as the disease progresses to

the advanced stage (Stem & Gardner 2013).

Similarly, ROP is a major cause of blindness in children born prematurely

before 31 weeks of gestation. In premature children, their peripheral retinal

vascularization is not complete (Smith 2003; Austeng et al. 2011). So, the retina

becomes hypoxic as development progresses in such children resulting in excess neovascularization. Continuous development of vasculature in the eyes results in formation of scar tissues eventually leading to retinal detachment and blindness in premature children. Factors secreted by RGCs such as succinate (via its receptor GPR91) and semaphorin 3A regulate neovascularization during pathogenesis of ROP (Joyal et al. 2011) indicating that neurons are an integral part of ROP pathogenesis. Mouse models of ROP also showed spatial neuronal and glial changes relative to the location of blood vessels in the eyes with normal tissues closer to the blood vessels (Downie et al. 2007).

Similar to diabetic retinopathy and ROP, other retinal pathologies associated with abnormal vasculature also include neuronal component. It is extremely critical to identify the neural components involved in progression of such diseases so that novel therapeutic methods can be developed in order to effectively treat blindness caused by such vascular abnormalities.

Stem cell niche and vasculature:

Few sites in adult mammalian body such as brain, bone marrow, blood vessels, liver and skeletal muscle contain a population of stem cell. As a result, these organs are able to regenerate new cells and tissues upon damage. Interestingly, zebrafish retina also contains neuronal stem cell niche, which enables the fish to regenerate its retina after injury, and allows continuous growth of the retina throughout life (persistent neurogenesis) (Johns 1977; Hitchcock et al. 2004; Otteson et al. 2001; Stenkamp 2011). One of the most common characteristics of all of these

different stem cell niches is their close localization to dense network of blood vessels. Such close association of blood vessels and stem cell niche has given rise to the concept of "stem cell zone" rather than just a specialized stem cell niche (Mounier et al. 2011).

Numerous studies have shown that the stem cells and the blood vessels communicate and regulate each other. Neurogenesis in adult mice brain takes place in areas of the brain richly supplied with blood vessels (Palmer et al. 2000; Shen et al. 2009). *In vitro* co-culture studies have shown that when endothelial cells physically contact neural stem cells, it results in division of neural stem cells (Shen et al. 2004). Satellite cells, the stem cells in human muscles, are also located within 20 microns from the capillaries in the muscles and the number of satellite cells are directly proportional to the number of capillaries (Christov et al. 2007). Satellite cells have been shown to promote angiogenesis in muscles by secreting soluble factor, VEGF (Christov et al. 2007). Co-culture studies have also shown that close association of neural stem cells and endothelial cells of brain regulate the formation and maintenance of vascular tube mediated by VEGF and brain derived neurotrophic factor (BDNF) (Li et al. 2006).Generally, neural stem cells and vascular endothelial cells regulate with each by secreting various types of diffusible signals (Goldberg & Hirschi 2009).

Factors involved in vertebrate retinal neurogenesis:

Several genes in zebrafish control retinal neurogenesis. Genes such as *pax6, rx1, rx2, ath5, neuroD* and *crx* are extremely critical for eye development in zebrafish

embryos. *Pax6* is a critical transcription factor required for eye morphogenesis in

nearly all metazoans (Nornes et al. 1998). Ectopic expression of *pax6 (eyeless)* leads

to development of ectopic eyes (Halder et al. 1995) whereas lack of *pax6* expression

causes an eyeless phenotype in *Drosophila* (Quiring et al. 1994). *Pax6* expression in

vertebrate eye primordia is maintained throughout the ocular neurogenesis and is

later restricted to RGC and amacrine cells (Macdonald et al. 1995). *Rx1* is a paired

class homeobox gene which is important for eye development (Chuang et al. 1999).

There are three types of *rx1* genes in zebrafish, *zrx 1, 2 and 3* (Chuang et al. 1999).

Rx1 is required for retinal neurogenesis and photoreceptor differentiation (Nelson et

al. 2009). Zebrafish *rx2* is expressed in regions that give rise to the neural retina

(Chuang & Raymond, 2001) and is also required for cone photoreceptor

differentiation (Chuang & Raymond, 2001; Nelson et al., 2009). *Ath5* is a proneural

gene involved in retinal neurogenesis and RGC differentiation (Masai et al. 2000; Kay

et al. 2005; Cremisi et al. 2003). *Ath5* is a basic-helix-loop-helix transcription factor

and is expressed in all vertebrates during early retinal development (Mu & Klein

2004; Kay et al. 2005). Overexpression of *ath5* in chicks and *Xenopus* increases the

number of RGCs while other retinal neuronal subtypes are reduced in number

(Kanekar et al. 1997; Liu et al. 2001). Another transcription factor *NeuroD,* plays an

important role in cell fate determination and differentiation (Morrow et al. 1999).

NeuroD is expressed in the later stages of retinal neurogenesis especially after

terminal mitosis of neural precursors (Morrow et al. 1999). It has been shown that

NeuroD is expressed in areas where photoreceptors and amacrine cells develop in

mouse retina and is required for differentiation of photoreceptors and amacrine cells

(Morrow et al. 1999). *Crx* is a homeodomain containing transcription factor that promotes retinogenesis by differentiation of retinal progenitor cells including photoreceptors and may be involved in patterning of the early optic primordium (Stenkamp 2007; Shen & Raymond 2004).

Models of zebrafish vascular studies:

Cloche: The word *cloche* means "bell shaped heart" in French and is named after bell shaped heart in zebrafish embryos carrying *cloche* mutation. Studies have shown that the *cloche* mutation acts early during vasculogenesis and hematopoiesis (Weinstein et al. 1996; Stainier et al. 1995). Although the molecular nature of *cloche* is yet to be identified, the phenotypic characteristics of *cloche* mutants ($clo^{-/-}$) include absence of nearly all the blood cells, edemic heart, absence of head and trunk endothelial cells and lack of endocardium (Stainier et al. 1995b; Sumanas et al. 2005). Additionally, $clo^{-/-}$ exhibit very weak to non-existent heartbeat, abnormally enlarged atrium, collapsed ventricle and failure of blood cell differentiation at a very early stage, around 24 hpf (Stainier et al. 1995). Epistasis analysis has shown that *cloche* acts upstream of critical genes such as *scl, lmo2, gata1, fli1* and *flk1* which are primarily involved in hematopoiesis and vasculogenesis and are not expressed in $clo^{-/-}$ (Xiong et al. 2008). The *cloche* mutation has been associated with the *lycat* gene, which has been mapped on the telomere of chromosome 13 near the microsatellite markers Z17223, Z22194 and Z10362 (Xiong et al. 2008). Studies in mouse have shown that *lycat* is initially expressed in the heart, lung and somites and become restricted to smooth muscle cells in the blood vessels (Xiong et al. 2008). *Lycat* is critical for hematopoietic and endothelial lineage development. The *lycat*

gene encodes a transmembrane protein called lysocardiolipin acyltransferase with a C-terminal ER localization signal in both mice and zebrafish (Wang et al. 2010; Xiong et al. 2008). In zebrafish embryos that are injected with morpholino to knockdown *lycat* gene expression, both the endothelial and hematopoietic lineage is reduced and formation of endocardium is eliminated (Xiong et al. 2008). *Lycat* overexpression in embryonic stem cells when they are differentiating into embryoid bodies leads to overpopulation of hematopoietic and endothelial cells (Wang et al. 2010). In zebrafish, *lycat* mRNA microinjection is able to partially rescue *cloche* phenotype, especially the red blood cell count (Wang et al. 2010). Cardiolipin, a membrane polyglycerophospholipid found in inner mitochondrial membrane, binds with calcium ions to maintain the membrane potential and membrane permeability (Wang et al. 2010). Acyl transferase proteins such as cardiolipin are involved in protein trafficking, sorting and development and play an important role in regulating embryonic patterning and organogenesis (Xiong et al. 2008; Nusse 2003; Linder & Deschenes 2003)**.** Therefore, *cloche* mutants allow the characterization of retinal phenotype in absence of vasculature and circulation (Figure 1.4).

    Silent heart: Silent heart (*sih*$^{-/-}$) zebrafish have a non-coding mutation in the cardiac *troponin T (tnnt2)* gene which results in a change at the invariant position of the splice acceptor sequence in intron 2, causing pleiotropic defects in mRNA splicing (Sehnert et al. 2002). This frameshift causes premature stop codon in exon 7 causing disruption in *tnnt2* transcription. *Tnnt2* is critical for sarcomere assembly and its mutation results in a non-contractile heart (Sehnert et al. 2002; Clark et al. 2011). Vasculature and heart development along with blood cell differentiation proceeds

normally in *sih*^{-/-}*,* unlike *clo*^{-/-}. *Sih*^{-/-} zebrafish show an edemic heart by 32 hpf and no circulation is observed at any developmental time point (Sehnert et al. 2002). *Sih*^{-/-} mutants serve as an animal model to study the potential roles of circulating factors during retinal neurogenesis in zebrafish embryos (Figure 1.4).

Vlad tepes: The specific role of circulating erythrocytes in early retinal development was evaluated using the *vlad tepes (vlt*^{-/-}*)* zebrafish mutants. Absence of vasculature and circulation results in absence of oxygen transport through erythrocytes to the developing eye. Although zebrafish embryos have been shown to develop normally in lower oxygen conditions (Pelster & Burggren 1996; Jacob et al. 2002), use of the *vlt*^{-/-} provided information on the effects of circulating erythrocytes in retinal development. *Vlt*^{-/-} mutants have a non-sense mutation in *gata1* gene which is required for erythropoiesis resulting in either highly reduced or no red blood cells circulating in the body starting from 24 hpf (Lyons et al. 2002). Vasculature and heart develop normally during embryonic development in *vlt*^{-/-} (Weinstein et al. 1996). Analysis of early ocular development in *vlt*^{-/-} provided information regarding the role of circulating blood cells in retinal neurogenesis in presence of normal vasculature and circulating materials besides erythrocytes (Figure 1.4).

Selective ablation of endothelial cells using GAL4/UAS system:

GAL4/UAS is a binary gene expression system used to pursue gene specific studies and was initially developed in *Drosophila melanogaster*. This system utilizes two specific genes, GAL4 and UAS, to manipulate genes or tissues of interest. GAL4 is a transcription activator initially discovered in yeast and consists of 881 amino

acids in total. N-terminus of *GAL4* gene has 74 amino acids which is responsible for DNA binding activity of GAL4 (Keegan et al. 1986; Asakawa & Kawakami 2008). GAL4 transcription activation is mapped to two groups of amino acids residues located between 148-196 and 768-881 (Keegan et al. 1986). GAL4 binds with a specific recognition sequence called Upstream Activator Sequence (UAS) to regulate expression of genes downstream of UAS sequence. Although initially discovered in yeast, GAL4/UAS system has been shown to work in other vertebrates and invertebrate models as well. Studies have shown that plasmid constructs containing full length GAL4 gene as well as GAL4 DNA binding domain driven by transcriptional activation domain from herpes simplex virus protein VP16 (GAL4-VP16) can direct expression of genes downstream of UAS (Asakawa & Kawakami 2008). However, for my studies, I used another version of GAL4 transcriptional activator called GAL4ff, which contains the DNA binding domain of GAL4 and two short VP16 transcriptional activation motifs (Asakawa & Kawakami 2008). Advantages of the GAL4ff over two versions of GAL4 transcription activator include stable germline transmission and reduced variegated transgene expression (Asakawa & Kawakami 2008).

GAL4/UAS gene expression system can be used to selectively ablate different tissues in a spatio-temporal manner. There are numerous other ways to ablate cells and tissues such as diptheria toxin A (DTA), Kid/Kis, HSV thymidine kinase/ganciclovir, tamoxifen-inducible c-Myc and toxic viral protein M2 (H37A) (Curado et al. 2008). However, each of these techniques have one or more drawbacks such as bystander effect, feasibility in all age groups of animal model, limitations regarding target cells, prolonged drug treatment required for the drug to

have desired effect, and limitations regarding animal models. Most of the

shortcomings of these cell ablation method can be overcome by GAL4/UAS system.

In my study, selective ablation of endothelial cells was accomplished by crossing two

transgenic lines of zebrafish, *Tg(cdh5:GAL4ff)* and *Tg(UAS-E1b:Eco.NfsB-mCherry)*.

When these two transgenic adults are crossed, they generate doubly transgenic

embryos, which express bacterial enzyme nitroreductase fused with fluorescent

protein, mCherry in the cells expressing cadherin5 in zebrafish embryos. Cadherin5

is a cell adhesion molecule and is expressed exclusively in the vascular endothelial

cells (Breviario et al. 1995). When a prodrug, Metronidazole (Met), is added to the

fish water containing the doubly transgenic embryos, Met reacts with bacterial

nitroreductase enzyme to produce a cytotoxin that crosslinks the DNA resulting in

apoptotic death of endothelial cells (Curado et al. 2008). Cell death using GAL4/UAS

and Met system is exclusively limited to the target cells and does not affect

neighboring cells, thereby, minimizing the unintended effects of "bystander effect"

(Curado et al. 2008). This method has been shown to effectively and selectively

ablate cardiomyocytes, hepatocytes and pancreatic beta cells (Pisharath et al. 2008;

Curado et al. 2007).

Figures

Figure 1.1. Systemic factors vs circulating factors. Endothelial cells of the vasculature can potentially regulate retinal neurogenesis by secreting paracrine factors in the developing retina. However, vasculature might just be a conduit for supplying signals secreted in other areas of zebrafish embryo via circulating action by the heart.
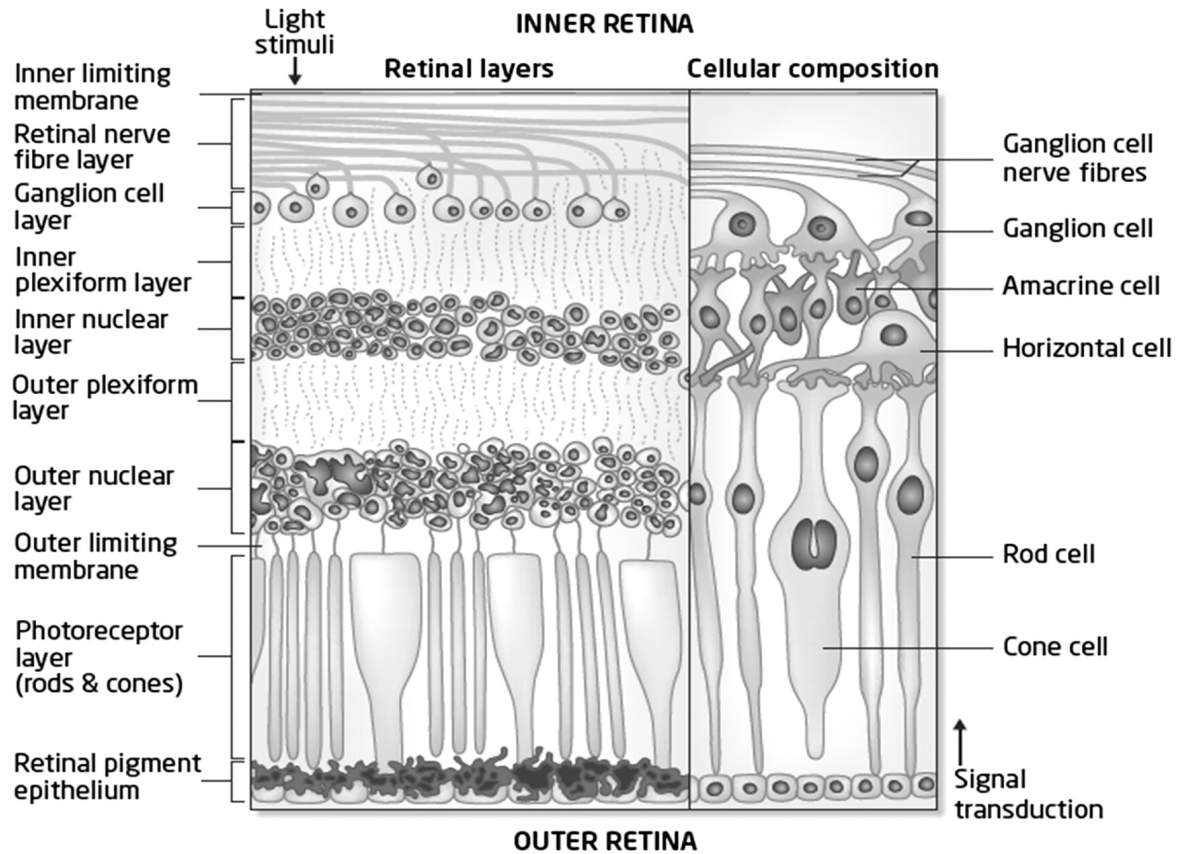
Figure 1.2. Retinal histological layers. A 2-D cartoon structure of human retina.

Three nuclear layers, a) ganglion cell layer (GCL), b) inner nuclear layer (INL), and c)

outer nuclear layer (ONL), consisting of cell bodies of neurons are separated by two

synaptic layers, inner plexiform layer (IPL) and outer plexiform layer (OPL).
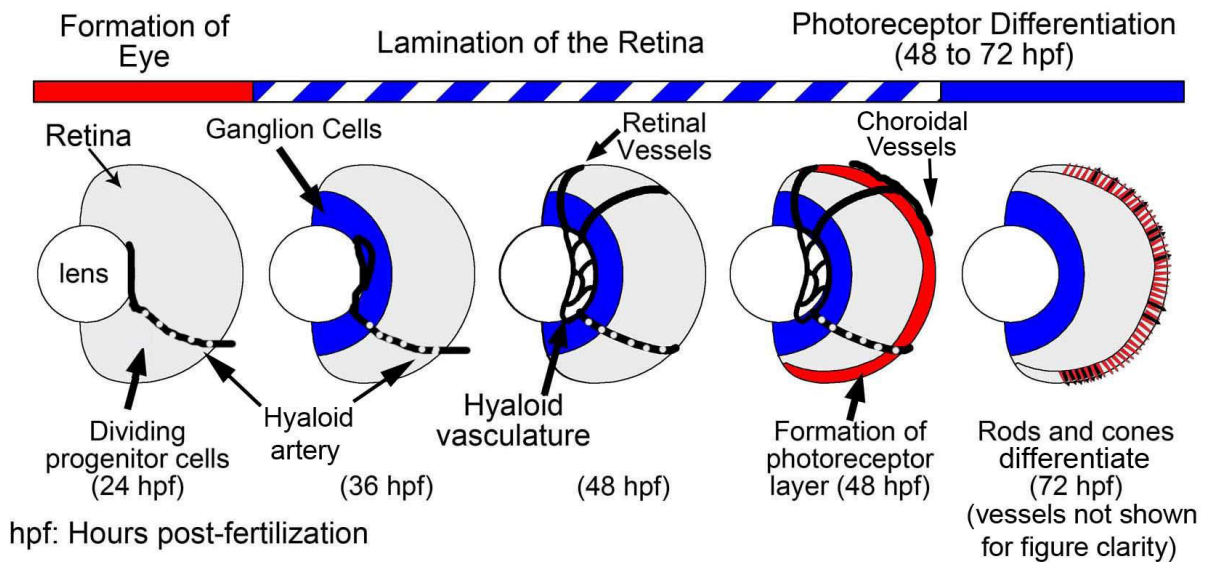
Figure 1.3. Retinal neurogenesis and hyaloid vasculature in zebrafish embryo.
Retinal neurogenesis starts at 24 hpf and is complete by 72 hpf. Hyaloid artery enters
the retina through optic disc and starts forming hyaloid vascular network starting at
24 hpf. Hyaloid vascular network covering the lens from underneath and retinal
vessels surrounding the lens is formed by 72 hpf (not shown in figure).

Animal models

wild-type + vasculature +circulation	*cloche (clo$^{-/-}$)* **- vasculature - circulation**	*silent heart (sih$^{-/-}$)* **+ vasculature - circulation**	*vlad tepes (vlt$^{-/-}$)* **+ vasculature + circulation - red blood cells**
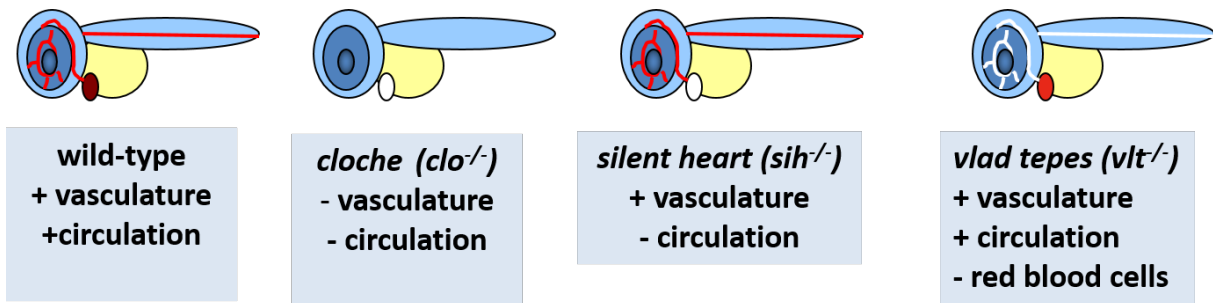
Figure 1.4. Cartoon representation of different zebrafish mutant models.

Wildtype embryos have both normal vasculature and circulation. The mutant models

lack either vasculature or circulation or some circulating factors or all of them.

References

Aizawa, Y. & Shoichet, M.S., 2012. The role of endothelial cells in the retinal stem and progenitor cell niche within a 3D engineered hydrogel matrix. *Biomaterials*, 33(21), pp.5198–5205. Available at: http://dx.doi.org/10.1016/j.biomaterials.2012.03.062.

Alvarez, Y. et al., 2007. Genetic determinants of hyaloid and retinal vasculature in zebrafish. *BMC developmental biology*, 7, p.114.

Asakawa, K. & Kawakami, K., 2008. Targeted gene expression by the GAL4-UAS system in zebrafish. *Development Growth and Differentiation*, 50(6), pp.391–399.

Austeng, D. et al., 2011. Screening for retinopathy of prematurity in infants born before 27 weeks' gestation in Sweden. *Archives of ophthalmology (Chicago, Ill. : 1960)*, 129(2), pp.167–72. Available at: http://www.ncbi.nlm.nih.gov/pubmed/21320961 [Accessed June 1, 2015].

Barlow, H.B. & Levick, W.R., 1965. The mechanism of directionally selective units in rabbit's retina. *The Journal of physiology*, 178(3), pp.477–504.

Baylor, D. A, Fuortes, M.G. & O'Bryan, P.M., 1971. Receptive fields of cones in the retina of the turtle. *The Journal of physiology*, 214(2), pp.265–294.

Breviario, F. et al., 1995. Functional Properties of Human Vascular Endothelial Cadherin (7B4/Cadherin-5), an Endothelium-Specific Cadherin. *Arteriosclerosis, Thrombosis, and Vascular Biology* , 15 (8), pp.1229–1239. Available at: http://atvb.ahajournals.org/content/15/8/1229.abstract.

Bringmann, A. et al., 2006. Müller cells in the healthy and diseased retina. *Progress in Retinal and Eye Research*, 25(4), pp.397–424.

Chow, R.L. & Lang, R.A., 2001. Early eye development in vertebrates. *Annual review of cell and developmental biology*, 17, pp.255–96. Available at: http://www.ncbi.nlm.nih.gov/pubmed/11687490 [Accessed May 25, 2015].

Christov, C. et al., 2007. Muscle satellite cells and endothelial cells: close neighbors and privileged partners. *Molecular biology of the cell*, 18(4), pp.1397–409. Available at: http://www.pubmedcentral.nih.gov/articlerender.fcgi?artid=1838982&tool=pmcentrez&rendertype=abstract [Accessed June 1, 2015].

Chuang, J.C., Mathers, P.H. & Raymond, P. a., 1999. Expression of three Rx homeobox genes in embryonic and adult zebrafish. *Mechanisms of Development*, 84, pp.195–198.

Chuang, J.C. & Raymond, P. a, 2001. Zebrafish genes rx1 and rx2 help define the region of forebrain that gives rise to retina. *Developmental biology*, 231(1), pp.13–30.

Ciulla, T.A., Amador, A.G. & Zinman, B., 2003. Diabetic Retinopathy and Diabetic Macular Edema: Pathophysiology, screening, and novel therapies. *Diabetes Care*, 26(9), pp.2653–2664. Available at: http://care.diabetesjournals.org/content/26/9/2653.short [Accessed April 29, 2015].

Clark, K.J. et al., 2011. In vivo protein trapping produces a functional expression codex of the vertebrate proteome. *Nature methods*, 8(6), pp.506–515.

Cremisi, F., Philpott, A. & Ohnuma, S.I., 2003. Cell cycle and cell fate interactions in neural development. *Current Opinion in Neurobiology*, 13(1), pp.26–33.

Cringle, S.J. et al., 2006. Oxygen distribution and consumption in the developing rat retina. *Investigative ophthalmology & visual science*, 47, pp.4072–4076.

Curado, S. et al., 2007. Conditional targeted cell ablation in zebrafish: A new tool for regeneration studies. *Developmental Dynamics*, 236(February), pp.1025–1035.

Curado, S., Stainier, D.Y. & Anderson, R.M., 2008. Nitroreductase-mediated cell/tissue ablation in zebrafish: a spatially and temporally controlled ablation method with applications in development and regenration studies. *Nature Protocols*, 3(6), pp.948–954.

Downie, L.E. et al., 2007. Neuronal and glial cell changes are determined by retinal vascularization in retinopathy of prematurity. *The Journal of comparative neurology*, 504(4), pp.404–17. Available at: http://www.ncbi.nlm.nih.gov/pubmed/17663451 [Accessed June 1, 2015].

Eilken, H.M. & Adams, R.H., 2010. Dynamics of endothelial cell behavior in sprouting angiogenesis. *Current Opinion in Cell Biology*, 22(5), pp.617–625. Available at: http://dx.doi.org/10.1016/j.ceb.2010.08.010.

Faigle, R. & Song, H., 2012. Signaling mechanisms regulating adult neural stem cells and neurogenesis. *Biochimica et Biophysica Acta (BBA) - General Subjects*, 1830(2), pp.2435–2448. Available at: http://dx.doi.org/10.1016/j.bbagen.2012.09.002.

Ferrara, N., 2010. Vascular endothelial growth factor and age-related macular degeneration: from basic science to therapy. *Nature medicine*, 16(10), pp.1107–1111. Available at: http://dx.doi.org/10.1038/nm1010-1107.

Ferris, F.L., Fine, S.L. & Hyman, L., 1984. Age-related macular degeneration and blindness due to neovascular maculopathy. *Archives of ophthalmology (Chicago, Ill. : 1960)*, 102(11), pp.1640–2. Available at: http://www.ncbi.nlm.nih.gov/pubmed/6208888 [Accessed June 1, 2015].

Fruttiger, M., 2007. Development of the retinal vasculature. *Angiogenesis*, 10(2), pp.77–88.

Gestri, G., Link, B.A. & Neuhauss, S.C., 2012. The Visual System of Zebrafish and its Use to Model Human Ocular Diseases. *Changes*, 29(6), pp.997–1003.

Geudens, I. & Gerhardt, H., 2011. Coordinating cell behaviour during blood vessel formation. *Development*, 138, pp.4569–4583.

Gibson, D.L. et al., 1990. Retinopathy of Prematurity-Induced Blindness: Birth Weight-Specific Survival and the New Epidemic. *Pediatrics*, 86(3), pp.405–412. Available at: http://pediatrics.aappublications.org/content/86/3/405.short [Accessed June 1, 2015].

Gilbert, S.F., 2000. Development of the Vertebrate Eye. Available at: http://www.ncbi.nlm.nih.gov/books/NBK10024/ [Accessed May 25, 2015].

Goldberg, J.S. & Hirschi, K.K., 2009. Diverse roles of the vasculature within the neural stem cell niche. *Regenerative medicine*, 4(6), pp.879–97. Available at: http://www.pubmedcentral.nih.gov/articlerender.fcgi?artid=2836203&tool=pmcen trez&rendertype=abstract [Accessed June 1, 2015].

Haigh, J.J., 2008. Role of VEGF in organogenesis. *Organogenesis*, 4(4), pp.247–256.

Halder, G., Callaerts, P. & Gehring, W.J., 1995. Induction of ectopic eyes by targeted expression of the eyeless gene in Drosophila. *Science (New York, N.Y.)*, 267(5205), pp.1788–1792.

Hartsock, A. et al., 2014. In vivo analysis of hyaloid vasculature morphogenesis in zebrafish: A role for the lens in maturation and maintenance of the hyaloid. *Developmental Biology*, 394(2), pp.327–339. Available at: http://linkinghub.elsevier.com/retrieve/pii/S0012160614003765.

Hilfer, S.R., 1983. Development of the eye of the chick embryo. *Scanning electron microscopy*, (Pt 3), pp.1353–69. Available at: http://www.ncbi.nlm.nih.gov/pubmed/6648345 [Accessed May 25, 2015].

Hitchcock, P. et al., 2004. Persistent and injury-induced neurogenesis in the vertebrate retina. *Progress in retinal and eye research*, 23(2), pp.183–94.

Available at: http://www.ncbi.nlm.nih.gov/pubmed/15094130 [Accessed June 2, 2015].

Iruela-Arispe, M., 2005. The Cell Biology of Angiogenesis. *Mcdb.Ucla.Edu*, pp.1–30. Available at: https://www.mcdb.ucla.edu/Research/Arispe/course224-W1.pdf.

Jacob, E. et al., 2002. Influence of hypoxia and of hypoxemia on the development of cardiac activity in zebrafish larvae. *American journal of physiology. Regulatory, integrative and comparative physiology*, 283(4), pp.R911–R917.

Jin, S.-W. et al., 2005. Cellular and molecular analyses of vascular tube and lumen formation in zebrafish. *Development (Cambridge, England)*, 132(23), pp.5199–209. Available at: http://www.ncbi.nlm.nih.gov/pubmed/16251212 [Accessed June 2, 2015].

Johns, P.R., 1977. Growth of the adult goldfish eye. III. Source of the new retinal cells. *The Journal of comparative neurology*, 176(3), pp.343–57. Available at: http://www.ncbi.nlm.nih.gov/pubmed/915042 [Accessed June 2, 2015].

Joyal, J.S. et al., 2011. Ischemic neurons prevent vascular regeneration of neural tissue by secreting semaphorin 3A. *Blood*, 117, pp.6024–6035.

Kahn, H.A. & Hiller, R., 1974. Blindness Caused by Diabetic Retinopathy. *American Journal of Ophthalmology*, 78(1), pp.58–67. Available at: http://www.sciencedirect.com/science/article/pii/0002939474900105 [Accessed June 1, 2015].

Kanekar, S. et al., 1997. Xath5 participates in a network of bHLH genes in the developing Xenopus retina. *Neuron*, 19(5), pp.981–994.

Kay, J.N., Link, B. a & Baier, H., 2005. Staggered cell-intrinsic timing of ath5 expression underlies the wave of ganglion cell neurogenesis in the zebrafish retina. *Development (Cambridge, England)*, 132(11), pp.2573–2585.

Keegan, L., GIII, G. & Ptashne, M., 1986. Separation of DNA Binding from the Transcription-Activating Function of a Eukaryotic Regulatory Protein. , 231(4739), pp.699–704.

Kempen, J.H. et al., 2004. The prevalence of diabetic retinopathy among adults in the United States. *Archives of ophthalmology*, 122(4), pp.552–63. Available at: http://archopht.jamanetwork.com/article.aspx?articleid=416212 [Accessed March 19, 2015].

Kitambi, S.S. et al., 2009. Small molecule screen for compounds that affect vascular development in the zebrafish retina. *Mechanisms of Development*, 126(5-6), pp.464–477. Available at: http://dx.doi.org/10.1016/j.mod.2009.01.002.

Li, Q. et al., 2006. Modeling the neurovascular niche: VEGF- and BDNF-mediated cross-talk between neural stem cells and endothelial cells: an in vitro study. *Journal of neuroscience research*, 84(8), pp.1656–68. Available at: http://www.ncbi.nlm.nih.gov/pubmed/17061253 [Accessed June 1, 2015].

Li, S. et al., 2013. Endothelial VEGF sculpts cortical cytoarchitecture. *The Journal of neuroscience : the official journal of the Society for Neuroscience*, 33(37), pp.14809–15. Available at: http://www.pubmedcentral.nih.gov/articlerender.fcgi?artid=3771035&tool=pmcentrez&rendertype=abstract.

Liang, D. et al., 2001. The role of vascular endothelial growth factor (VEGF) in vasculogenesis, angiogenesis, and hematopoiesis in zebrafish development. *Mechanisms of development*, 108, pp.29–43.

Linder, M.E. & Deschenes, R.J., 2003. New insights into the mechanisms of protein palmitoylation. *Biochemistry*, 42(15), pp.4311–4320.

Liu, W., Mo, Z. & Xiang, M., 2001. The Ath5 proneural genes function upstream of Brn3 POU domain transcription factor genes to promote retinal ganglion cell development. *Proceedings of the National Academy of Sciences of the United States of America*, 98(4), pp.1649–1654.

Lutty, G. a. & McLeod, D.S., 2003. Retinal vascular development and oxygen-induced retinopathy: A role for adenosine. *Progress in Retinal and Eye Research*, 22, pp.95–111.

Lyons, S.E. et al., 2002. A nonsense mutation in zebrafish gata1 causes the bloodless phenotype in vlad tepes. *Proceedings of the National Academy of Sciences of the United States of America*, 99, pp.5454–5459.

Macdonald, R. et al., 1995. Midline signalling is required for Pax gene regulation and patterning of the eyes. *Development (Cambridge, England)*, 121(10), pp.3267–3278.

Mackenzie, F. & Ruhrberg, C., 2012. Diverse roles for VEGF-A in the nervous system. , 1380, pp.1371–1380. Available at: http://discovery.ucl.ac.uk/1344914/.

Masai, I. et al., 2000. Midline signals regulate retinal neurogenesis in zebrafish. *Neuron*, 27(2), pp.251–263.

Morrow, E.M. et al., 1999. NeuroD regulates multiple functions in the developing neural retina in rodent. *Development (Cambridge, England)*, 126, pp.23–36.

Mounier, R., Chrétien, F. & Chazaud, B., 2011. Blood vessels and the satellite cell niche. *Current topics in developmental biology*, 96, pp.121–38. Available at: http://www.ncbi.nlm.nih.gov/pubmed/21621069 [Accessed June 1, 2015].

Mu, X. & Klein, W.H., 2004. A gene regulatory hierarchy for retinal ganglion cell specification and differentiation. *Seminars in Cell and Developmental Biology*, 15(1), pp.115–123.

Nasevicius, a, Larson, J. & Ekker, S.C., 2000. Distinct requirements for zebrafish angiogenesis revealed by a VEGF-A morphant. *Yeast (Chichester, England)*, 17(4), pp.294–301.

Nelson, S.M., Park, L. & Stenkamp, D.L., 2009. Retinal homeobox 1 is required for retinal neurogenesis and photoreceptor differentiation in embryonic zebrafish. *Developmental Biology*, 328(1), pp.24–39.

Neumann, H., Kotter, M.R. & Franklin, R.J.M., 2009. Debris clearance by microglia: An essential link between degeneration and regeneration. *Brain*, 132(2), pp.288–295.

Newman, E. & Reichenbach, A., 1996. The Müller cell: A functional element of the retina. *Trends in Neurosciences*, 19(8), pp.307–312.

Nornes, S. et al., 1998. Zebrafish contains two Pax6 genes involved in eye development. *Mechanisms of Development*, 77(2), pp.185–196.

Nusse, R., 2003. Wnts and Hedgehogs: lipid-modified proteins and similarities in signaling mechanisms at the cell surface. *Development (Cambridge, England)*, 130(22), pp.5297–5305.

Otteson, D.C., D'Costa, A.R. & Hitchcock, P.F., 2001. Putative stem cells and the lineage of rod photoreceptors in the mature retina of the goldfish. *Developmental biology*, 232(1), pp.62–76. Available at: http://www.ncbi.nlm.nih.gov/pubmed/11254348 [Accessed June 2, 2015].

Paik, E.J. & Zon, L.I., 2010. Hematopoietic development in the zebrafish. *International Journal of Developmental Biology*, 54(6-7), pp.1127–1137.

Palmer, T.D., Willhoite, A.R. & Gage, F.H., 2000. Vascular niche for adult hippocampal neurogenesis. *Journal of Comparative Neurology*, 425(July), pp.479–494.

Pelster, B. & Burggren, W.W., 1996. Disruption of hemoglobin oxygen transport does not impact oxygen-dependent physiological processes in developing embryos of zebra fish (Danio rerio). *Circulation research*, 79, pp.358–362.

Pisharath, H. et al., 2008. Targeted ablation of beta cellls in the embryonic zebrafish pancreas using E.coli nitroreductase. , 124(3), pp.218–229.

Quiring, R. et al., 1994. Homology of the eyeless gene of Drosophila to the Small eye gene in mice and Aniridia in humans. *Science (New York, N.Y.)*, 265(5173), pp.785–789.

Reichenbach, A. & Bringmann, A., 2013. New functions of m??ller cells. *Glia*, 61(5), pp.651–678.

Risau, W., 1997. Mechanisms of angiogenesis. *Nature*, 386, pp.671–674.

Saint-Geniez, M. & D'Amore, P. a., 2004. Development and pathology of the hyaloid, choroidal and retinal vasculature. *International Journal of Developmental Biology*, 48(8-9), pp.1045–1058.

Sehnert, A.J. et al., 2002. Cardiac troponin T is essential in sarcomere assembly and cardiac contractility. *Nature genetics*, 31(April), pp.106–110.

Shen, Q. et al., 2009. Adult SVZ stem cells lie in a vascular niche: A quantitative analysis of niche cell-cell interactions. *Cell*, 3(3), pp.289–300.

Shen, Q. et al., 2004. Endothelial cells stimulate self-renewal and expand neurogenesis of neural stem cells. *Science (New York, N.Y.)*, 304(5675), pp.1338–40. Available at: http://www.ncbi.nlm.nih.gov/pubmed/15060285 [Accessed March 12, 2015].

Shen, Y.C. & Raymond, P. a., 2004. Zebrafish cone-rod (crx) homeobox gene promotes retinogenesis. *Developmental Biology*, 269, pp.237–251.

Smith, L.E.H., 2003. Pathogenesis of retinopathy of prematurity. *Seminars in neonatology : SN*, 8(6), pp.469–73. Available at: http://www.sciencedirect.com/science/article/pii/S1084275603001192 [Accessed June 1, 2015].

Stainier, D.Y. et al., 1995. *Cloche*, an early acting zebrafish gene, is required by both the endothelial and hematopoietic lineages. *Development (Cambridge, England)*, 121, pp.3141–3150.

Stainier, D.Y. et al., 1996. Mutations affecting the formation and function of the cardiovascular system in the zebrafish embryo. *Development (Cambridge, England)*, 123, pp.285–292.

Stainier, D.Y., Lee, R.K. & Fishman, M.C., 1993. Cardiovascular development in the zebrafish. I. Myocardial fate map and heart tube formation. *Development (Cambridge, England)*, 119(1), pp.31–40.

Stem, M.S. & Gardner, T.W., 2013. Neurodegeneration in the pathogenesis of diabetic retinopathy: molecular mechanisms and therapeutic implications. *Current medicinal chemistry*, 20(26), pp.3241–50. Available at: http://www.pubmedcentral.nih.gov/articlerender.fcgi?artid=4071765&tool=pmcen trez&rendertype=abstract [Accessed April 25, 2015].

Stenkamp, D.L., 2007. Neurogenesis in the fish retina. *International review of cytology*, 259, pp.173–224. Available at: http://www.pubmedcentral.nih.gov/articlerender.fcgi?artid=2897061&tool=pmcen trez&rendertype=abstract [Accessed June 2, 2015].

Stenkamp, D.L., 2011. The rod photoreceptor lineage of teleost fish. *Progress in retinal and eye research*, 30(6), pp.395–404. Available at: http://www.pubmedcentral.nih.gov/articlerender.fcgi?artid=3196835&tool=pmcen trez&rendertype=abstract [Accessed June 2, 2015].

Sumanas, S., Jorniak, T. & Lin, S., 2005. Identification of novel vascular endothelial-specific genes by the microarray analysis of the zebrafish *cloche* mutants. *Blood*, 106, pp.534–541.

Vailhé, B., Vittet, D. & Feige, J.J., 2001. In vitro models of vasculogenesis and angiogenesis. *Laboratory investigation; a journal of technical methods and pathology*, 81(4), pp.439–452.

Wang, W. et al., 2010. Expression of the Lycat gene in the mouse cardiovascular and female reproductive systems. *Developmental Dynamics*, 239(April), pp.1827–1837.

Wangsa-Wirawan, N.D. & Linsenmeier, R.A., 2003. Retinal oxygen: fundamental and clinical aspects. *Archives of ophthalmology (Chicago, Ill. : 1960)*, 121(4), pp.547–57. Available at: http://www.ncbi.nlm.nih.gov/pubmed/12695252 [Accessed May 25, 2015].

Weinstein, B.M. et al., 1996. Hematopoietic mutations in the zebrafish. *Development (Cambridge, England)*, 123, pp.303–309.

Weiss, O. et al., 2012. Abnormal vasculature interferes with optic fissure closure in lmo2 mutant zebrafish embryos. *Developmental Biology*, 369(2), pp.191–198. Available at: http://dx.doi.org/10.1016/j.ydbio.2012.06.029.

Xiong, J.-W. et al., 2008. An Acyltransferase Controls the Generation of Hematopoietic and Endothelial Lineages in Zebrafish. *Circulation Research*, 102(9), pp.1057–1064.

Chapter 2: Abnormal retinal development in *cloche* mutant zebrafish

Susov Dhakal[1,2]*, Craig B. Stevens[1]*, Meyrav Sebbagh[3], Omri Weiss[3], Ruth A. Frey[1],

Seth Adamson[1], Eric A. Shelden[4], Adi Inbal[3], and Deborah L. Stenkamp[1,2]

Abstract**:**

Background**:** Functions for the early embryonic vasculature in regulating the development of central nervous system tissues, such as the retina, have been suggested by *in vitro* studies and vascular gain-of-function experiments. Here we use an avascular zebrafish embryo, *cloche-/-* (*clo-/-*), to begin to identify necessary developmental functions of the ocular vasculature in regulating development and patterning of the neural retina, *in vivo*. These studies are possible in zebrafish embryos, which do not yet rely upon the vasculature for tissue oxygenation.

Results**:** *clo-/-* embryos lacked early ocular vasculature and were microphthalmic, with reduced retinal cell proliferation and cell survival. Retinas of *clo* mutants were disorganized, with irregular synaptic layers, mispatterned expression domains of retinal transcription factors, morphologically abnormal Müller glia, reduced differentiation of specific retinal cell types, and sporadically distributed cone photoreceptors. Blockade of p53-mediated cell death did not completely rescue this phenotype and revealed ectopic cones in the inner nuclear layer. *clo-/-* retinas did not express a molecular marker for hypoxia.

<u>Conclusions</u>**:** The disorganized retinal phenotype of the *clo-/-* embryo is consistent with a neural and glial developmental patterning role for the early ocular vasculature that is independent of its eventual function in gas exchange.

<u>Introduction</u>**:**

Cells of the central nervous system (CNS) are the most metabolically active in the body and have a high demand for oxygen and nutrient delivery from the vasculature. In addition, specialized neural stem cell niches require immediate access to a blood supply, for metabolic support as well as for endocrine or paracrine factors provided by the circulating blood or the cells of the blood vessels (Ottone et al., 2014; Raymond et al., 2006). Major glial cell types of the CNS – Müller glia in the retina, and astrocytes elsewhere – establish an intimate association with endothelial cells of blood vessels by forming endfeet that induce tight junctions and create the blood-retinal barrier and blood-brain barrier (Alvarez et al., 2007; Hartsock et al., 2014; Xie et al., 2010). Numerous disorders of the CNS involve coincident or causative vascular pathology. Examples of such disorders from the neural retina include diabetic retinopathy (Shin et al., 2014), the wet form of age-related macular degeneration (van Lookeren Campagne et al., 2014) and retinopathy of prematurity (Hartnett, 2015).

There is an emerging interest in understanding how the developing vasculature of the CNS interacts with progenitor cells, and developing neurons and glia, during embryogenesis (Aizawa and Shoichet, 2012). Goals of these efforts include determining vascular-neuronal developmental interactions necessary for the establishment of mature tissue morphologies that allow for healthy metabolic

relationships, and identifying signaling factors that underlie any communication between the developing vessels and developing neural tissue. For example, in the *frizzled* mutant mouse, and in a mouse model overexpressing vascular endothelial growth factor (VEGF) in the lens, extra blood vessels develop and are associated with abnormal retinal neurogenesis (Rutland et al., 2007; Zhang et al., 2008). In a zebrafish model, an abnormally dilated hyaloid vein interferes with closure of the optic fissure, demonstrating interactions between blood vessels and the optic cup in influencing eye morphogenesis (Weiss et al., 2012). In addition, co-culture studies suggest that direct cellular contact of neural progenitors with endothelial cells influences neural progenitor proliferation (Shen et al., 2004) and retinal cell differentiation (Aizawa and Shoichet, 2012) *in vitro*. Insights from further studies are likely to reveal vascular-neuronal relationships that may aid in understanding pathologies of the CNS, which involve the vasculature.

One challenge to the *in vivo* study of vascular effects on neuronal development is that experimental manipulation of the vasculature in mammals results in an unavoidable disruption of tissue oxygenation. Such experimental manipulations would therefore be unable to uncouple developmental signaling roles of the vasculature from nourishment roles. To overcome this obstacle we are pursuing developmental roles of the vasculature in the zebrafish (*Danio rerio*) embryo. During embryonic development, zebrafish tissues are not dependent upon hemoglobin-mediated oxygen transport, and can instead utilize diffusion for gas exchange (Pelster and Burggren, 1996). In addition to this important advantage, the zebrafish offers avascular genetic models (Stainier et al., 1996; Stainier et al., 1995; Xiong et

al., 2008), transgenic tools for the visualization of vasculature (Covassin et al., 2009; Jin et al., 2005; Lawson and Weinstein, 2002; Nasevicius et al., 2000), and numerous retina-specific developmental markers (Stenkamp, 2007).

In vertebrates, the vasculature and the neural retina undergo development concomitantly, suggesting opportunities for developmental signaling interactions. Specifically in zebrafish, the hyaloid artery invades the eye through the choroid fissure at 18-20 hpf (Hartsock et al., 2014), and then branches to form the system of hyaloid capillaries that lie between the lens and retina (Alvarez et al., 2007; Hartsock et al., 2014; Kitambi et al., 2009). This hyaloid network is established over 24-32 hpf, corresponding to the time of retinal progenitor proliferation and initial differentiation of retinal ganglion cells (RGCs) (Hu and Easter, 1999). A second vascular system, the superficial vessels, forms on the surface of the eye from 23 hpf to 54 hpf (Kaufman et al., 2015), corresponding to the time of generation and differentiation of more distal retinal cell types including retinal bipolar cells, photoreceptors, and Müller glia (Hu and Easter, 1999).

To begin to test developmental roles for the early ocular vasculature in regulating retinal neurogenesis and patterning, we used embryonic *cloche* (*clo*) mutant zebrafish. *Clo* mutant embryos display severe defects in development of vascular endothelial cells, endocardial cells, and hematopoietic cells (Stainier et al., 1995). Here we verified the lack of early ocular vasculature in *clo-/-* embryos, and evaluated the process of retinal neurogenesis using histology, cell-specific immunological markers, and *in situ* hybridization for specific retinal transcription factors. We report defects in retinal cell proliferation and survival in *clo-/-*, and striking

defects in retinal organization that include disrupted expression patterns of retinal transcription factors, abnormal morphology of Müller glia and of synaptic layers, and ectopic cone photoreceptors that are revealed when cell death is blocked. These abnormalities are not related to tissue hypoxia or to the complete lack of microglia and they are not secondary to lens defects. Our results are consistent with possible non-metabolic, developmental patterning functions for the early ocular vasculature in the control of retinal neurogenesis.

Experimental Procedures:

Animals

Zebrafish were maintained in monitored aquatic housing units on recirculating system water at 28.5°C. Embryos were collected according to Westerfield (Westerfield, 2007), with the time of spawning considered to be zero hours postfertilization (hpf) and embryonic age timed accordingly thereafter. Embryos used for some of the histological analyses were kept transparent by incubating them in system water containing 0.003% phenothiourea (PTU) to inhibit melanin synthesis (Westerfield, 2007). All experiments using animals were approved by the University of Idaho's Animal Care and Use Committee or by the Authority for Biological and Biomedical Models in the Hebrew University of Jerusalem. Adults carrying the *cloche (clo) m39* mutation (Stainier et al., 1995) were the generous gift of Leonard Zon; those carrying the *m378* mutation (Stainier et al., 1996) were kindly provided by Karina Yaniv. Crosses of heterozygous carriers were used to obtain *clo-/-* embryos. The *clo-/-* heart defect was reliably identified beginning at 29 hpf, and eye phenotypes in both *clo* mutant alleles were similar. For all analyses *clo-/-* embryos

were compared to normal siblings. *Tg(kdrl:EGFP)s843* has been described (Jin et al.,

2005).

Visualization of early ocular vasculature

Early ocular vasculature was imaged in live embryos carrying the *kdrl:EGFP*

transgene using a Zeiss LSM 700 confocal microscope. An additional analysis of

ocular vascular development was performed by staining for the endogenous alkaline

phosphatase found in developing vasculature cells, and was performed as previously

described (Zoeller et al., 2008). Briefly, embryos were fixed for 1 hour in phosphate-

buffered (pH 7.4) 4% paraformaldehyde in 5% sucrose at room temperature, washed

in phosphate-buffered saline with 0.5% Triton X-100 (PBST), dehydrated through a

methanol series and were stored at -20°C. Tissues were incubated in 100% acetone

at -20°C for 30 minutes followed by washing twice in PBST at room temperature.

Embryos were equilibrated in alkaline phosphatase staining solution three times for

15 minutes at room temperature. Embryos were then incubated in staining solution

with nitroblue tetrazolium and 5-bromo-4-chloro-3-indolyl-phosphate (NBT-BCIP)

substrates, or with Fast Red, according to the manufacturer's instructions (Roche).

The reaction was stopped by washing embryos repeatedly with PBST, and eyes were

dissected manually and mounted in glycerol for viewing on a Leica DMR (for NBT-

BCIP) or an Olympus Fluoview confocal microscope (for Fast Red).

Histology

Embryos were fixed in 4% paraformaldehyde overnight at 4°C, washed with

PBT, dehydrated in EtOH series and embedded in JB4 resin (Polysciences, Inc.)

according to manufacturer's instructions. 4 μm sections were cut with LKB 8800

Ultratome III microtome and stained with methylene blue – azure II (Humphrey and Pittman, 1974).

Tissues were processed for immunocytochemical staining and *in situ* hybridization according to published protocols (Barthel and Raymond, 1990). Briefly, embryos were fixed in phosphate buffered, 4% paraformaldehyde containing 5% sucrose for one hour, washed with buffered 5% sucrose, cryoprotected overnight in buffered 20% sucrose, then embedded in a 1:2 mixture of OCT medium and 20% sucrose. Sections were cut at 5-14 μm on a Microm cryostat or Leica CM3050 S cryostat.

Morphometric analysis of eye and lens size

Live whole embryos at specific developmental stages were immobilized using 0.017% Tricaine (Sigma) and aligned for photography in a trough molded into an agarose plate. Images were captured using a Nikon stereomicroscope (Meridian Instruments, Freeland, WA) fitted with a CCD camera. For each specimen the outline of the eye and lens were traced using Photoshop CS6 (Adobe) to generate a silhouette. This silhouette was analyzed in ImageJ/FIJI (Schneider et al., 2012) in order to obtain a Feret Diameter (a method for estimating the particle diameter of potentially irregularly-shaped particles). The statistical analyses of significance (ANOVA) were performed in the R statistical environment (R Core Development Team, 2000).

Immunocytochemistry and in situ hybridization

Fixation and preparation of embryos for immunocytochemistry and *in situ* hybridization were performed as previously described (Barthel and Raymond, 1990;

Nelson et al., 2008; Stevens et al., 2011). The following antibodies were used:

mouse monoclonal ZPR1, labels red- and green-sensitive cones (Larison and

Bremiller, 1990) (1:500; Zebrafish International Research Center; ZIRC); mouse

monoclonal ZN8, labels embryonic retinal ganglion cells (Hu and Easter, 1999)

(1:500; ZIRC); mouse monoclonal ZRF1, labels Müller glia (Marcus and Easter,

1995) (1:20; ZIRC); rabbit polyclonal anti-GFP (1:1000; Torrey Pines Biolabs), mouse

monoclonal 1D1, labels rod opsin (Fadool, 2003) (1:100; the gift of James Fadool,

Florida State University); mouse monoclonal anti-HuC/D, labels RGCs and amacrine

cells (1:200; Developmental Studies Hybridoma Bank); rabbit polyclonal anti-protein

kinase C (PKC), labels a subpopulation of retinal bipolar cells (1:200; Santa Cruz

Biotechnologies); mouse monoclonal anti-phosphohistone 3 (PH-3; 1:1000; Cell

Signaling Technologies); mouse monoclonal anti-synaptic vesicle 2 (SV2; 1:2000;

Developmental Studies Hybridoma Bank); mouse monoclonal anti-cleaved caspase 3

(CC3; 1:200; Abcam); mouse monoclonal 4C4, labels microglia (Raymond et al.,

2006) (1:200; gift of Peter Hitchcock, University of Michigan). Immunocytochemistry

was performed as described (Stevens et al., 2011). Primary antibodies were detected

with an Alexa Fluor 647 or Cy3 or fluorescein-conjugated secondary antibody

(Jackson Immunoresearch) at 1:200 or 1:500 and samples were mounted with

VectaShield containing DAPI (Vector Labs).

 In situ hybridization was performed as previously described for cryosections

(Nelson et al., 2008; Stevens et al., 2011) and for whole mounts (Stenkamp and

Frey, 2003). Digoxigenin-labeled cRNA probes were generated by *in vitro* reverse

transcription from plasmids containing the following cDNAs: zebrafish *pax6a* and *crx*

(gifts of P. Raymond), *rx1* (gift of P. Mathers), *NeuroD* (gift of P. Hitchcock), *atoh7/ath5* (gift of S. Wilson), *six3b* {Kobayashi, 1998 #178}, and *phd3/elgn3* (BioScience Life Sciences).

Quantification of labeling by antibodies

Images of immunologically-labeled histological sections were captured using a Leica DMR compound microscope with a SPOT camera system (Diagnostic Instruments). Fluorescently-labeled tissues were viewed using epifluorescence or using Zeiss LSM 700 confocal microscope. Specific cell types were analyzed as follows: *Rod photoreceptors:* 1D1 labeling was quantified by counting in each section the number of labeled cells located dorsal to the optic nerve. All cells ventral to the optic nerve were considered part of the "ventral patch" of rods where the density of rod photoreceptors prevented accurate counting (Raymond et al., 1995; Stevens et al., 2011). The total number of rods was then divided by the number of sections counted to determine the average number of rods per section. *Cone photoreceptors:* Two scores were used. The first score was based on the extent of labeling in each sample, and included three categories (*None* = no labeled cells; *Few* = 1 to 10 labeled cells; *Many* > 10 labeled cells). The second score, applied only to samples scored as *Few* or *Many,* was based on the pattern of ZPR1 staining (*Sporadic* = large gaps between the labeled cells; *Discontinuous* = 1 to 2 unlabeled cells in between; *Dense* = no unlabeled gaps between the labeled cells) (Kashyap et al., 2011; Nelson et al., 2009). *Ganglion cell layer:* The ganglion cell layer (GCL) was detected using the antibody ZN-8 (Hu and Easter, 1999). The volume of the GCL for each eye was estimated as follows: In all images of ZN8 labeling the area representing the GCL

was traced digitally using Photoshop CS6. The area of each resulting silhouette was determined using ImageJ/FIJI (Schneider et al., 2012). The area of each section was multiplied by the section thickness in order to determine the volume and these results were summed for all sections in order to estimate the volume of the GCL. *PH-3 labeling.* Nuclei positive for PH-3 were counted in order to estimate the number of cells undergoing mitosis. Fragmentary labeling for PH-3 due to sections cutting through only a small part of a mitotic nucleus was avoided by counting only labeled nuclei above 7 μm in diameter size, considered to represent the whole nucleus. *CC3 labeling.* Cellular profiles positive for CC3 were counted to estimate the number of cells undergoing apoptosis in sections; we counted CC3+ fragments in embryonic hemi-brains and retinas. Double-counting of cell fragments derived from the same cell was avoided by counting only labeled profiles above 3 μm in diameter, and performing counts on sections separated by 10 μM. *4C4 labeling.* Numbers of 4C4+ cell clusters were counted to assess the presence of mature microglia. Double-counting of clusters was avoided by performing counts on sections separated by 20 μm (counting every fifth, 5-μm section).

Statistically significant differences in these measures between genotypes were determined using Student's T-Test, performed in the R statistical environment (R Core Development Team, 2000), or Fisher's exact test in the case of proportional data.

Neutral red uptake and quantification

Live embryos were incubated in 2.5 μg/ml neutral red in the dark from 49-53 hpf, and were imaged as whole mounts using DIC optics, with images collected in 4-6

focal planes for each embryo, in order to sample all neutral red-labeled cells. Neutral red+ profiles were traced, and areas measured in ImageJ/FIJI on projected stacks of images representing each embryo eye.

Morpholino-mediated knockdown of p53

Antisense morpholino oligonucleotides (MO) targeting the translation start site to *p53* mRNA (Plaster et al., 2006), MO4-*tp53*, were purchased from Gene Tools (Philomath, OR), and resuspended in water. Embryos obtained from a heterozygote cross of *clo+/-* zebrafish were injected at the one-cell stage with 2 ng *p53* MO. *clo* mutant embryos in these experiments were identified by heart phenotype.

Hypoxia treatments

Hypoxic conditions were achieved using previous methods (Tucker et al., 2011). System water was filtered and then boiled to remove dissolved gasses, and then 0.2 mg/ml sodium sulfite was added, and the water was cooled under N_2 gas to 28.5°C. Levels of O_2 were measured with a YSI DO200 O_2 meter, and were between 0.08 and 0.12 ppm O_2. Embryos were incubated in airtight 250 ml flasks containing deoxygenated system water for 90 mins, and then placed individually in culture wells containing normoxic system water for 30 mins prior to fixation.

Results**:**

Lack of early ocular vasculature in clo-/- embryos

The *cloche* mutation in zebrafish affects the development of endothelial and hematopoietic lineages, and mutants lack functional hearts, blood cells, and most blood vessels (Liao et al., 1997; Stainier et al., 1995). We verified that ocular vasculature was absent in *clo* mutants (*m378* and *m39* alleles) using two

complementary strategies. Firstly, we established *cloche* on the *kdrl:EGFP*

transgenic background, in which all vascular endothelial cells express EGFP under

regulatory elements of the *kdrl* gene (VEGF receptor 2, *vegfr2*) (Jin et al., 2005).

Confocal images revealed that *clo+; kdrl:EGFP* embryos develop EGFP+ ocular

vascular networks from 24 – 54 hpf, including the hyaloid artery, hyaloid capillaries,

and the superficial vasculature (Fig. 2.1A,C) (Alvarez et al., 2007; Kitambi et al.,

2009). In contrast, eyes of *clo-/-; kdrl:EGFP* embryos showed the complete absence

of EGFP+ blood vessels within the developing eye at the same developmental stages

(Fig. 2.1B,D). Interestingly, *clo-/-* embryos displayed some evidence of blood vessel

formation outside of the eye, including the branchial arch vessels, at 54 hpf (Fig.

2.1E,F). Secondly, we examined eyes of non-transgenic *clo-/-* embryos for the

presence of endogenous alkaline phosphatase activity, which is characteristic of

endothelial cells (Zoeller et al., 2008). At 48 hpf, wildtype siblings of *clo* mutants

showed staining of superficial vasculature (data not shown) in addition to staining of

hyaloid capillaries surrounding the lens (Fig. 2.1G). By contrast, *clo* mutant eyes

displayed no alkaline phosphatase activity, indicating the absence of endothelial cells

(Fig. 2.1H). The absence of two markers of endothelial cells within the developing

eye indicates that embryonic eyes of *clo* mutants do not develop early ocular

vasculature.

Reduced embryonic eye growth in clo mutants

clo-/- embryonic eyes appeared reduced in size as compared with their

wildtype siblings (Fig. 2.1I-L). Circumferences of eyes and lenses from live embryos

at 30, 36, 48, and 72 hpf were measured in order to estimate their diameters (n=10-

15 for each age and genotype; see Experimental Procedures). At all sampling times, *clo-/-* eyes were significantly smaller than wildtype eyes (Fig. 2.1M-P). No eye growth was apparent in *clo-/-* eyes between 36 and 48 hpf, as the 48 hpf *clo-/-* eyes were not significantly larger than 36 hpf *clo-/-* eyes (Fig. 2.1N,O). Interestingly, at 30 and 36 hpf *clo-/-* lenses were not significantly different in size than wildtype lenses (Fig. 2.1M,N), and at 48 hpf *clo-/-* lenses had increased significantly in size (Fig. 2.1N,O; p<0.01). However, at 48 and 72 hpf *clo-/-* lenses were significantly smaller than those of their wildtype siblings (Fig. 2.1O,P; p<0.001). Together these findings suggest that *clo* mutants have defects in eye growth that are not likely strictly related to, or secondary to, lens defects (Goishi et al., 2006).

Disrupted retinal, RPE, and lens histology in clo mutants

We evaluated further the phenotype of *clo* mutant eyes using histological sections prepared from *clo-/-* embryos at 72 hpf, when the wildtype retina displays laminar organization (Fig. 2.1Q) and visual function is possible (Easter and Nicola, 1996). *clo-/-* retinas were poorly organized, with a reduced and irregular inner plexiform layer (IPL; where bipolar cells synapse with ganglion cells), and a strongly reduced outer plexiform layer (OPL; where photoreceptors synapse with bipolar cells). All retinal nuclear layers also appeared reduced in thickness and were disorganized (Fig. 2.1R). The *clo-/-* retinas also showed evidence of cell death, with gaps in the retinal tissue associated with darkly stained and pyknotic nuclei, particularly in the retinal ganglion cell (RGC) layer and the inner nuclear layer (INL) (Fig. 2.1R). We note that within a clutch of *clo* mutants, this phenotype showed some variability, with some embryos displaying fewer pyknotic nuclei and less disorganized

retinal layers (not shown). However, microphthalmia and the reduced thickness of plexiform layers were consistently observed. The retinal pigmented epithelium (RPE) was visibly thinner in *clo-/-* than in wildtype embryos, particularly in ventral retina, and in some mutant embryos the ventral RPE was missing (data not shown). Lenses of *clo-/-* embryos were also abnormal, with the absence of concentric lens fibers (Fig. 2.1R), perhaps related to reduced crystallin synthesis as previously reported (Goishi et al., 2006). In addition, *clo-/-* lenses displayed cell-free gaps between the lens epithelium and the developing lens fibers, particularly in the region of the lens equator (Fig. 2.1R). These findings indicate that *clo* mutant embryos fail to develop normally laminated retinas, as well as show defects in developing RPE and lens tissues.

Reduced retinal cell proliferation and increased cell death in clo mutants

The developmental time when the growth of *clo-/-* eyes is significantly disrupted (30-72 hpf) corresponds to the periods of retinal progenitor proliferation, neurogenesis, and cell differentiation (Hu and Easter, 1999). Next we tested whether some of the reduced eye growth in *clo* mutants may be related to defects in cell proliferation, by staining cryosections obtained from 30 hpf and 54 hpf embryos with an antibody targeting phosphorylated histone-3 (PH3), an M-phase marker. At 30 hpf, wildtype and *clo-/-* retinas contained mitotic cells at the apical surface of the retina (Fig. 2.2A,B), and numbers of PH3+ cells were not significantly different in *clo-/-* as compared to wildtype retinas (Fig. 2.2E), suggesting that reduced retinal proliferation may not contribute to reduced eye size in *clo* mutants at this developmental time. At 54 hpf, wildtype and *clo-/-* retinas contained mitotic cells in

the emerging ONL, the INL, and in the circumferential germinal zone (CGZ) (Fig. 2.2C,D). In *clo-/-* embryos, mitotic cells in the retina were present in significantly fewer numbers (Fig. 2.2F). An additional analysis of PH3+ cells within specific retinal layers/regions revealed significantly fewer M-phase cells specifically at the apical surface of the retina/future ONL (Fig. 2.2G). Therefore, reduced retinal proliferation likely contributes to the lack of eye growth during later stages of neurogenesis in *clo-/-* embryos.

The gaps in retinal tissue and presence of pyknotic cell bodies, together with reduced eye size (Fig. 2.1) suggested that increased cell death in *clo-/-* embryos was likely. We explicitly evaluated caspase 3-mediated cell death in the retinas of *clo* mutants and their normal siblings by using an anti-cleaved caspase 3 (CC3) antibody. In sections derived from 30 hpf embryos, we observed virtually no CC3+ cells in developing retinas of either wildtype or *clo-/-* embryos (data not shown). However, in sections of 54 hpf embryos, numbers of CC3+ cells were slightly but significantly higher in *clo-/-* retinas than in wildtype retinas (Fig. 2.3A,B,E; $p<0.001$), indicating an increased rate of cell death during late retinal neurogenesis. In sections processed at 72 hpf the numbers of CC3+ profiles increased further, with bands or clusters of staining predominantly in the GCL, and in the INL region that normally contains cell bodies of bipolar cells and Müller glia, and in the distal retina (possibly cells of the ONL but due to disorganized structure this cannot be unambiguously determined; Fig. 2.3C-E). Of particular interest was the comparative lack of increased cell death in the brains of *clo-/-* embryos (Fig. 2.3E; numbers are per hemi-brain), suggesting a potentially specific retinal requirement for vasculature at 54-72 hpf.

Reduced differentiation of retinal neurons in clo mutants

The thinned and irregular plexiform layers in *clo-/-* retinas suggested that formation of synaptic processes may be impaired. Indirect immunofluorescence studies using an antibody that detects synaptic vesicle 2 (SV2) confirmed that synaptic terminals appeared less abundant in *clo-/-* retinas at 72 hpf, and showed irregular patterns (Fig. 2.4A-C). These irregular patterns of SV2 staining may indicate faulty growth and targeting of the synaptic terminals themselves, and/or specifically of the SV2 protein.

clo-/- retinas displayed disorganized RGC layers (Fig. 2.1R), suggesting that differentiation of RGCs may be affected. In addition, RGCs are the retinal neurons that reside in closest proximity to a vasculature bed – the hyaloid – which is missing in *clo* mutants (Fig. 2.1B,D,H). We labeled the ganglion cell layer (GCL) with the antibody ZN8 at 54 hpf, when embryonic RGC neurogenesis is complete (Hu and Easter, 1999). The size of the ZN8-positive domain appeared reduced in *clo-/-* as compared with wildtype embryos (Fig. 2.4D,E). We used a subset of ZN8-stained cryosections from n=9 embryos to estimate the volume of the GCL (see Experimental Procedures). This analysis revealed a significantly reduced GCL volume in *clo-/-* retinas; approximately 48% (Fig. 2.4F). To determine whether this outcome was simply related to reduced overall eye size, we used the same set of cryosections to estimate the volume of the unlabeled portion of each eye and then obtain ratios of GCL volumes to the non-GCL volume of the eye. In wildtype embryos this ratio was 0.08, while in *clo-/-* embryos this ratio was 0.10, a statistically significant difference ($p<0.05$), and one that indicates the GCL of *clo-/-* embryos is actually less reduced in

size as compared with the remainder of the eye. Collectively these findings suggest that the *clo* mutation impairs the differentiation of RGCs, but may have greater impacts on other cell types of the developing eye.

Neurons of the INL were next analyzed by staining cryosections from 72 hpf embryos with anti-HuC/D, which stains amacrine as well as ganglion cells (Fig. 2.4G), and with anti-protein kinase Cα (PKCα), which stains a subpopulation of retinal bipolar cells (Fig. 2.4I). HuC/D+ cells in the GCL and inner half of the INL were evident in both wildtype retinas (Fig. 2.4G), and the domain of HuC/D immunoreactivity in *clo-/-* retinas was greatly expanded as compared to the corresponding ZN8 staining domain (compare Fig. 2.4H with Fig. 2.4E), suggesting that initial amacrine cell differentiation took place in *clo* mutants. Moreover, the Hu staining pattern further revealed a conspicuously reduced and disorganized IPL (Fig. 2.4H). In the anti-PKCα studies, *clo-/-* retinas displayed a range of staining patterns. In some *clo* mutants, particularly those that showed highly disorganized retinal lamination, PKCα staining was entirely absent (Fig. 2.4J). However, in *clo* mutants with evidence of some lamination, faint PKCα+ cellular profiles were present, but with no obvious cellular processes (Fig. 2.4K).

The differentiation of rod and cone photoreceptors was detected in 72 hpf cryosections using the antibodies 1D1, which stains the rod visual pigment, rhodopsin (Fadool, 2003), ZPR1, which stains an unknown surface epitope on double cones (pairs of red- and green-sensitive cones) (Larison and Bremiller, 1990), and peanut lectin, which stains all cones (Garlipp et al., 2012) (Fig. 2.5A,C, and data not shown). The presence of rods in *clo* mutants appeared greatly reduced, with most

clo-/- samples showing only a small patch of rods ventral to the optic nerve (Fig.

2.5B), and significantly fewer 1D1+ rods dorsal to the optic nerve (Fig. 2.5E). Staining

with ZPR1 (Fig. 2.5D) and peanut lectin (data not shown) was also reduced in *clo*

mutants as compared with their wildtype siblings, but still showed a sporadic

distribution of irregularly-shaped ZPR1+ cones in regions dorsal to the ventral patch

(Fig. 2.5D). We scored patterns of ZPR1 staining to quantify the extent of cell staining

(none, few, or many ZPR1+ cells) and the distribution of stained cells (sporadic,

discontinuous, or dense within the ONL) (see Methods and (Kashyap et al., 2011)). In

clo-/- embryos, both the extent of staining (Fig. 2.5F) and the distribution of stained

cells (Fig. 2.5F`) were significantly different from those of wildtype siblings (p<0.001

for each comparison).

　　　In summary, the differentiation of specific retinal neuronal cell types was

reduced or irregular, and the organization of retinal layers was abnormal in *clo*

mutants, suggesting that the early ocular vasculature, or the *clo* gene product more

directly, may have a regulatory role in retinal patterning, as well as in lens

development (Goishi et al., 2006). These defects were not limited to the cell type

(RGCs) normally in closest proximity to the hyaloid vasculature.

Reduced differentiation of Müller glia, and reduced numbers of microglia in clo

mutants

　　　We next evaluated the presence and differentiation of two non-neuronal

components of the retina, Müller glia and microglia. Müller glia were selected for

evaluation because they must interact with the developing vasculature as they

mature and develop their proximal endfeet (Alvarez et al., 2007), and in *clo* mutant

eyes such interactions would not be possible. Using anti-glial fibrillary acidic protein (GFAP) antibody (ZRF1) and cryosections obtained from 72 hpf wildtype embryos, we detected radial arrays of Müller glia, with prominent endfeet at the vitreal surface of the developing retina (Fig. 2.6A). In contrast, cryosections obtained from *clo-/-* embryos showed greatly reduced GFAP immunoreactivity, as well as disorganized patterns of staining (Fig. 2.6B, C). In some mutants, the few GFAP+ profiles that were present appeared most prominent at the vitreal surface, where Müller glia would normally establish endfeet, but with little staining elsewhere (Fig. 2.6C), suggesting abnormal glial morphology and/or abnormal targeting of glial cytoskeletal proteins. Interestingly, many of the *clo* mutant brains displayed prominent GFAP staining, and radially organized glial processes (Fig. 2.6B, C). These results indicate significant and potentially retina-selective defects in Müller glial differentiation in *clo* mutants.

We also evaluated retinal microglia, because, to our knowledge, their presence in *clo* mutants has not been ascertained, although the hematopoietic lineages that require a functional *cloche* gene include the myeloid lineage (Lyons et al., 2001), which is known to give rise to microglial progenitors (Greter and Merad, 2013). Mature microglia were detected using the 4C4 antibody (Nelson et al., 2013). In wildtype retinas processed at 72 hpf, microglia were found sporadically, and generally in clusters, with wide variability in their presence vs. absence in any particular section (Fig. 2.6D). We therefore processed 10-30 sections of five embryos of each genotype to analyze the amount and distribution of microglia. This analysis suggested that *clo* mutant retinas also harbored microglia, which were distributed sporadically and also found in clusters (Fig. 2.6E). However, a significantly smaller

proportion of cryosections derived from *clo-/-* eyes contained microglia as compared with wildtype (p<0.0001; Fisher exact test; Fig. 2.6F). These results suggest that microglia are present within the *clo-/-* retina, but in reduced numbers. Because 4C4 antibody detects only mature microglia, we next tested whether phagocytic microglial progenitors invaded the retina in high numbers, using the uptake of neutral red dye (49-53 hpf) to label this cell population (Herbomel et al., 2001). Both wildtype and *clo-/-* retinas showed neutral red+ cells and/or clusters of cells (Fig. 2.6G,H). We quantified the percentage of each embryonic retina that was covered with neutral red+ profiles, by tracing stained cells in flattened projections of focal planes that contained neutral red+ cells (Fig. 2.6G', H'). The "percent coverage" of the retina by neutral red+ cells in *clo-/-* embryos was not significantly different from that in their wildtype siblings (Fig.2.6I). Collectively these results suggest that in *clo-/-*, microglial progenitors invade the retina in numbers similar to those in wildtype embryos, but then many of these progenitors fail to either mature, and/or proliferate, and/or survive, resulting in highly reduced numbers of mature microglia in *clo-/-* retinas at 72 hpf.

Irregular expression patterns of specific retinal transcription factors in clo mutants

The generation and differentiation of retinal neurons requires coordinated expression of specific retinal transcription factors (Kay et al., 2001; Macdonald et al., 1995; Nelson et al., 2008; Nelson et al., 2009; Ochocinska and Hitchcock, 2009). We therefore examined expression of transcription factors that are required for normal neurogenesis and differentiation of retinal cell types. Expression of *atoh7* (*ath5*) is required for RGC neurogenesis (Kay et al., 2001), and in wildtype embryos a wave of

atoh7 expression is propagated through the retinal neuroepithelium from 25 to 36 hpf (Masai et al., 2000) (Fig. 2.7A). *clo* mutants processed at 30 hpf showed a pattern of *atoh7* expression similar to that of wildtype siblings (Fig. 2.7B), suggesting that abnormal *atoh7* expression is not likely involved in generating the retinal phenotype of *clo-/-*. Expression of *six3b*, which encodes a transcription factor that is expressed in proliferating eye progenitors at 30 hpf was also normal in *clo* mutants (data not shown).

The transcription factor Pax6 is essential for eye development and is expressed in retinal progenitors during progenitor proliferation, and then during retinal neurogenesis becomes restricted to RGCs and amacrine cells (Hitchcock et al., 1996; Macdonald et al., 1995), and the circumferential germinal zone (CGZ) (Raymond et al., 2006) (Fig. 2.7C,E). In *clo* mutant retinas, *pax6a* expression appeared normal in distribution and was present throughout the retinal neuroepithelium at 30 hpf (Fig. 2.7D). However, at 49 hpf, *pax6a* expression was highly unusual in that it was not restricted to the emerging RGC and INL (Fig. 2.7F). In addition, the hybridization signals appeared weak and patchy in distribution (Fig. 2.7F). Hence, it is possible that the abnormal distribution of *pax6* expression, at least in part, underlies the disorganized phenotype of *clo-/-* retinas, and may reflect earlier events in retinal development that lead to this abnormal expression.

Because we observed impaired photoreceptor differentiation and patterning in *clo* mutants, we next examined expression of several transcription factors involved in photoreceptor development. *neurod1* regulates retinal progenitor cell proliferation and promotes the generation of photoreceptors (Ochocinska and Hitchcock, 2009).

At 49 hpf, *neurod1* is expressed throughout the emerging ONL, and in cells organized in loose patches in the INL and occasionally in the GCL (Fig. 2.7G); some of the INL cells are those of the dedicated lineage that gives rise to rod photoreceptors (Nelson et al., 2008; Ochocinska and Hitchcock, 2007). The *clo-/-* retinas displayed a similar overall pattern of *neurod1* expression, but the ONL showed occasional gaps in labeling and reduced intensity of staining, and far fewer cells in the INL appeared to be labeled (Fig. 2.7H). Expression of *rx1* (*rax*) is required for retinal neurogenesis and for photoreceptor differentiation (Nelson et al., 2009). At 30 hpf, *rx1* is expressed throughout the retinal neuroepithelium (Chuang et al., 1999; Nelson et al., 2009), and we observed this expression pattern in *clo-/-* and wildtype retinas (data not shown). At 54 hpf, *rx1* is expressed in the CGZ, and weakly in the emerging ONL of wildtype retinas (Fig. 2.7I). A similar *rx1* expression pattern was observed in *clo* mutant retinas (Fig. 2.7J). Finally, we analyzed expression of *crx* mRNA, which encodes a transcription factor that activates numerous photoreceptor-specific genes (Chen et al., 1997). In wildtype zebrafish embryos, this gene is expressed in the ONL as well as in the outer INL (Liu et al., 2001) (Fig. 2.7K); some of these *crx+* cells of the INL are of the rod lineage (Nelson et al., 2008). In *clo* mutant embryos, a similar pattern was observed, although occasionally cells of the ONL showed gaps in *crx* expression (Fig. 2.7L).

In summary, expression patterns of critical retinal transcription factors appeared normal in *clo* mutant embryos during the early waves of retinal neurogenesis, around 30 hpf. However, domains of some specific transcription

factors, particularly *pax6*, *neurod1*, and to a lesser extent *crx*, appeared mispatterned and/or weaker in expression as the ONL becomes established.

Abnormal retinal phenotype and ectopic cones in clo mutants when cell death is blocked

We considered that some of the features of the retinal phenotype in *clo-/-* may be secondary to retinal cell death, particularly because of the significantly higher rate of cell death at a developmental time (54-72 hpf) when some cell types are still being generated and then are differentiating (Hu and Easter, 1999). Therefore we evaluated retinal histology in *clo-/-* embryos in which cell death mediated by the tumor suppressor p53 was blocked through the use of a *p53*-targeting antisense morpholino oligonucleotide (MO-*tp53*; (Plaster et al., 2006)). The *clo-/-*, *p53*-morphant retinas showed virtually no gaps in the retinal tissue, and visibly fewer pyknotic cell bodies as compared to *clo-/-* retinas (Fig. 2.8A-C), indicating that the MO-*tp53* was effective at blocking much of the retinal cell death. However, *clo-/-*; *p53*-morphant retinas still showed thinned or disorganized plexiform layers, and nuclear layers that were reduced in thickness and disorganized as compared to wildtype retinas (Fig. 2.8A-C), suggesting that these aspects of the *clo-/-* retinal phenotype are not likely related to retinal cell death. Interestingly, the lens phenotype of *clo* mutants was partially rescued in the *p53* morphants; the tissue gaps between the lens epithelium and developing lens fibers were not evident, but the concentric lens fibers themselves did not appear to be differentiated and still contained nuclei (Fig. 2.8A-C). These findings collectively suggest that retinal and lens abnormalities

in *clo* mutant zebrafish are not solely related to an increased rate of p53-mediated cell death.

Cone photoreceptors and Müller glia were specifically evaluated in *clo-/-;p53* morphants by immunostaining with ZPR1 (Fig. 2.8D-E) and ZRF1 (Fig. 2.8H-J) antibodies, respectively. In many cases, cones in *clo-/-;p53* morphants appeared to remain patchy and irregular in distribution, and reduced in number as compared to wildtype cones. Quantification using the cone distribution categories revealed no significant rescue of the extent of ZPR1 labeling (p=0.11), but a significant rescue of the ZPR1 pattern (p<0.05), such that many of the *clo-/-;p53* morphants displayed dense or discontinuous labeling patterns rather than sporadic patterns (Fig. 2.8G). Interestingly, the *clo-/-;p53* morphants also showed ectopic ZPR1+ cells within the INL (Fig. 2.8F) (71% of morphants; n=14), suggesting that *clo-/-* retinas may develop ectopic cones that die when p53-mediated cell death is permitted. Müller glia in *clo-/-;p53* morphants did not appear to be rescued in morphology or in apparent number as compared with the *clo-/-* Müller glia (Fig. 2.8H-J, also see Fig. 2.6B,C). The *clo-/-* Müller glial phenotype is therefore not related to p53-mediated cell death.

No evidence of hypoxia in clo mutant retinas

The absence of a cardiovascular system in *cloche* mutant zebrafish embryos may underlie the abnormal development of the retina and lens. Potential mechanisms include lack of critical (paracrine) factor(s) provided by endothelial cells, and/or lack of critical endocrine or other factor(s) delivered by the circulating blood. The absence of circulating oxygen (O_2) is an unlikely explanation, as zebrafish tissues are not dependent upon the circulation for oxygen until larval stage [6

dpf;(Pelster and Burggren, 1996)]. However, to confirm whether the absence of

circulating O_2 contributed to the eye phenotype, we performed *in situ* hybridizations

for the presence of *phd3* mRNA. The *phd3/egln3* gene encodes prolyl hydroxylase

domain containing protein 3/egl-9 family hypoxia-inducible factor 3, a cellular oxygen

sensor that regulates the response to hypoxia and that is transcriptionally

upregulated by hypoxia (Santhakumar et al., 2012). Cryosections derived from *clo-/-*

mutants or wildtype embryos showed no positive hybridization signals (Fig. 2.9A,C),

while those derived from wildtype embryos subjected to 90 minutes of hypoxia and

then processed in parallel with the remaining samples, showed *phd3* hybridization

signal in retinal cells (Fig. 2.9B). These results suggest that tissues of *clo* mutants are

not hypoxic, and hence the eye phenotype of *clo-/-* embryos is not the consequence

of hypoxia.

Discussion**:**

        The major findings of this study can be summarized as follows: 1. The

embryonic *clo-/-* eye lacks vasculature and is microphthalmic, with defects in cell

proliferation and survival, and in the generation and patterning of specific retinal cell

types. 2. Retinal patterning defects in *clo-/-* embryos include unusual expression

patterns of key retinal transcription factors, abnormal morphology of Müller glia and of

synaptic layers, and ectopic cones that are revealed when cell death is blocked. 3.

Retinal defects in *clo-/-* embryos are not strictly related to cell death, or to retinal

hypoxia, or to the complete lack of microglia, and they are not secondary to lens

defects. Together these findings suggest a regulatory (non-metabolic) role for the

early ocular vasculature in regulating retinal neurogenesis and patterning.

Embryonic eyes of *cloche* mutants indeed showed a strikingly abnormal phenotype, distinct in many ways from other zebrafish microphthalmic phenotypes (Kashyap et al., 2007;Liu et al., 2007; Stenkamp et al., 2002). Defects in retinal cell proliferation and cell survival were accompanied by the presence of thinned and disorganized plexiform layers and mis-projected synaptic terminals, reduced and mispatterned retinal neurons, reduced and morphologically abnormal Müller glia, and disrupted expression of *pax6a* and *neuroD1.* This phenotype suggests roles for the ocular vasculature in regulating generation, survival, migration/patterning, and morphological differentiation of distinct classes of retinal cells. The distinctive nature of this phenotype is underscored by the observation that many of its features are unrelated to cell death. Blocking p53-mediated cell death in *clo-/-* embryos resulted in very little evidence of rescue other than the reduction of pyknotic (dying) cells. *clo-/- ;p53* morphants still showed microphthlamia, thinned and irregular retinal plexiform layers, and fewer and morphologically undifferentiated Müller glia. Blocking cell death also unmasked an additional phenotype, in the form of ectopic ZPR1+ cells in the INL. Together with the misregulation of expression of *pax6a* and *neuroD1* expression in the *clo-/-* retina, these results are consistent with ocular vasculature playing a role in regulating one or more of the following: radial migration of cone progenitors; radial positioning of cone precursors; onset of expression of cone markers in the cone lineage; and/or suppressing expression of photoreceptor antigens in inner retinal cells. Given the presence of laminar disruptions and the lack of radially organized Müller glia, a migration or positioning defect is the most parsimonious explanation. Resolution of these alternatives will benefit from live imaging of specific retinal cell

populations in the presence or absence of normal early ocular vasculature. It is possible that the hyaloid vasculature generates factors that provide apicobasal polarity information to the developing retina.

The *clo-/-* microphthalmic phenotype bears some resemblance to the retinal phenotype described for embryos in which migration of microglial precursors was inhibited by morpholino-mediated knockdown of expression of the *colony stimulating factor 1 receptor a* (*csf-1r*; *fms*) gene (Huang et al., 2012). Although numbers of mature microglia in *clo-/-* retina were severely reduced, it not likely that the unusual features of the *clo-/-* retina are solely due to this paucity of microglia. In the *csf-1r* morphant retinas, cell proliferation is increased rather than decreased, retinal layers are generated, but no neuronal cell types differentiate because cell cycle exit is impaired (Huang et al., 2012). These features are distinct from those we describe here for *clo-/-* retina. However, it is possible that the highly reduced number of microglia (as opposed to no microglia at all) may be involved in the generation of the *clo-/-* retinal phenotype. To resolve this question, we are developing alternative strategies to manipulate the early ocular vasculature without interfering with the development, migration, or maturation of microglia.

A previous report described lens defects in *clo-/-* embryos (both *m39* and *s5* alleles) (Goishi et al., 2006). These defects consisted of decreased synthesis of lens crystalline proteins beginning at 2.5 dpf, and ultimately resulting in the formation of cataracts (Goishi et al., 2006). The present study is consistent with this observation, and in addition we report cell-free gaps between the lens epithelium and the developing lens fibers (Fig. 2.1R), and reduced lens size/failed lens growth at 2 dpf
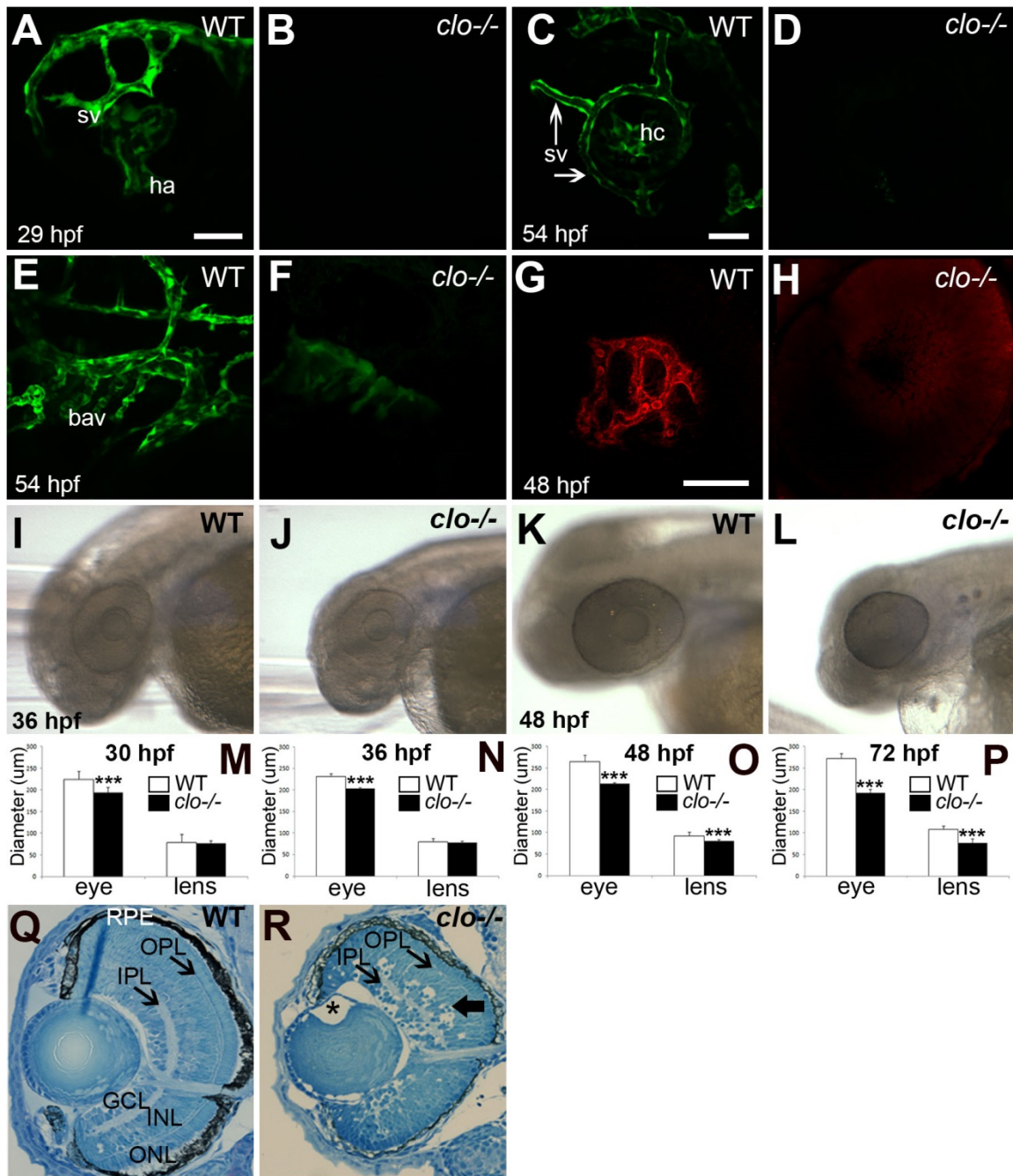
(Fig. 2.1O). These defects appear later than general microphthalmia (at 30 hpf; Fig. 2.1M), and instead appear at the same time as the earliest manifestations of a retinal phenotype (48-54 hpf), suggesting that retinal defects are likely not secondary to lens defects.

The distinctive and disorganized retinal phenotype of the *clo-/-* embryo offers initial insights into roles for the vasculature in regulating retinal development – roles that are not related to tissue oxygenation. The pursuit of developmental vascular-retinal interactions may further reveal regulatory mechanisms important for understanding the neural progenitor niche and the progression of retinal disorders that involve the vasculature.

Acknowledgments**:**

Figures

- A: WT, sv, ha, 29 hpf
- B: clo-/-
- C: WT, sv, hc, 54 hpf
- D: clo-/-
- E: WT, bav, 54 hpf
- F: clo-/-
- G: WT, 48 hpf
- H: clo-/-
- I: WT, 36 hpf
- J: clo-/-
- K: WT, 48 hpf
- L: clo-/-
- M: 30 hpf, Diameter (um), WT, clo-/-, ***, eye, lens
- N: 36 hpf, Diameter (um), WT, clo-/-, ***, eye, lens
- O: 48 hpf, Diameter (um), WT, clo-/-, ***, ***, eye, lens
- P: 72 hpf, Diameter (um), WT, clo-/-, ***, ***, eye, lens
- Q: WT, RPE, OPL, IPL, GCL, INL, ONL
- R: clo-/-, IPL, OPL, *

Figure 2.1. Ocular abnormalities in *cloche* mutant embryos. A.-F. Confocal images of *kdrl:EGFP* wildtype (A,C,E) and *clo-/-* (B,D,F) blood vessels (green). Hyaloid artery (ha) has invaded the eye and superficial vessels (sv) begin to form at 29 hpf in wildtype (A) but not *clo-/-* (B). Hyaloid capillaries (hc), and superficial vasculature (sv) have developed at 54 hpf in wildtype (C) but not *clo-/-* (D). Branchial arch vessels (bav) are present at 54 hpf in wildtype (E), and are strongly reduced in *clo-/-* (F). G-H. Confocal images of Fast Red staining of endogenous alkaline phosphatase; focal plane of hyaloid capillaries, which are present in wildtype (G) but not *clo-/-* (H). I-L. Live, wildtype (I, K) and *clo-/-* (J,L) embryos imaged at 36 hpf (I,J) and 48 hpf (K,L). M-P. Eye diameters and lens diameters of wildtype and *clo-/-* embryos at 30 (M), 36 (N), 48 (O) and 72 (P) hpf; ***, $p < 0.001$. Q-R. Histology of wildtype (Q) and *clo-/-* (R) eyes at 72 hpf; GCL, ganglion cell layer; INL, inner nuclear layer; ONL, outer nuclear layer; IPL, inner plexiform layer; OPL, outer plexiform layer; RPE, retinal pigmented epithelium. In R, asterisk (*) denotes gap between lens epithelium and developing lens fibers; wide arrow points to pyknotic cells in INL. Scale bars = 50 µm (in A, applies to A,B; in C, applies to C-F and Q-R; in G, applies to G,H).
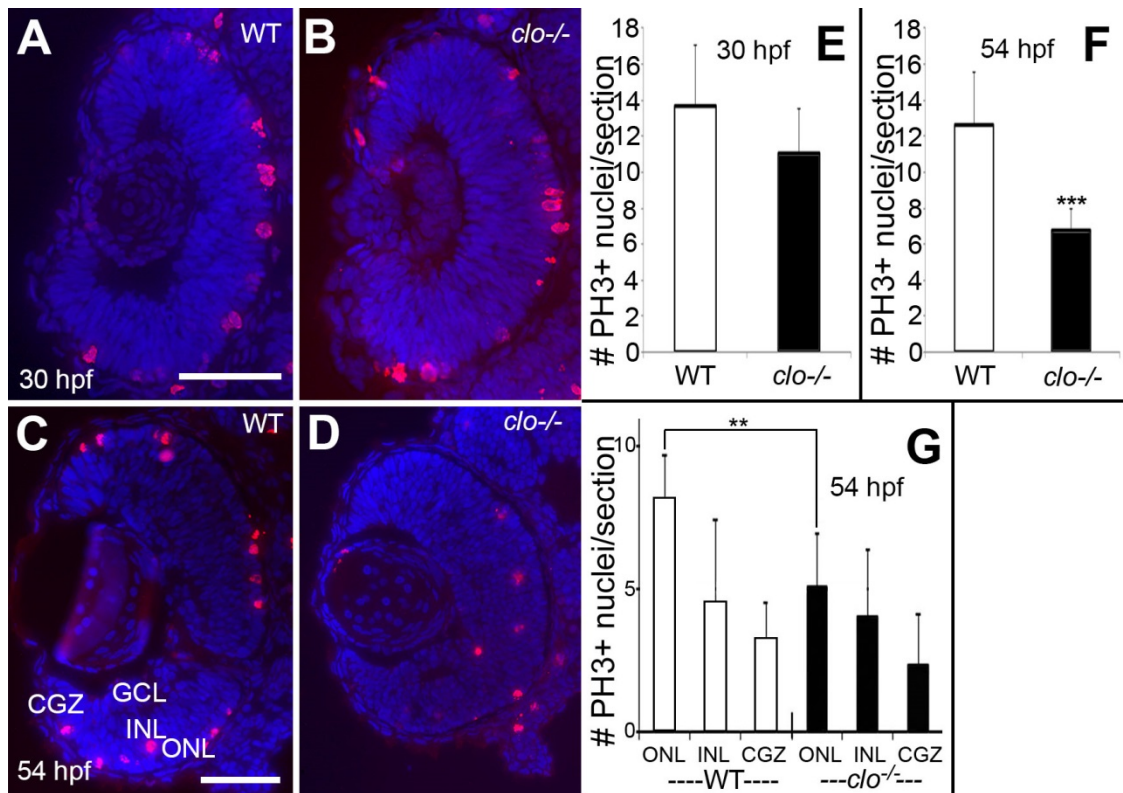
Figure 2.2. Reduced retinal progenitor proliferation at 54 hpf but not 30 hpf in
cloche **mutant embryos**. A-D. Immunofluorescence images of wildtype (A,C) and
clo-/- (B,D) retinas stained with anti-phosphohistone 3 (PH3) and counterstained with
DAPI (blue); samples obtained at 30 hpf (A,B) and 54 hpf (C,D). E-G. Numbers of
PH3+ nuclei/section are not significantly different in *clo-/-* vs. wildtype retinas at 30
hpf (E), but are significantly different at 54 hpf (F; p<0.001); these differences are
most evident in the outer nuclear layer (G; ONL; p<0.001), but not in the inner
nuclear layer (INL) or circumferential germinal zone (CGZ). Scale bars = 50 µm (A
applies to A,B; C applies to C,D).
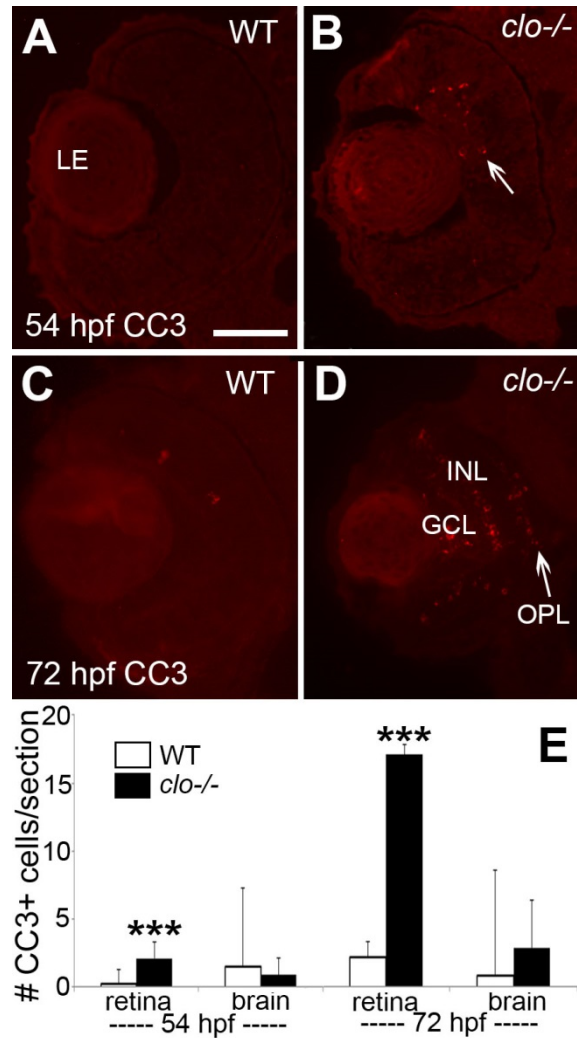
Figure 2.3. Increased retinal cell death during late retinal neurogenesis in

cloche **mutant embryos.** A-D. Immunofluorescence images of wildtype (A,C) and

clo-/- (B, D) retinas stained with anti-cleaved caspase 3 (CC3); samples obtained at

54 hpf (A,B) and 72 hpf (C,D). Arrow in B indicates examples of CC3+ cells. E.

Numbers of CC3+ cells are significantly (***; p<0.001) increased in *clo-/-* retinas at 54

hpf and 72 hpf, but not in *clo-/-* brains. Bar in A (applies to all images) = 50 µm; LE,

lens; GCL, ganglion cell layer; INL, inner nuclear layer; OPL, outer plexiform layer
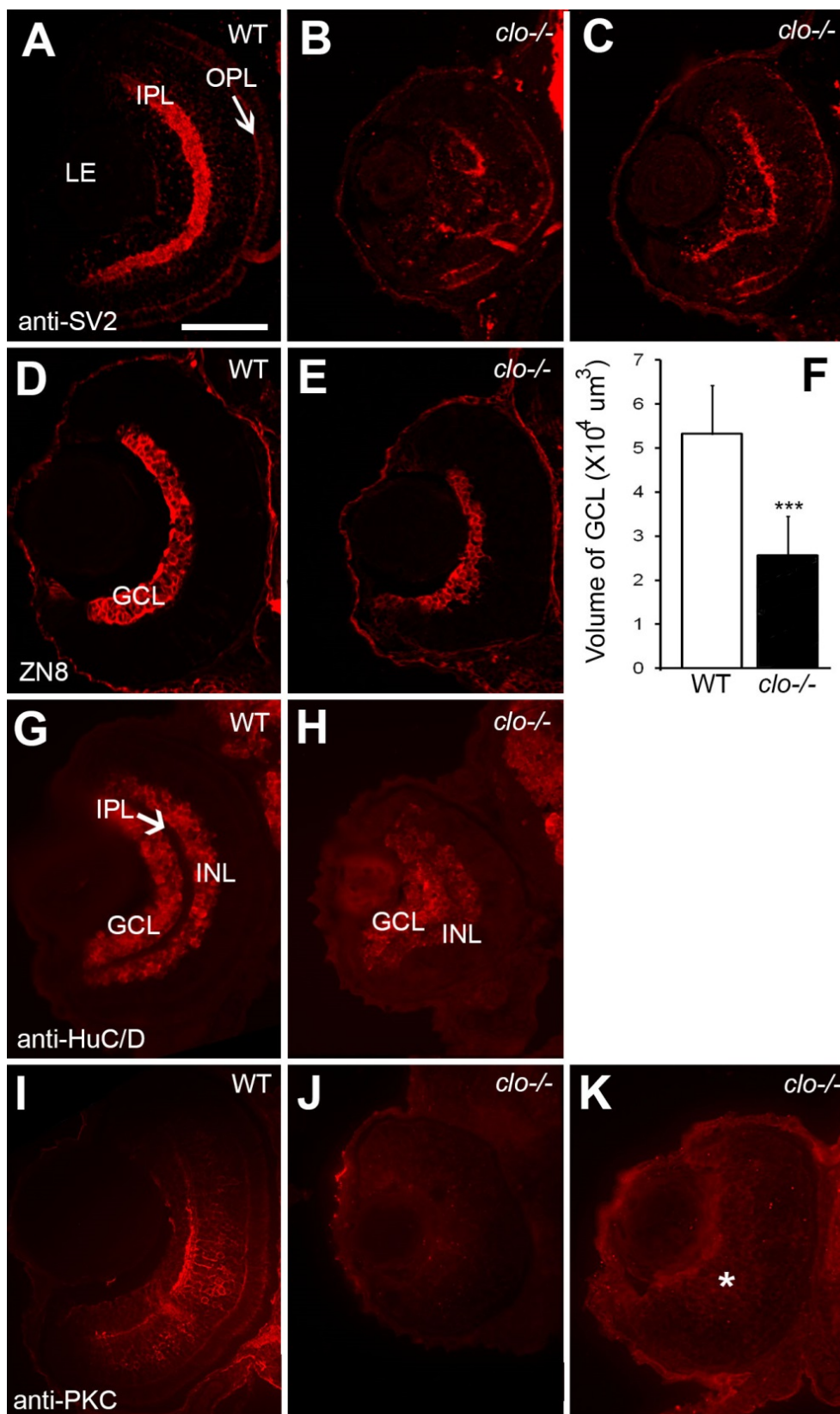
Figure 2.4. Abnormal differentiation of specific inner retinal neurons in *cloche*

mutant embryos. A.-C. Immunofluorescence images of 72 hpf retinas of wildtype (A)

and *clo-/-* (B,C) embryos stained for synaptic vesicle 2 (SV2). D,E.

Immunofluorescence images of 72 hpf retinas of wildtype (D) and *clo-/-* (E) embryos

stained with the ZN8 antibody, detecting retinal ganglion cells. F. Volume of GCL is

significantly (***, $p < 0.001$) reduced in *clo-/-* retinas. G-H. Immunofluorescence

images of 72 hpf retinas of wildtype (G) and *clo-/-* (H) embryos stained with an

antibody detecting HuC/D, present in ganglion cells and amacrine cells. I-K.

Immunofluorescence images of 72 hpf retinas of wildtype (I) and *clo-/-* (J,K) embryos

stained with an antibody detecting PKCα, specific to bipolar cells. * in K indicates

diffuse staining of material lacking typical bipolar cell morphology. Scale bar in A

(applies to all images) = 50 µm. LE, lens; IPL, inner plexiform layer; OPL, outer

plexiform layer; GCL, ganglion cell layer; INL, inner nuclear layer.
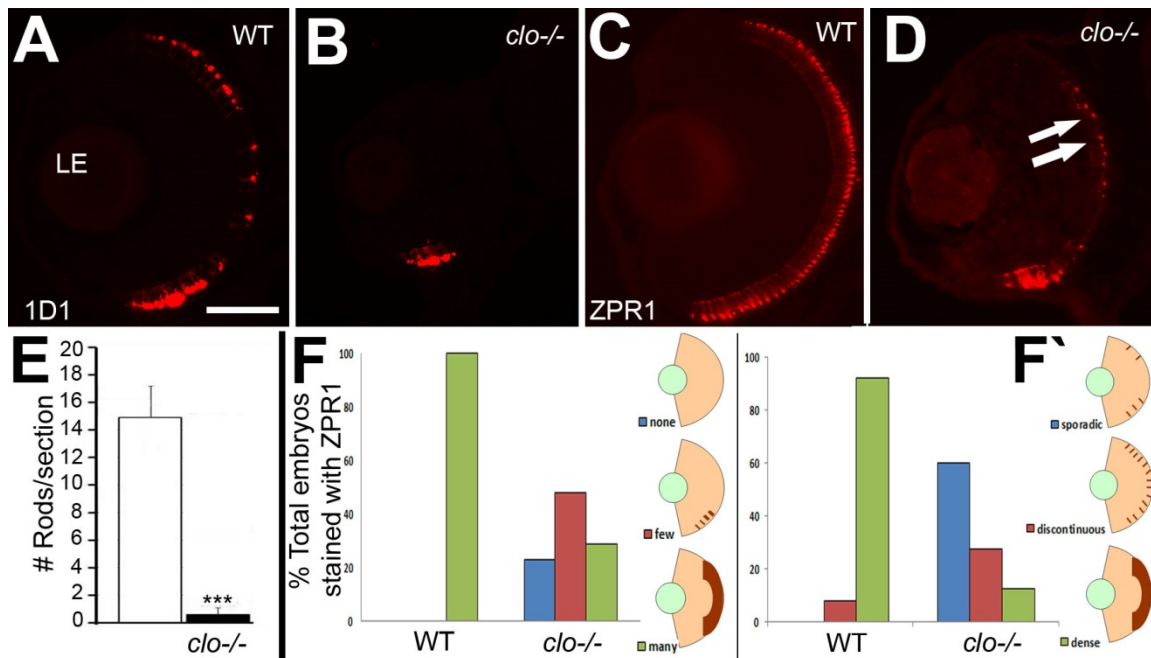
Figure 2.5. Reduced and mispatterned differentiation of photoreceptors in

cloche **mutant embryos.** A-B**.** Immunofluorescence images of 72 hpf retinas of

wildtype (A) and *clo-/-* (B) embryos stained with the 1D1 antibody, detecting rod

photoreceptors. C-D. Immunofluorescence images of 72 hpf retinas of wildtype (D)

and *clo-/-* (E) embryos stained with the ZPR1 antibody, detecting cone

photoreceptors. Arrows in D show developing cones flanking a region of the ONL that

is not ZPR1+. E. Numbers of 1D1+ cells are significantly (***, p<0.001) reduced in

clo-/- retinas. F. The extent of ZPR1 labeling (F) and the distribution of ZPR1+ cells

(F`) is also significantly different in *clo-/-* retinas as compared to wildtype (p<<0.001).

LE, lens. Scale bar in A (applies to all images) = 50 μm.

A **WT** — r, b, LE, *, ZRF1, 72hpf
B **clo-/-** — *
C **clo-/-** — *
D **WT** — 4C4, 72hpf
E **clo-/-**
F — % sections with microglia; WT, clo-/-; ***
G **WT** — NR, 53hpf
H **clo-/-**
G` H`
I — % retinal coverage by NR+ cells; WT, clo-/-

Figure 2.6. Abnormal differentiation of Müller glia, and reduced microglia in

***cloche* mutant embryos.** A-C. Immunofluorescence images of 72 hpf retinas of

wildtype (A) and *clo-/-* (B,C) embryos stained with the ZRF1 antibody detecting

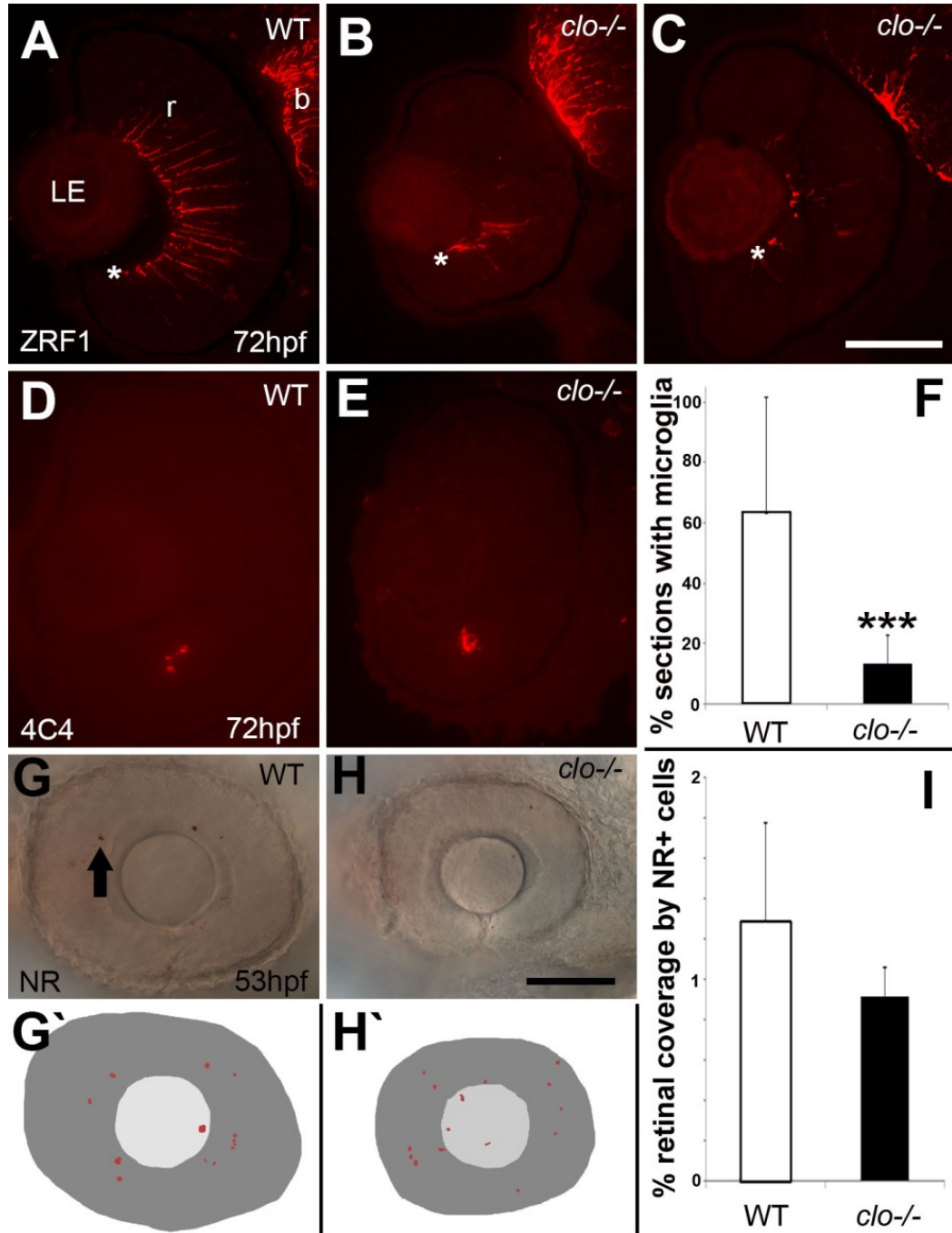GFAP, specific to Müller glia. * indicates vitreal surface of retina (r), where Müller glia

establish endfeet. b, brain. D-E. Immunofluorescence images of 72 hpf retinas of

wildtype (D) and *clo-/-* (E) embryos stained with the 4C4 antibody that labels

microglia. F. The % of cryosections per eye that contained microglia was significantly

reduced in *clo-/-* embryos as compared with wildtype embryos (***, $p<0.0001$). G-H.

Neutral red uptake in retinal cells of wildtype (G) and *clo-/-* (H) embryos from 49 to 53

hpf. G`-H`. Tracings of flattened projections of neutral red (NR) stained wildtype (G`)

and *clo-/-* (H`) eyes; arrow in G shows an NR+ cell. I. Percent retinal coverage by

neutral red+ profiles. LE, lens. Scale bar in C (applies to A-E) = 50 µm; scale bar in H

(applies to G-H`) = 50 µm.

A WT 30 hpf *atoh7*
B *clo-/-*
C WT *pax6*
D *clo-/-*
E WT GCL INL 49 hpf *pax6*
F *clo-/-* *
G WT GCL INL ONL *NeuroD*
H *clo-/-*
I WT CGZ ONL 54 hpf *rx1*
J *clo-/-*
K WT INL ONL *crx*
L *clo-/-*
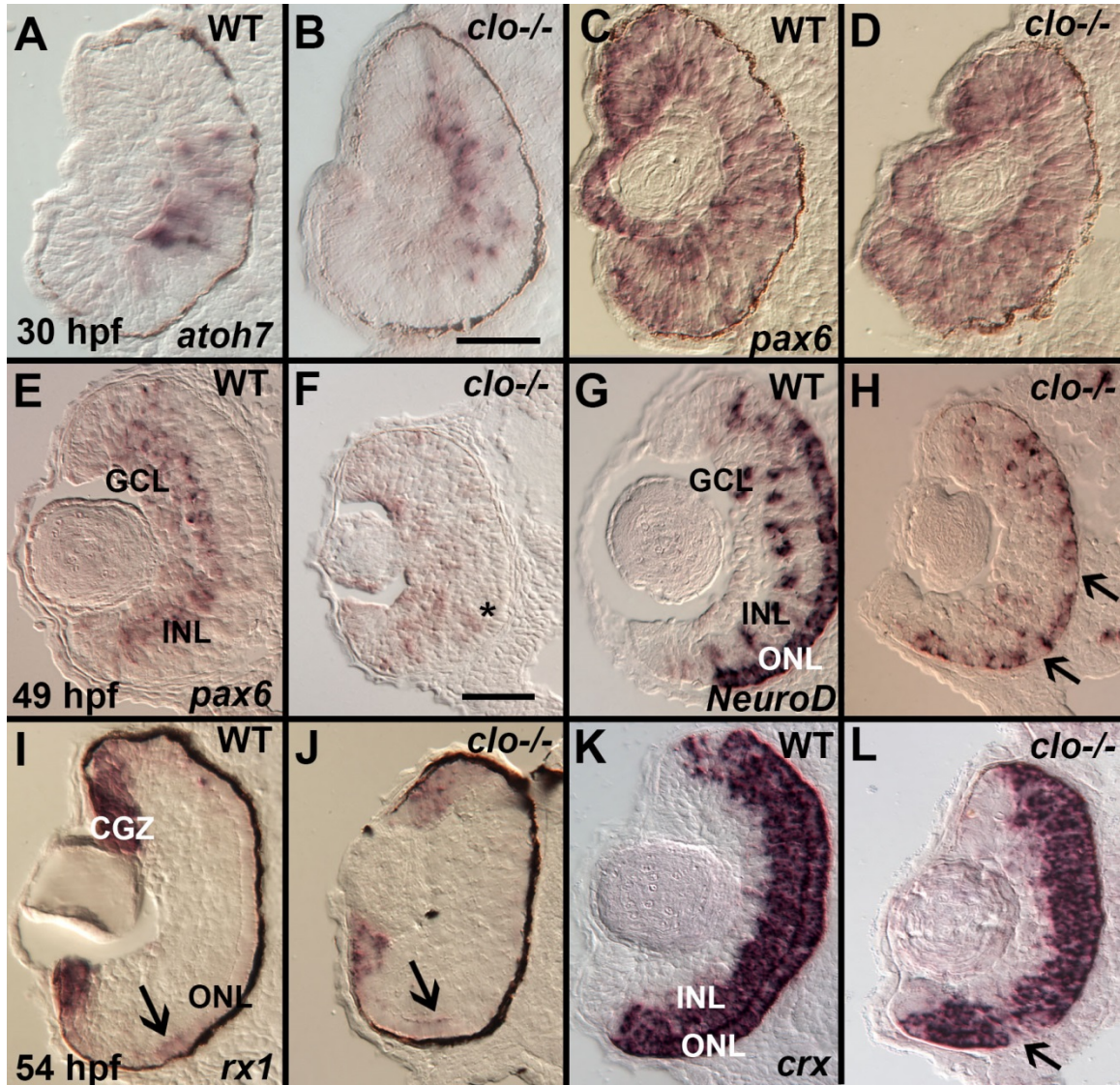
Figure 2.7. Irregular expression of specific retinal transcription factors in

***cloche* mutant embryos.** A.-D. At 30 hpf *atoh7/ath5* is expressed in a ventral cluster

of retinal progenitor cells in both wildtype (A) and *clo-/-* (B), and *pax6* is expressed in

all retinal progenitors in both wildtype (C) and *clo-/-* (D) embryos. E.-F. At 49 hpf *pax6*

is expressed in the ganglion cell layer (GCL) and inner half of the inner nuclear layer

(INL) of wildtype embryos (E), but is more diffusely distributed (such as in the cells

near the asterisk) and weakly expressed in *clo-/-* (F). G.-H. At 49 hpf, *NeuroD* is

expressed in the ONL, and in radial clusters of cells in the INL and occasionally the

GCL in wildtype (G), but is reduced in distribution in all of these locations in *clo-/-* (H),

resulting in patches of ONL lacking *NeuroD* (arrows). I.-J. At 54 hpf, *rx1* is expressed

in the circumferential germinal zone (CGZ) and weakly in the emerging outer nuclear

layer (ONL, arrows) in WT (I) and *clo-/-* (J); K.-L. At 54 hpf *crx* is expressed in the

ONL and the outer half of the INL in wildtype (K), and shows a similar distribution and

hybridization intensity in *clo-/-* (L), but with occasional patches of ONL lacking *crx*

expression (arrow). Scale bars = 50 µm (B, applies to A-D; F, applies to E-L).

Sections in panels E-H, and K-L were derived from embryos treated with PTU and so

do not have melanin pigment within the retinal pigmented epithelium.

A WT

B *clo-/-* uninj

C *lclo-/-* p53 MO

72 hpf

D WT

LE

ZPR1

E *clo-/-* uninj

F *clo-/-* p53 MO

G

% Total embryos stained with ZPR1

none
few
many

WT   *clo-/-*   *clo-/-*;p53MO

G`

sporadic
discontinuous
dense

WT   *clo-/-*   *clo-/-*;p53MO

H WT

ZRF1

I *clo-/-* uninj

J *clo-/-* p53 MO
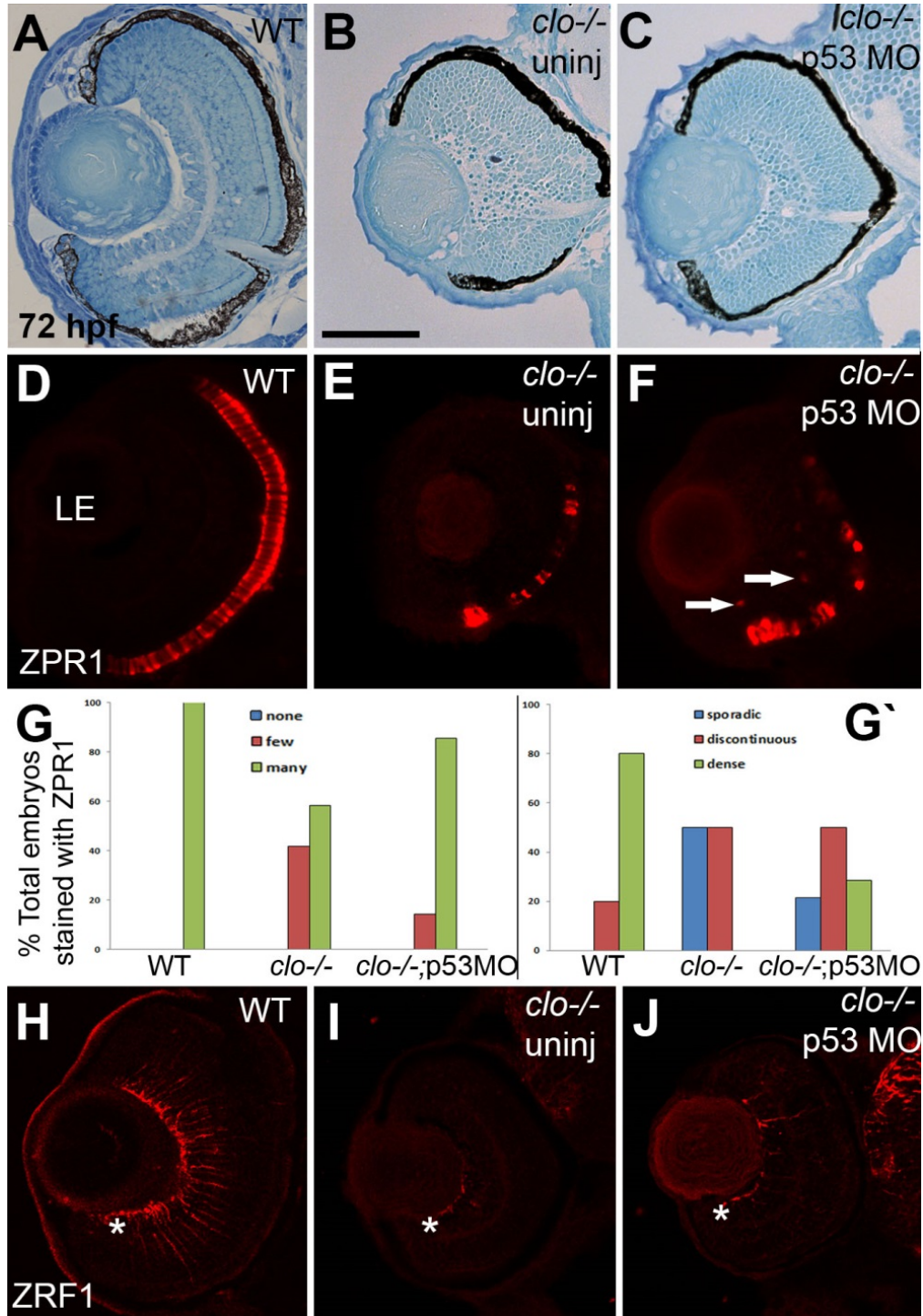
Figure 2.8. Partial rescue of *cloche* ocular phenotype by blocking cell death. A-

C. Eye histology of wildtype (A) and *clo-/-* (B) embryos at 72 hpf, and of *clo-/-*

embryos injected with a morpholino targeting p53 (p53 MO; C). D-F. ZPR1 (cone

photoreceptor) staining in wildtype (D), *clo-/-* (E), and *clo-/-* p53 morphants (F).

Arrows in F show ectopic ZPR1+ profiles. G. The extent of ZPR1 labeling (G) is not

significantly rescued in *clo-/-* p53 morphants (p=0.11), but the distribution of ZPR1+

cells (G`) is significantly different in *clo-/-* morphant retinas as compared to *clo-/-*

(p<0.03). H-J. ZRF1 (Müller glia) staining in wildtype (H), *clo-/-* (I), and *clo-/-*p53

morphants (J), showing no rescue of the presence or morphology of Műller glia (*

asterisks denotes normal location of endfeet). LE, lens. Scale bar in B (applies to all

images) = 50 µm.
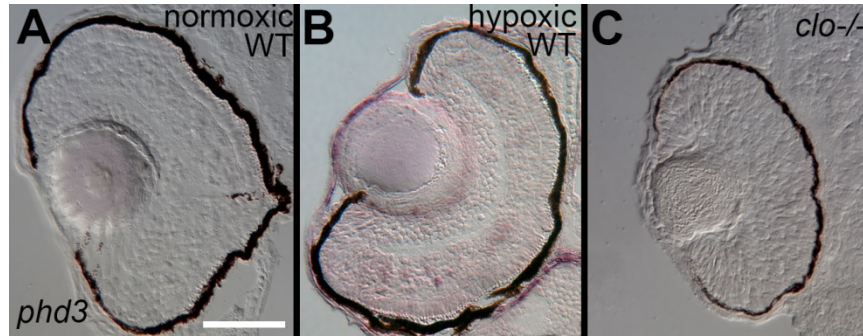
Figure 2.9. No evidence for hypoxia in *cloche* mutant retinas. A-C. *In situ* hybridization for *phd3* mRNA in wildtype normoxic embryos (A), wildtype hypoxic embryos showing positive hybridization signals (B), and *clo-/-* embryos. Scale bar in A (applies to all) = 50 μm.

References

Aizawa, Y., Shoichet, M.S., 2012. The role of endothelial cells in the retinal stem and progenitor cell niche within a 3D engineered hydrogel matrix. Biomaterials 33, 5198-5205.

Alvarez, Y., Cederlund, M.L., Cottell, D.C., Bill, B.R., Ekker, S.C., Torres-Vazquez, J., Weinstein, B.M., Hyde, D.R., Vihtelic, T.S., Kennedy, B.N., 2007. Genetic determinants of hyaloid and retinal vasculature in zebrafish. BMC developmental biology 7, 114.

Barthel, L.K., Raymond, P.A., 1990. Improved method for obtaining 3-microns cryosections for immunocytochemistry. The journal of histochemistry and cytochemistry : official journal of the Histochemistry Society 38, 1383-1388.

Chen, S., Wang, Q.L., Nie, Z., Sun, H., Lennon, G., Copeland, N.G., Gilbert, D.J., Jenkins, N.A., Zack, D.J., 1997. Crx, a novel Otx-like paired-homeodomain protein, binds to and transactivates photoreceptor cell-specific genes. Neuron 19, 1017-1030.

Chuang, J.C., Mathers, P.H., Raymond, P.A., 1999. Expression of three Rx homeobox genes in embryonic and adult zebrafish. Mechanisms of development 84, 195-198.

Covassin, L.D., Siekmann, A.F., Kacergis, M.C., Laver, E., Moore, J.C., Villefranc, J.A., Weinstein, B.M., Lawson, N.D., 2009. A genetic screen for vascular mutants in zebrafish reveals dynamic roles for Vegf/Plcg1 signaling during artery development. Developmental biology 329, 212-226.

Easter, S.S., Jr., Nicola, G.N., 1996. The development of vision in the zebrafish (Danio rerio). Developmental biology 180, 646-663.

Fadool, J.M., 2003. Development of a rod photoreceptor mosaic revealed in transgenic zebrafish. Developmental biology 258, 277-290.

Garlipp, M.A., Nowak, K.R., Gonzalez-Fernandez, F., 2012. Cone outer segment extracellular matrix as binding domain for interphotoreceptor retinoid-binding protein. The Journal of comparative neurology 520, 756-769.

Goishi, K., Shimizu, A., Najarro, G., Watanabe, S., Rogers, R., Zon, L.I., Klagsbrun, M., 2006. AlphaA-crystallin expression prevents gamma-crystallin insolubility and cataract formation in the zebrafish *cloche* mutant lens. Development (Cambridge, England) 133, 2585-2593.

Greter, M., Merad, M., 2013. Regulation of microglia development and homeostasis. Glia 61, 121-127.

Hartnett, M.E., 2015. Pathophysiology and mechanisms of severe retinopathy of prematurity. Ophthalmology 122, 200-210.

Hartsock, A., Lee, C., Arnold, V., Gross, J.M., 2014. In vivo analysis of hyaloid vasculature morphogenesis in zebrafish: A role for the lens in maturation and maintenance of the hyaloid. Developmental biology 394, 327-339.

Herbomel, P., Thisse, B., Thisse, C., 2001. Zebrafish early macrophages colonize cephalic mesenchyme and developing brain, retina, and epidermis through a M-CSF receptor-dependent invasive process. Developmental biology 238, 274-288.

Hitchcock, P.F., Macdonald, R.E., VanDeRyt, J.T., Wilson, S.W., 1996. Antibodies against Pax6 immunostain amacrine and ganglion cells and neuronal progenitors, but not rod precursors, in the normal and regenerating retina of the goldfish. Journal of neurobiology 29, 399-413.

Hu, M., Easter, S.S., 1999. Retinal neurogenesis: the formation of the initial central patch of postmitotic cells. Developmental biology 207, 309-321.

Huang, T., Cui, J., Li, L., Hitchcock, P.F., Li, Y., 2012. The role of microglia in the neurogenesis of zebrafish retina. Biochemical and biophysical research communications 421, 214-220.

Humphrey, C.D., Pittman, F.E., 1974. A simple methylene blue-azure II-basic fuchsin stain for epoxy-embedded tissue sections. Stain technology 49, 9-14.

Jin, S.W., Beis, D., Mitchell, T., Chen, J.N., Stainier, D.Y., 2005. Cellular and molecular analyses of vascular tube and lumen formation in zebrafish. Development (Cambridge, England) 132, 5199-5209.

Kashyap, B., Frederickson, L.C., Stenkamp, D.L., 2007. Mechanisms for persistent microphthalmia following ethanol exposure during retinal neurogenesis in zebrafish embryos. Visual neuroscience 24, 409-421.

Kashyap, B., Frey, R.A., Stenkamp, D.L., 2011. Ethanol-induced microphthalmia is not mediated by changes in retinoic acid or sonic hedgehog signaling during retinal neurogenesis. Alcoholism, clinical and experimental research 35, 1644-1661.

Kay, J.N., Finger-Baier, K.C., Roeser, T., Staub, W., Baier, H., 2001. Retinal ganglion cell genesis requires lakritz, a Zebrafish atonal Homolog. Neuron 30, 725-736.

Kitambi, S.S., McCulloch, K.J., Peterson, R.T., Malicki, J.J., 2009. Small molecule screen for compounds that affect vascular development in the zebrafish retina. Mechanisms of development 126, 464-477.

Larison, K.D., Bremiller, R., 1990. Early onset of phenotype and cell patterning in the embryonic zebrafish retina. Development (Cambridge, England) 109, 567-576.

Lawson, N.D., Weinstein, B.M., 2002. In vivo imaging of embryonic vascular development using transgenic zebrafish. Developmental biology 248, 307-318.

Liao, W., Bisgrove, B.W., Sawyer, H., Hug, B., Bell, B., Peters, K., Grunwald, D.J., Stainier, D.Y., 1997. The zebrafish gene *cloche* acts upstream of a flk-1 homologue to regulate endothelial cell differentiation. Development (Cambridge, England) 124, 381-389.

Liu, Q., Frey, R.A., Babb-Clendenon, S.G., Liu, B., Francl, J., Wilson, A.L., Marrs, J.A., Stenkamp, D.L., 2007. Differential expression of photoreceptor-specific genes in the retina of a zebrafish cadherin2 mutant glass onion and zebrafish cadherin4 morphants. Experimental eye research 84, 163-175.

Liu, Y., Shen, Y., Rest, J.S., Raymond, P.A., Zack, D.J., 2001. Isolation and characterization of a zebrafish homologue of the cone rod homeobox gene. Investigative ophthalmology & visual science 42, 481-487.

Lyons, S.E., Shue, B.C., Oates, A.C., Zon, L.I., Liu, P.P., 2001. A novel myeloid-restricted zebrafish CCAAT/enhancer-binding protein with a potent transcriptional activation domain. Blood 97, 2611-2617.

Ma, N., Huang, Z., Chen, X., He, F., Wang, K., Liu, W., Zhao, L., Xu, X., Liao, W., Ruan, H., Luo, S., Zhang, W., 2011. Characterization of a weak allele of zebrafish *cloche* mutant. PloS one 6, e27540.

Macdonald, R., Barth, K.A., Xu, Q., Holder, N., Mikkola, I., Wilson, S.W., 1995. Midline signalling is required for Pax gene regulation and patterning of the eyes. Development (Cambridge, England) 121, 3267-3278.

Marcus, R.C., Easter, S.S., Jr., 1995. Expression of glial fibrillary acidic protein and its relation to tract formation in embryonic zebrafish (Danio rerio). The Journal of comparative neurology 359, 365-381.

Masai, I., Stemple, D.L., Okamoto, H., Wilson, S.W., 2000. Midline signals regulate retinal neurogenesis in zebrafish. Neuron 27, 251-263.

Nasevicius, A., Larson, J., Ekker, S.C., 2000. Distinct requirements for zebrafish angiogenesis revealed by a VEGF-A morphant. Yeast (Chichester, England) 17, 294-301.

Nelson, C.M., Ackerman, K.M., O'Hayer, P., Bailey, T.J., Gorsuch, R.A., Hyde, D.R., 2013. Tumor necrosis factor-alpha is produced by dying retinal neurons and is

required for Müller glia proliferation during zebrafish retinal regeneration. J Neurosci 33, 6524-6539.

Nelson, S.M., Frey, R.A., Wardwell, S.L., Stenkamp, D.L., 2008. The developmental sequence of gene expression within the rod photoreceptor lineage in embryonic zebrafish. Dev Dyn 237, 2903-2917.

Nelson, S.M., Park, L., Stenkamp, D.L., 2009. Retinal homeobox 1 is required for retinal neurogenesis and photoreceptor differentiation in embryonic zebrafish. Developmental biology 328, 24-39.

Ochocinska, M.J., Hitchcock, P.F., 2007. Dynamic expression of the basic helix-loop-helix transcription factor neuroD in the rod and cone photoreceptor lineages in the retina of the embryonic and larval zebrafish. The Journal of comparative neurology 501, 1-12.

Ochocinska, M.J., Hitchcock, P.F., 2009. NeuroD regulates proliferation of photoreceptor progenitors in the retina of the zebrafish. Mechanisms of development 126, 128-141.

Ottone, C., Krusche, B., Whitby, A., Clements, M., Quadrato, G., Pitulescu, M.E., Adams, R.H., Parrinello, S., 2014. Direct cell-cell contact with the vascular niche maintains quiescent neural stem cells. Nature cell biology 16, 1045-1056.

Pelster, B., Burggren, W.W., 1996. Disruption of hemoglobin oxygen transport does not impact oxygen-dependent physiological processes in developing embryos of zebra fish (Danio rerio). Circulation research 79, 358-362.

Plaster, N., Sonntag, C., Busse, C.E., Hammerschmidt, M., 2006. p53 deficiency rescues apoptosis and differentiation of multiple cell types in zebrafish flathead mutants deficient for zygotic DNA polymerase delta1. Cell death and differentiation 13, 223-235.

Raymond, P.A., Barthel, L.K., Bernardos, R.L., Perkowski, J.J., 2006. Molecular characterization of retinal stem cells and their niches in adult zebrafish. BMC developmental biology 6, 36.

Raymond, P.A., Barthel, L.K., Curran, G.A., 1995. Developmental patterning of rod and cone photoreceptors in embryonic zebrafish. The Journal of comparative neurology 359, 537-550.

Rutland, C.S., Mitchell, C.A., Nasir, M., Konerding, M.A., Drexler, H.C., 2007. Microphthalmia, persistent hyperplastic hyaloid vasculature and lens anomalies following overexpression of VEGF-A188 from the alphaA-crystallin promoter. Molecular vision 13, 47-56.

Santhakumar, K., Judson, E.C., Elks, P.M., McKee, S., Elworthy, S., van Rooijen, E., Walmsley, S.S., Renshaw, S.A., Cross, S.S., van Eeden, F.J., 2012. A zebrafish model to study and therapeutically manipulate hypoxia signaling in tumorigenesis. Cancer research 72, 4017-4027.

Schneider, C.A., Rasband, W.S., Eliceiri, K.W., 2012. NIH Image to ImageJ: 25 years of image analysis. Nature methods 9, 671-675.

Shen, Q., Goderie, S.K., Jin, L., Karanth, N., Sun, Y., Abramova, N., Vincent, P., Pumiglia, K., Temple, S., 2004. Endothelial cells stimulate self-renewal and expand neurogenesis of neural stem cells. Science (New York, N.Y 304, 1338-1340.

Shin, E.S., Sorenson, C.M., Sheibani, N., 2014. Diabetes and retinal vascular dysfunction. Journal of ophthalmic & vision research 9, 362-373.

Stainier, D.Y., Fouquet, B., Chen, J.N., Warren, K.S., Weinstein, B.M., Meiler, S.E., Mohideen, M.A., Neuhauss, S.C., Solnica-Krezel, L., Schier, A.F., Zwartkruis, F., Stemple, D.L., Malicki, J., Driever, W., Fishman, M.C., 1996. Mutations affecting the formation and function of the cardiovascular system in the zebrafish embryo. Development (Cambridge, England) 123, 285-292.

Stainier, D.Y., Weinstein, B.M., Detrich, H.W., 3rd, Zon, L.I., Fishman, M.C., 1995. *Cloche*, an early acting zebrafish gene, is required by both the endothelial and hematopoietic lineages. Development (Cambridge, England) 121, 3141-3150.

Stenkamp, D.L., 2007. Neurogenesis in the fish retina. International review of cytology 259, 173-224.

Stenkamp, D.L., Frey, R.A., 2003. Extraretinal and retinal hedgehog signaling sequentially regulate retinal differentiation in zebrafish. Developmental biology 258, 349-363.

Stenkamp, D.L., Frey, R.A., Mallory, D.E., Shupe, E.E., 2002. Embryonic retinal gene expression in sonic-you mutant zebrafish. Dev Dyn 225, 344-350.

Stevens, C.B., Cameron, D.A., Stenkamp, D.L., 2011. Plasticity of photoreceptor-generating retinal progenitors revealed by prolonged retinoic acid exposure. BMC developmental biology 11, 51.

Tucker, N.R., Middleton, R.C., Le, Q.P., Shelden, E.A., 2011. HSF1 is essential for the resistance of zebrafish eye and brain tissues to hypoxia/reperfusion injury. PloS one 6, e22268.

van Lookeren Campagne, M., LeCouter, J., Yaspan, B.L., Ye, W., 2014. Mechanisms of age-related macular degeneration and therapeutic opportunities. The Journal of pathology 232, 151-164.

Weiss, O., Kaufman, R., Michaeli, N., Inbal, A., 2012. Abnormal vasculature interferes with optic fissure closure in lmo2 mutant zebrafish embryos. Developmental biology 369, 191-198.

Westerfield, M., 2007. The Zebrafish Book; A guide for the laboratory use of zebrafish (Danio rerio). University of Oregon Press, Eugene, OR.

Xie, J., Farage, E., Sugimoto, M., Anand-Apte, B., 2010. A novel transgenic zebrafish model for blood-brain and blood-retinal barrier development. BMC developmental biology 10, 76.

Xiong, J.W., Yu, Q., Zhang, J., Mably, J.D., 2008. An acyltransferase controls the generation of hematopoietic and endothelial lineages in zebrafish. Circulation research 102, 1057-1064.

Zhang, J., Fuhrmann, S., Vetter, M.L., 2008. A nonautonomous role for retinal frizzled-5 in regulating hyaloid vitreous vasculature development. Investigative ophthalmology & visual science 49, 5561-5567.

Zoeller, J.J., McQuillan, A., Whitelock, J., Ho, S.Y., Iozzo, R.V., 2008. A central function for perlecan in skeletal muscle and cardiovascular development. The Journal of cell biology 181, 381-394.

Chapter 3: Roles of the early ocular vasculature during retinal neurogenesis in zebrafish retina

Susov Dhakal, Megan Batty, Josilyn Sejd, Adi Inbal, and Deborah L. Stenkamp

Publication status: Manuscript in progress

<u>Abstract:</u>

<u>Background:</u> Developmental roles of the early ocular vasculature during retinal neurogenesis in vertebrates remain unknown. *In vivo* and *in vitro* studies have indicated a potential regulatory relationship between the vascular endothelial cells and neural stem cells. Here, we selectively destroy vascular endothelial cells of zebrafish embryos using GAL4/UAS system of gene expression and evaluate their retinal phenotype to identify specific roles of vasculature during retinal development. We also evaluate retinal phenotypes of *silent heart* and *vlad tepes* mutant zebrafish embryos to identify roles of circulating factors and circulating red blood cells respectively during retinal neurogenesis.

<u>Results:</u> Our results indicate that when vasculature is disrupted during retinal neurogenesis, the eyes become microphthalmic and have disorganized lamination. Similarly, destruction of vascular endothelial cells also cause defects with cell proliferation and cell survival. Selective reduction of vasculature affects differentiation of photoreceptors, bipolar cells, Müller glia and formation of regular synaptic layers. Disruption of vascular endothelial cells also affects expression of retina specific transcription factors. Absence of circulating factors or circulating red blood cells does not affect retinal neurogenesis in zebrafish embryos.

<u>Conclusions:</u> Abnormal retinal phenotypes in zebrafish embryos with disrupted vascular endothelial cells suggest that vasculature has developmental roles during retinal neurogenesis and provides systemic factors to the developing retina. This is further supported by the fact that neurogenesis proceeds normally in *silent heart* and *vlad tepes* mutants.

<u>Introduction</u>**:**

The roles of the ocular vasculature during retinal neurogenesis in vertebrates have been mostly limited to fulfilling the metabolic and nutritive demands of the developing retina. Any potential developmental roles of the early ocular vasculature during eye development remain unknown and unstudied. It is critical to understand the developmental roles of ocular vasculature during retinal neurogenesis in order to develop novel treatment therapeutic techniques to treat vascular related ocular pathologies such as persistent fetal vasculature syndrome and retinopathy of prematurity (ROP).

Vascular system is one of the first organ systems to complete development in a developing vertebrate embryo. Developing organs are in close association with single-layered endothelial cells lining the inside of the blood vessels and they communicate with vascular endothelial cells to regulate organogenesis via extracellular matrix (Cleaver & Melton 2003). Vasculature is very closely associated with retinal neurons during the period of embryonic development in vertebrates. There are several instances indicating potential regulatory relationship between the endothelial cells of the vasculature and neural stem cells. Sites of mammalian brain

where neurogenesis have been shown to occur have a very dense blood vessel network (Palmer et al. 2000; Shen et al. 2009) suggesting that neural stem cells communicate with the blood vessels to regulate neurogenesis in the brain. Optic fissure closure is affected in zebrafish *lmo2* embryos that have abnormal vasculature (Weiss et al. 2012). Overexpression of vascular endothelial growth factor A (VEGF-A) in the lens of mouse embryos causes excess blood vessel growth, microphthalmia and abnormal retinal morphology (Rutland et al. 2007). Conditional knockout of *Frizzled-5* in mouse retina leads to failure of hyaloid vasculature regression and abnormal retinal development (Zhang et al. 2008) indicating that retinal neurons and blood vessels have regulatory relationship. *In vitro* cell culture studies have also shown that neural progenitor cells are stimulated to divide upon physical contact from endothelial cells (Shen et al. 2004). Co-culture studies have also shown that retinal progenitor cells undergo self-renewal in presence of endothelial cells (Parameswaran et al. 2014).

Using mammalian model to study the relationship between the ocular vasculature and developing retina is extremely difficult to accomplish because as soon as the vasculature is manipulated tissue oxygenation is disrupted resulting in death of the organism. Therefore, zebrafish embryo is an ideal model organism to conduct this study because ablation of blood vessels in zebrafish embryos does not have lethal effect as zebrafish embryos have been shown to not require active circulation of oxygen for their survival until 5 days post fertilization (dpf) (Pelster & Burggren 1996; Jacob et al. 2002; Dhakal et al. 2015, under revision). Previously, we have shown that *cloche* zebrafish mutants, which lack most of the endothelial,

endocardial and hematopoietic cells, have severe defects in retinal development (Dhakal et al. 2015, under revision). However, molecular nature of *cloche* remains unknown. Therefore, in order to identify specific roles of systemic factors from vasculature and circulating factors from circulation for normal retinal neurogenesis, we used transgenic and mutant zebrafish embryos in this study. We selectively destroyed the vascular endothelial cells in zebrafish embryos by using GAL4/UAS gene expression system under the regulatory action of vascular endothelial cell specific promoter, *cadherin5* (Lampugnani et al. 1992; Breviario et al. 1995) and a prodrug, Metronidazole (Met) (Curado et al. 2007; Pisharath et al. 2008). We used *silent heart (sih-/-)* mutants to investigate the roles of circulating materials for normal retinal neurogenesis. *Sih-/-* have a non-coding mutation in *troponin2 (tnnt2)* gene in their heart muscle resulting in non-contractile heart (Sehnert et al. 2002). In order to test specific roles of circulating blood cells, we analyzed the retinal phenotype of *vlad tepes (vlt-/-)* mutant zebrafish embryos. *Vlt-/-* have a non-sense mutation in *gata1* transcription factor resulting in absence of red blood cells (Lyons et al. 2002).

Here, we report that, upon disruption of blood vessels retinal neurogenesis is severely affected in zebrafish embryos. The eyes become microphthalmic and differentiation of neuronal and non-neuronal cells of the retina is either reduced or absent in zebrafish embryos with disrupted vasculature. Similarly, expression of transcription factors required for differentiation of retinal neurons is also reduced or absent in absence of vasculature. In contrast, when vasculature is present but circulation or circulating materials are absent, retinal neurogenesis proceeds normally. Our results indicate that ocular vasculature provides local paracrine signals

to the developing neurons whereas circulating materials within the vasculature may not be critical for initial retinal development.

Experimental procedures:

Animal care

The University of Idaho Institutional Animal Care and Use Committee (IACUC) approved all the protocols used in this study. Adult zebrafish were maintained according as described (Westerfield 2007) at 28.5°C in aquatic housing units with recirculating water and in a 14-hour light cycle. The embryo was considered 0 hpf at the time of spawning and the embryos were staged as described (Westerfield 2007). Embryos were kept transparent by treating them with 0.003% phenylthiourea (PTU) to inhibit melanin synthesis (Westerfield 2007) for eye morphometrics. *Silent heart* mutant embryos were identified by visualizing at their non-contractile hearts at 30 hpf under dissecting microscope. *Vlad tepes* mutants were identified by observing circulating blood cells under a dissecting microscope (Lyons et al. 2002).

Tg(cdh5:GAL4ff) was generously gifted by Dr. Jesus Torres Vazquez (New York University). *Tg(UAS-E1b:Eco.NfsB-mCherry)* and *vlad tepes* lines were purchased from Zebrafish International Resource Center (ZIRC). *Silent heart* fish were kindly provided by Dr. Jeffrey Essner (Iowa State University).

Metronidazole treatment

Doubly transgenic zebrafish embryos obtained from crossing hemizygous *Tg(cdh5:GAL4ff)* and hemizygous *Tg(UAS-E1b:Eco.NfsB-mCherry)* were treated with

10mM metronidazole (Met) (Sigma-Aldrich) prepared in 0.2% dimethylsulfoxide (DMSO) starting at 12 hpf and maintained in the dark to prevent photoinactvation of Met (Curado et al. 2008). Met solution was replaced at 24 hpf and after every exposure to light (eg. post sorting of doubly transgenic embryos). The doubly transgenic embryos were sorted for mCherry expression in their vascular endothelial cells at 30 hpf.

Visualization of vasculature ablation

We verified vascular disruption in multiple ways. First, we established a timeline by which significant destruction of vasculature was achieved by Met treatment in doubly transgenic embryos. Significant vasculature disruption was assumed to occur when there was no visible circulation present in the embryos. We viewed the embryos under dissecting microscope at different developmental time points and tracked the number of embryos without circulating materials until 48 hpf.

Second, we used Nikon-Andor spinning disk confocal microscope to visualize ocular vessels at 48 hpf. Whole mount zebrafish embryos were fixed using 4% paraformaldehyde for 1 hour at room temperature followed by three 30 min rinses in PBS. The embryos were then stored in PBS at 4°C. Before imaging, the fixed whole mount embryos were mounted in 0.1% low melting point agarose to immobilize them. The images were collected at 0.4-micron interval for at least 45 sections per eye using a confocal laser-scanning microscope fitted to an inverted microscope using Apo LWD 40X lens with a 561nm solid-state laser. The images were processed using NIS elements viewer software.

Third, we verified vasculature reduction by imaging eyes of living embryos for the presence of circulating materials through the ocular vessels at 48 hpf. Live embryos were anesthetized using tricaine (MS-222) followed by mounting the whole embryos in 0.1% low melting point agarose prepared in tricaine (MS-222) solution with an eye facing up. The eyes were imaged in a single focal plane continuously Apo LWD 40X lens for 1 minute with each image exposed for 40 msec using transmitted light to visualize circulating materials in the eye, especially around the lens, at 48 hpf.

Tissue preparation

Embryos were fixed as described (Barthel & Raymond 1990). In short, embryos were fixed in 4% paraformaldehyde in 5% sucrose buffered phosphate solution for 1 hour at room temperature. Fixed embryos were washed by incubating them in increasing concentration of sucrose solution starting from 5% and ending with 20% and were cryoprotected overnight in a rotating shaker at 4°C in 20% sucrose phosphate solution. The fixed embryos were embedded in an embedding medium consisting of 1 part OCT medium (Sakura Finetek, Torrance, CA) and 2 parts 20% sucrose phosphate solution and the tissue blocks were stored at -20°C. 5 micron sections were sectioned using a Leica CM3050 cryostat. The slides were dried in a vacuum desiccator overnight and stored at -20°C.

Immunocytochemistry (ICC) and in situ hybridization

ICC experiments were performed as described (Stevens et al. 2011). Briefly, prior to addition of primary antibodies, the slides were incubated with PBST solution

consisting of 20% goat serum in phosphate buffered saline containing 0.5% Triton X-100 (Sigma, St. Louis,MO) for 30 minutes. The following primary antibodies were used: mouse monoclonal Zn8, labels retinal ganglion cells (Hu & Easter 1999) (1:10, ZIRC); mouse monoclonal anti-HuC/D, labels retinal ganglion and amacrine cells (1:200, Developmental Studies Hybridoma Bank); rabbit polyclonal anti protein kinase C (PKC) alpha, labels subpopulation of rod bipolar cells (1:200, Santa Cruz Biotechnologies); mouse monoclonal 1D1, labels rhodopsin (Fadool 2003) (1:100, generous gift from Dr. James Fadool); mouse monoclonal ZPR1, labels red and green-sensitive cones (Larison & Bremiller 1990) (1:100, ZIRC); mouse monoclonal ZRF1, labels Müller glia (Marcus & Easter 1995) (1:20, ZIRC); mouse monoclonal SV2, labels synaptic vesicle 2 (1:2000, Developmental Studies Hybridoma Bank); rabbit polyclonal cleaved caspase-3, labels apoptotic cells (1:200, AbCam); rabbit polyclonal antiphosphohistone-3, labels M-phase cells (PH3, 1:1000, Cell Signaling Technologies); rabbit anti L-plastin, labels pan leucocytes (Hochmann et al. 2012) (1:10000, generous gift of Dr. Michael Redd). After adding the primary antibodies, the slides were stored at 4°C overnight. Primary antibody was detected using either fluorescein conjugated secondary antibody (1:200 or 1:500) or Cy3-conjugated secondary antibody (1:200 or 1:500). The slides were mounted with Vectashield mounting medium containing DAPI (Vector labs).

In situ hybridizations were performed as previously described (Stevens et al. 2011). In vitro transcription was used to generate digoxigenin labeled cRNA probe from the plasmids. Following cRNA probes were used; *pax6a* and *crx* (gifts from P.

Raymond); *NeuroD* (gift from P. Hitchcock), *phd3/elgn3* (BioScience Life Sciences). Hypoxic samples were prepared as described (Tucker et al. 2011).

Histology

Retinal lamination was analyzed using hematoxylin (Sigma-Aldrich) and eosin (Sigma-Aldrich) staining procedure. Briefly, the slides were hydrated in PBST followed by incubation in hematoxylin for 5 minutes followed by washes in acid alcohol (70% EtOH, 29% H_2O, 1% HCl) and Scott's tap water solution (1% $NaHCO_3$). Then, the slides were incubated in eosin for a minute followed by rinsing with water. Finally, the slides were dehydrated in the increasing concentrations of alcohol and xylene and mounted in permout (Fisher Scientific).

Photography and Statistics

To measure eye and lens size, embryos were positioned with their sides facing up on a petri dish and imaged with Nikon stereomicroscope with a CCD camera (Meridian Instruments, Freeland, WA). The images were collected such that clear boundaries of the eye and the lens were in same focal plane. Black and white silhouette was created by selecting the eye and the lens boundary for each image using photoshop CS (Adobe). Feret's diameter (a method of estimating a diameter for irregularly shaped objects) was measured for each silhouette image using image J software (NIH). For epifluorescence images, Leica DMR compound microscope with SPOT camera system (Diagnostic Instruments) was used. All the images were prepared using Adobe Photoshop. Statistical analyses were performed using Microsoft Excel (Microsoft).

Cell counts

Following methods were used to count the fluorescent labeled cells. *Rod photoreceptors:* All 1D1 label positive cells located dorsal to the optic nerve were counted to determine the average number of 1D1+ cells per section per retina. A dense patch of cells located in the ventral retina was excluded from 1D1 counts to avoid inaccuracies with the cell counts (Raymond et al. 1995; Stevens et al. 2011). *Microglia:* Microglial cells labeled by L-plastin antibody were counted to obtain average number of microglia present per section per retina. To avoid double counting, only those sections that were at least 15 microns apart were counted. *Cell proliferation:* Nuclei of proliferating cells in M-phase labeled by PH3 antibodies were counted to estimate average number of proliferating cells per section per retina. Double counting was avoided by counting nuclei that were at least 15 microns apart in the same embryonic section. *Cell death:* Cells undergoing apoptosis were labeled by anti-CC3 antibody. Total number of CC3+ profiles in the retina was counted to determine average number of CC3+ cells per section per retina. Double counting was avoided by counting the sections that were at least 15 microns apart. CC3+ cells that were at least 3 microns in diameter were only included in the count to maintain consistency and to avoid counting fragmented cells.

Results**:**

Verification of vasculature ablation

To selectively ablate vasculature, we used GAL4/UAS system of gene expression and vascular endothelial cell specific promoter *cadherin5* (*cdh5*)

(Breviario et al. 1995; Lampugnani et al. 1992). When hemizygous transgenic adult zebrafish, *Tg(cdh5:GAL4ff)* and *Tg(UAS-E1b:Eco.NfsB-mCherry)* were mated, they produced doubly transgenic embryos, *Tg(cdh5:GAL4-UASNfsBmCherry),* which expressed fusion protein mCherry tagged with bacterial nitroreductase enzyme (nfsB:mCherry) exclusively in the vascular endothelial cells. Met, a prodrug, reacts with bacterial enzyme nitroreductase (nfsB) to produce a cytotoxic metabolite which crosslinks DNA strands leading to selective cell death of endothelial cells (Curado et al. 2008). Doubly transgenic embryos treated with Met are referred to as avascular embryos for rest of this manuscript whereas doubly transgenic embryos treated with DMSO are referred to as DMSO controls. Hemizygous or wildtype embryos from the same clutch that generated doubly transgenic embryos treated and were treated with Met are referred to as Met control embryos.

Embryos were treated with Met starting at 12 hpf because first evidence of vascular endothelial cells in retina is seen around 18 hpf in zebrafish embryos (Hartsock et al. 2014). We verified disruption of retinal vasculature in Met treated doubly transgenic embryos at different developmental times. At 36 hpf, circulation was present in both DMSO control and Met control embryos (n=8 each) and Met treated doubly transgenic embryos (n=8) (Fig. 3.1C). However, circulation appeared to be reduced but not completely absent at 42 hpf in Met treated doubly transgenic embryos. By 48 hpf, 100% of the doubly transgenic embryos treated with Met lacked any circulation suggesting that significant disruption in vasculature was achieved (Fig. 3.1C). Ocular vasculature of embryonic zebrafish appears as a ring-like structure surrounding the lens and supplied by nasal retinal vessels (nrv), through

which blood enters the eye, along with dorsal and ventral retinal vessel, through which blood is drained out of the eye by 48 hpf (Hartsock et al. 2014; Kitambi et al. 2009). DMSO control embryos at 48 hpf showed the evidence of ring vessels around the lens along with nrv, vrv and drv (Fig. 3.1A). In addition, the network of hyaloid vessels (hv) under the lens was also observed in DMSO control embryos at 48 hpf (Fig. 3.1A). In contrast, experimentally avascular embryos had extremely reduced mCherry expression in the eyes at 48 hpf (Fig. 3.1B). Some remnants of the nrv and a few patches of mCherry around the lens are present in these embryos indicating that most of the vasculature was reduced at 48 hpf. In zebrafish embryos, rod and cone photoreceptors, bipolar cells and Müller glia are generated between 48 hpf and 72 hpf.

Additionally, we verified the absence of vasculature and circulation in Met treated doubly transgenic embryos at 48 hpf by visualizing circulation and circulating materials in the eye. In control embryos, circulating materials were seen entering the ring vessels around the lens through nrv and leaving the retina through vrv and drv. In contrast, no evidence of circulation or circulating materials was seen in Met treated doubly transgenic embryos suggesting that vasculature was absent in them (See supplemental video, Fig 3.1D).

Lens and eye size

We used Feret's statistical diameter to calculate diameter of the lens and the eyes of embryos at 48 hpf and 72 hpf. At 48 hpf, we did not find any difference in lens and eye diameter between control and experimentally avascular embryos (Fig.

3.2A) (ANOVA). By 72 hpf, both lens and eye diameter were significantly smaller in experimentally avascular embryos than in control embryos (Fig. 3.2B) (ANOVA, $p<0.01$ (lens), $p<0.0001$(eye), Tukey test). The lens grew marginally between 48 hpf and 72 hpf in absence of vasculature but eyes did not grow at all over the same time period. Average eye diameter was reduced at 72 hpf in absence of vascular endothelial cells when compared with eye diameters of embryos at 48 hpf. To summarize, there is no difference between eye and lens size in absence of vasculature in zebrafish embryos at 48 hpf but both eyes and lens significantly smaller in absence of normal vasculature at 72 hpf.

Cell proliferation and cell death

Previously, we have shown that the retinal neurons undergo significantly higher cell death starting around 54 hpf in *cloche* mutants (Dhakal et al. 2015, under revision). Abnormal retinal phenotype in *cloche* mutants is not completely rescued even when cell death is blocked after injecting *p53* morpholino. Similarly, *cloche* mutants have defects in cell proliferation by 54 hpf (Dhakal et al. 2015, under revision). Therefore, we tested for cell death and cell proliferation in experimentally avascular embryos in order to determine whether differences in either one or combination of both might be contributing to abnormal retinal phenotype and microphthalmic eyes at 72 hpf. We used anti-phosphohistone-3 (PH3) antibody to label mitotic cells at M-phase in 48 hpf embryos to label the dividing progenitor cells giving rise to retinal neuronal cells except RGCs and amacrine cells. In control embryos, mitotic progenitor cells (PH3+) were present in the ONL, INL and circumferential germinal zone (CGZ) (Fig. 3.3 A, B). In case of experimentally

avascular embryos, our results show that PH3+ cells were mostly present in ONL but reduced in CGZ at 48 hpf (Fig. 3.3C). The number of PH3+ cells was also significantly lower in experimentally avascular embryos ($p<0.05$, ANOVA, Tukey test) (Fig. 3.3D) indicating that fewer dividing cells might be contributing to lack of growth in their eyes between 48 hpf to 72 hpf ultimately resulting in microphthalmia.

To evaluate cell death in developing retinas, we used anti cleaved caspase-3 (CC3) to label the cells undergoing apoptosis mediated by cleaved caspase-3 signaling pathway. Zebrafish retina develops with very few cells undergoing cell death during the process of neurogenesis. Cell death in developing neural retina in zebrafish reaches its peak at 36 hpf and cell death is extremely reduced after 48 hpf (Cole & Ross 2001). At 48 hpf, we observed very few CC3+ cells in the retina of controls and vasculature disrupted embryos and there was no significant difference in number of CC3+ cells in (Fig. 3.4D). By 72 hpf, there was statistically significant increase in number of labeled CC3+ cells in embryos with reduced vasculature compared to controls ($p<0.01$, ANOVA, Tukey test) (Fig. 3.4 A-C, E). CC3+ cells were not spatially restricted in the retina and were present in all retinal layers. Therefore, increased cellular death in the retina of zebrafish embryos lacking vascular endothelial cells is likely one of reasons behind abnormal retinal phenotype at 72 hpf.

Retinal lamination

We examined laminar organization of the retina at 72 hpf in zebrafish embryos with disrupted blood vessels using H&E staining. At 72 hpf, experimentally avascular

zebrafish embryos had highly disorganized retinas (Fig. 3.5C). These embryos had

no distinct ganglion cell layer (GCL) when compared to the controls (Fig. 3.5 A, B).

The inner plexiform layer (IPL), where bipolar and amacrine cells synapse with retinal

ganglion cells was hardly identifiable. The inner nuclear layer (INL) consisting of

bipolar, amacrine and horizontal cell bodies was highly disorganized and was difficult

to identify in experimentally avascular embryos. The outer plexiform layer (OPL),

where photoreceptors form synapses with bipolar and horizontal cells, was non-

existent in embryos with reduced vasculature. Cell morphology and organization of

the photoreceptors in the outer nuclear layer (ONL) also appeared abnormal in

embryos with reduced vasculature. Overall, the retinal lamination was extremely

disorganized with no distinct neuronal and synaptic layers in absence of vasculature

in zebrafish embryos. We, then, examined retinal lamination of *sih-/-* and *vlt-/-*

mutants at 72 hpf. In both cases, the retinas were very well organized with distinct

and identifiable cellular and synaptic layers at 72 hpf similar to the wildtypes (Fig. 3.5

D, E).

Photoreceptor differentiation

Embryonic rod and cone photoreceptor neurogenesis is competed by 72 hpf in

zebrafish embryos (Stenkamp 2007). We used 1D1 antibody to label rhodopsin in rod

photoreceptors and zpr-1 antibodies to examine red and green double-cone

photoreceptors at 72 hpf. Rod photoreceptors were present throughout the ONL in

control embryos at 72 hpf (Fig. 3.6 A, B). In contrast, rods were limited to ventral

retina as a single patch of cells in experimentally avascular embryos (Fig. 3.6C). We

also quantified average number of labeled rod photoreceptors in the ONL per retina

per section excluding the patch of labeled cells in ventral retina in control and

experimental embryos and found that the average number of 1D1 labeled rod

photoreceptors present in the ONL of experimentally avascular embryos were

significantly lower than the control embryos (p<0.01, ANOVA, Tukey test) (Fig. 3.6K).

Rod photoreceptors were present throughout the ONL of both *sih-/-* and *vlt-/-* mutants

(Fig. 3.6 D, E) similar to the wildtypes indicating that neurogenesis and initial

differentiation are unaffected in absence of circulation and blood cells respectively.

Next, we analyzed differentiation of cone photoreceptors. At 72 hpf, red and

green sensitive double cones were present throughout the ONL of the control

embryos as indicated by zpr1+ labels (Fig. 3.6 F, G). Similar to the rods, cone

photoreceptors were either absent or limited to ventral retina as a patch in avascular

embryos (Fig. 3.6H). In *sih-/-* and *vlt-/-* mutants, cone photoreceptors seem to

develop normally similar to the wildtypes (Fig. 3.6 I, J). Taken together, differentiation

of rod and cone photoreceptors is severely reduced in absence of vascular

endothelial cells but not in absence of circulating materials or circulating blood cells.

Neuron differentiation and synapses

Retinal ganglion cells (RGC) and amacrine cells are the first types of retinal

neurons to exit cell cycle and their neurogenesis is complete by 36 hpf and 48 hpf

respectively during retinal neurogenesis in zebrafish embryos (Stenkamp 2007). We

evaluated differentiation of retinal ganglion cells at 48 hpf and 72 hpf by labeling the

cells with Zn8 antibody. At 48 hpf, when the retinal neurogenesis of the ganglion cells

is already complete, we observed a distinct GCL and Zn8 labels were present

throughout the GCL in both control and experimentally avascular embryos (data not shown). GCL appeared smaller and thinner in experimentally avascular embryos at 72 hpf (Fig. 3.7 A-C). Especially, the edges of GCL appeared thinner and looked abnormal compared to the controls in experimentally avascular embryos. Interestingly, the axons from the GCL appeared to leave the retina through optic nerve normally in embryos with reduced blood vessels.

We next analyzed the presence of amacrine cells at 72 hpf and performed ICC experiments with retinal sections targeted with anti HuC/D antibody that labels RGCs and ACs. HuC/D antibody labels were present throughout the inner INL in both controls (Fig. 3.7 D, E). In experimentally avascular embryos, HuC/D labeled amacrine cells were present around the INL suggesting that amacrine cells were present in in absence of blood vessels (Fig. 3.7F). Anti-HuC/D antibodies also labeled RGC in experimentally avascular embryos. Presence of HuC/D labels in the GCL also provided additional verification of RGC differentiation in experimentally avascular embryos. These results indicate that absence of blood vessels during retinal development in embryonic zebrafish affected normal differentiation of RGCs but not the amacrine cells.

Bipolar cell neurogenesis is complete around 60 hpf in zebrafish (Schmitt & Dowling 1999; Connaughton 2011). We used anti PKC-α antibody to label a sub-population of rod bipolar cells at 72 hpf. In control embryos, PKC-α labeled bipolar cell bodies were present throughout the outer INL (Fig. 3.7 G, H). In contrast, very few to no labeled bipolar cells were present in experimentally avascular embryos

(Fig. 3.7I). Therefore, bipolar cell differentiation is reduced in absence of vasculature in zebrafish embryos.

We also analyzed the formation of synaptic layers in Met treated doubly transgenic embryos at 72 hpf. In the DMSO and Met controls, IPL appeared as a distinct layer between the GCL and INL (Fig. 3.7 J, K). In experimentally avascular embryos, IPL was diffused and appeared smaller at 72 hpf suggesting that synapse formation was likely affected (Fig. 3.7L). Similarly, OPL containing the synapses between photoreceptors and bipolar cells was present as a thin layer between the INL and ONL in control embryos (Fig. 3.7 J, K). OPL was absent in zebrafish embryos with reduced blood vessels (Fig. 3.7L) indicating that synapse formation was affected.

Glial differentiation

Müller glia are the principal cells that provide structural integrity to the retina and span across the retina by extending their endfeet from inner limiting membrane to the outer limiting membrane (Newman & Reichenbach 1996; Willbold 1998). We used anti-glial fibrillary acidic protein (GFAP) antibody, Zrf-1, to label Müller glia in the zebrafish retina at 72 hpf. The control embryos showed presence of Müller glia with their endfeet extending from the vitreal surface to the photoreceptor layers (Fig. 3.8 A, B). In contrast, Met treated doubly transgenic embryos had highly reduced labeled Müller glia and their endfeet were non-existent suggesting that differentiation of Müller glia was affected in absence of vasculature (Fig. 3.8C). *Silent heart* mutants

also appeared to have normal Müller glia differentiation at 72 hpf (preliminary data, data not shown).

Previously, we have shown that *cloche* mutant embryos have reduced microglia in their retina at 72 hpf (Dhakal et al. 2015, under revision) leaving the open possibility that the retinal phenotype in *cloche* mutants could be related to reduced microglia. Another study has also shown that retinal neurogenesis is affected in absence of microglia (Huang et al. 2012). Microglia migrate from yolk sac to the brain and retina as early macrophages around 26-30 hpf and differentiate into mature microglia around 55 hpf during development in zebrafish embryos (Herbomel et al. 2001). Therefore, we tested for presence of microglia in experimentally avascular embryos in order to verify that their abnormal retinal phenotype was not primarily due to absent or reduced microglia. We labeled microglia with a pan leucocyte marker L-plastin in 72 hpf embryos. About 30-35 microglial cells are normally present at random locations in developing neural retina in zebrafish embryos by 72 hpf (Herbomel et al. 2001). L-plastin labels indicating presence of microglia were present within the IPL and INL in all control and Met treated embryos at 72 hpf (Fig. 3.8 D- F). The labeling pattern of L-plastin is consistent with reported locations of microglia in zebrafish embryos as described previously (Herbomel et al. 2001). We, then, quantified the average number of L-plastin labeled microglia per section per retina at 72 hpf and found that there was no significant difference in number of microglia present in experimentally avascular embryos when compared with the control embryos (Fig. 3.8G). Therefore, abnormal retinal phenotypes in experimentally avascular embryos in presence of microglia suggest that blood vessels are required

for normal neurogenesis in zebrafish embryos. This result also rules out the possibility that abnormal retinal phenotype in *cloche* mutants is related to reduced microglia.

Retinal transcription factors expression

Several transcription factors are involved in differentiation of different cell types in developing zebrafish retina. We tested the expression of a few retinal transcription factors required for neurogenesis in zebrafish embryos using *in situ* hybridization technique. First, we analyzed the expression of *pax6a* gene, which is required for overall eye development, and is present in retinal progenitor cells including CGZ and eventually being limited to RGCs and amacrine cells (Nornes et al. 1998; Macdonald et al. 1995). *Pax6a* was expressed normally in the GCL and CGZ in both control and Met treated doubly transgenic embryos at 48 hpf (data not shown). By 60 hpf, *pax6a* was still expressed in the GCL but reduced in CGZ in Met treated doubly transgenic embryos. In contrast, control embryos had uniform *pax6a* expression throughout GCL and slightly reduced expression in CGZ at 60hpf (Fig. 3.9, A-C). Therefore, *pax6a* expression is affected in absence of vascular endothelial cells and reduced *pax6a* expression could contribute to abnormal GCL in embryos with reduced blood vessels at 72 hpf.

Next, we analyzed the expression of the transcription factor *NeuroD*, which is required for differentiation of photoreceptors and amacrine cells in zebrafish embryos (Morrow et al. 1999). At 48 hpf, *NeuroD* was expressed throughout the developing ONL as a continuous long patch and in the developing INL as small patches in all

embryos (data not shown). By 60 hpf, *NeuroD* was still expressed in the ONL and INL in control embryos (Fig. 3.9 D, E). In contrast, *NeuroD* expression was extremely reduced, diffused, and limited to small patches within ONL and minimal to absent in INL in Met treated doubly transgenic embryos (Fig. 3.9F).

Lastly, we tested *crx* gene expression at 48 hpf and 72 hpf. *Crx* gene encodes a transcription factor, which is required for expression of photoreceptor-specific genes (Shen & Raymond 2004; Stenkamp 2007). *Crx* mRNA transcripts were present throughout the ONL and outer INL in control and Met treated embryos at 48 hpf suggesting that *crx* expression is normal until 48 hpf (data not shown). When the control and Met treated embryos were evaluated for *crx* expression at 60 hpf, we observed extremely faint patches of *crx* expression present in the ONL and no expression in the outer INL in embryos with disrupted vasculature (Fig. 3.9I). Therefore, reduced *NeuroD* and *crx* expression by 60 hpf in Met treated doubly transgenic embryos are very likely to contribute to reduced presence of photoreceptors at 72 hpf. These results also suggest that endothelial cells of vasculature are likely to be involved in providing signals to the developing retina which help to maintain the expression of various transcription factors required for normal retinal development.

Hypoxia

Studies have shown that zebrafish embryos do not require active circulation of oxygen for their metabolic needs until 5 dpf (Pelster & Burggren 1996; Jacob et al. 2002). *Cloche* mutants also did not show any evidence of hypoxia in their retina at 72

hpf (Dhakal et al. 2015, under revision). In order to verify that the abnormal retinal phenotype observed in embryos lacking vasculature was not due to hypoxia, we performed an *in situ* hybridization experiment to detect the expression of *prolyl-hydroxylase3* (*phd3*) gene, whose expression is upregulated in response to hypoxic conditions in cells at 72 hpf (D'Angelo et al. 2003). The embryos treated to hypoxic controls expressed *phd3* in patches (arrows) in their retina (Fig. 3.10A). In contrast, control and Met treated embryonic retinas did not show any evidence of expression of *phd3* at 72 hpf suggesting that their retina were not hypoxic (Fig. 3.10 B-D) and abnormal retinal phenotype in absence of vascular endothelial cells is not due to hypoxia.

Discussion**:**

In this study, we demonstrated that vascular endothelial cells are required for normal retinal neurogenesis in zebrafish embryos. Here, we selectively destroyed vascular endothelial cells in zebrafish embryos using GAL4/UAS system of gene expression. Our results indicate that endothelial cells of the vasculature have regulatory roles during retinal neurogenesis in zebrafish embryos and retinal progenitor cells require factors derived from the vascular endothelial cells. Normal retinal development in *sih-/-* and *vlt-/-* embryos suggest that the "factors" from the vasculature that are required by the developing retinal neurons are not likely to be circulating factors. Our findings are consistent with other studies that have shown interactions between endothelial cells and neuronal progenitor cells in other parts of the vertebrate body such as brain (Palmer et al. 2000; Shen et al. 2009). Our findings

are also consistent with the co-culture studies that have shown that endothelial cells regulate cell cycle of neural stem cells (Parameswaran et al. 2014).

Previously, we have shown that, in *cloche* mutant zebrafish embryos, which lack most of the endothelial cells from early developmental stage, retinal neurogenesis is affected as early as 48 hpf (Dhakal et al. 2015, under revision). We found that endothelial cell disruption by using Met had delayed effect and blood vessels were not significantly reduced until 48 hpf. However, in both cases, retinal lamination was disrupted at 72 hpf and development of photoreceptors, bipolar cells and Müller glia were affected. Additionally, *cloche* mutants also had defective RGC and reduced microglia. Therefore, these additional defects in *cloche* could likely be caused by *cloche* mutation rather than absence of vascular endothelial cells. *Cloche* mutants also had significantly smaller eyes as early as 30 hpf and they had significantly higher cell death in their retina by 54 hpf. In contrast, vascular endothelial cell ablation did not cause microphthalmia and increased retinal cell death until 72 hpf indicating that *cloche* mutation is likely causing reduced growth and increased cell death early in developing zebrafish embryos. Very little to no effect on retinal development of cells (RGCs and amacrine cells) that are generated by 48 hpf could also be likely due to delayed ablation of vasculature when treated with Met. Taking these two results together, we can conclude that it is extremely likely that the endothelial cells regulates retinal progenitor neurons constantly and any disruption in such regulation can have adverse developmental effects on retinal neurons.

Previous studies have shown that vascular endothelial cells in the brain secrete different growth factors such as insulin-like growth factor-1 (IGF-1) and brain-
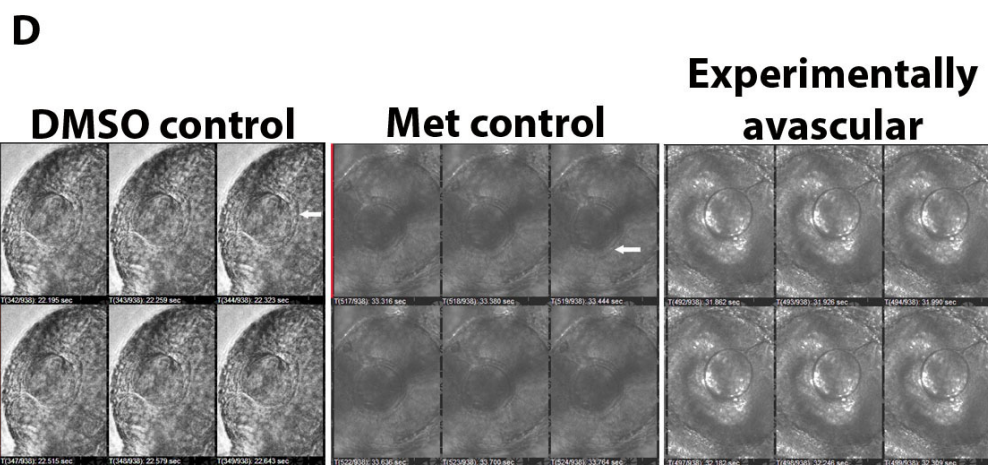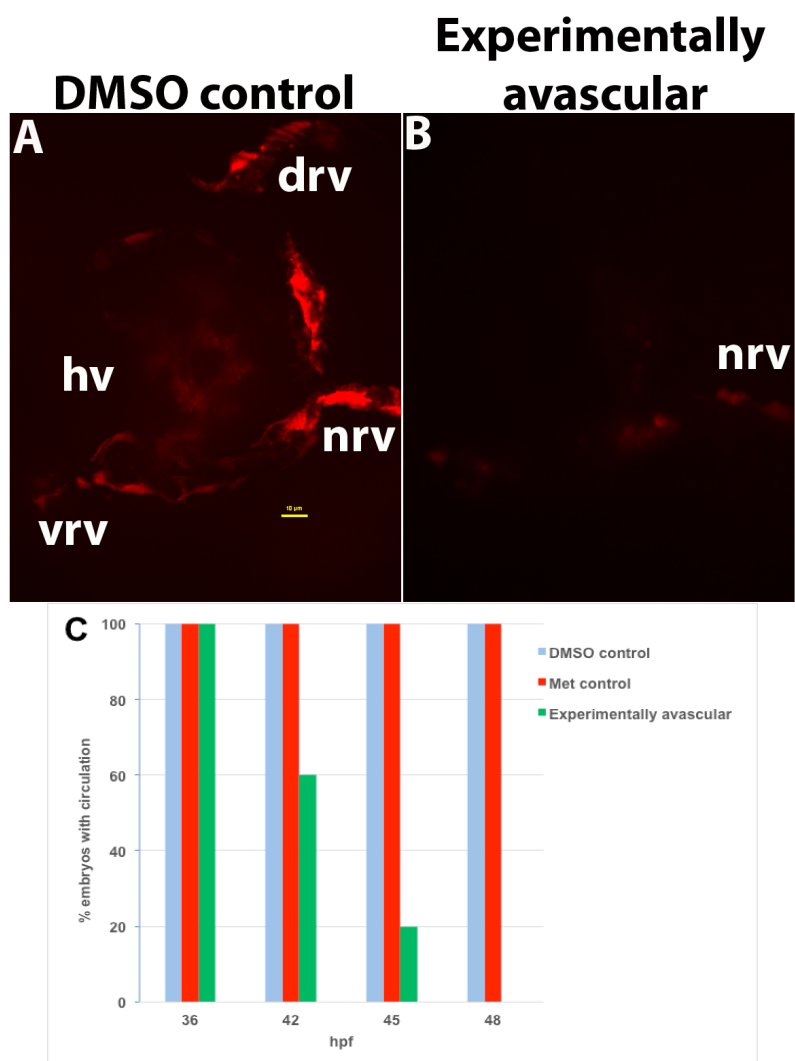
derived neurotrophic factor (BDNF) to regulate neuronal development, survival and respond after neuronal injury (Nakahashi et al. 2000; Wang et al. 2013). Similarly, endothelial cells have been shown to express genes that regulate cell cycle, cell commitment, epigenetic changes for cell renewal and receptors for different ligands such as Notch, FGF, VEGF, etc. (Parameswaran et al. 2014) in neural stem cell culture *in vitro*. Based on our findings in this study, we can also speculate that vascular endothelial cells in the retina also secrete factors to regulate cell cycle and cell survival to regulate neurogenesis. Future studies should focus on identifying such signals used by vascular endothelial cells to regulate retinal neurogenesis.

The findings of this study indicate that vascular endothelial cells have regulatory roles during retinal neurogenesis and such regulation occurs likely via paracrine signaling. Identification of such signaling molecules secreted by the vasculature to regulate retinal neurogenesis can be used to develop novel therapeutic methods to treat retinal pathologies associated with vascular abnormalities.
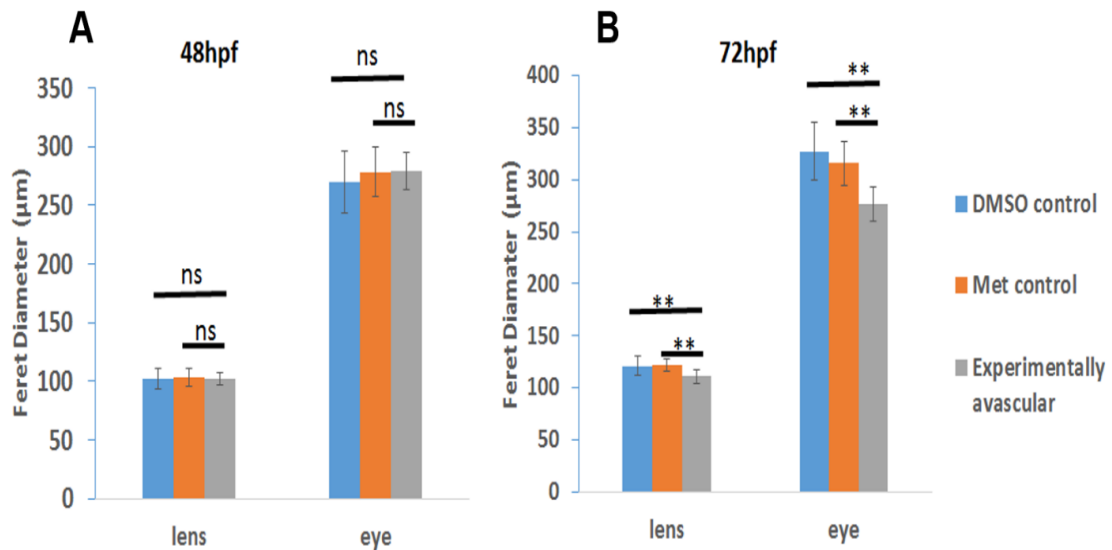
Figures

DMSO control

Experimentally avascular

A — drv, hv, nrv, vrv

B — nrv

C — % embryos with circulation vs hpf (36, 42, 45, 48)

DMSO control · Met control · Experimentally avascular

D — DMSO control · Met control · Experimentally avascular

Figure 3.1. Verification of vasculature disruption (A.-B.). Confocal images of

DMSO control (A) and experimentally avascular embryo (B). Hyaloid vasculature (hv)
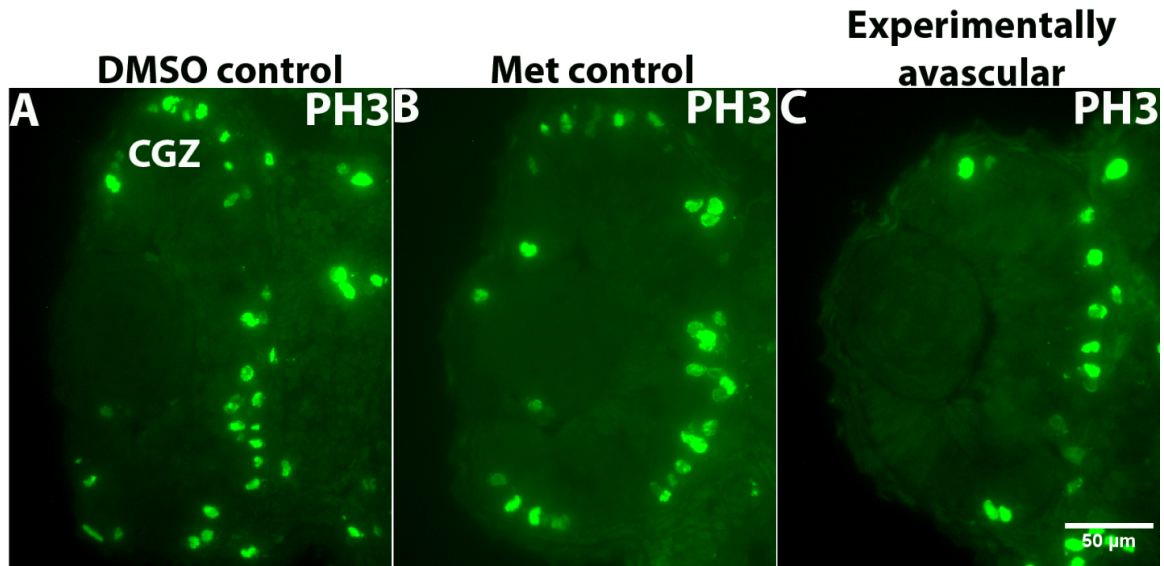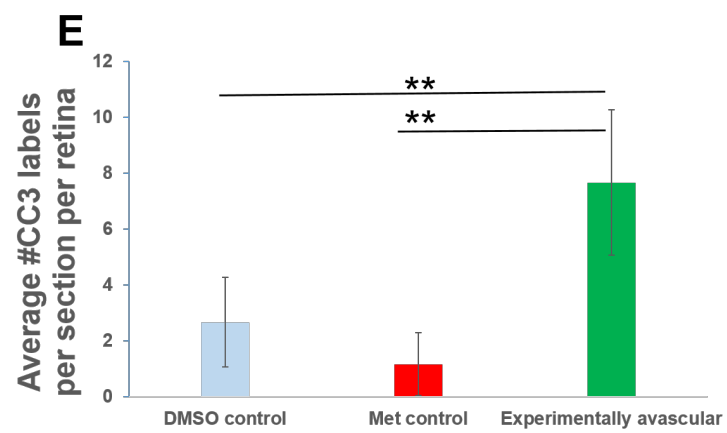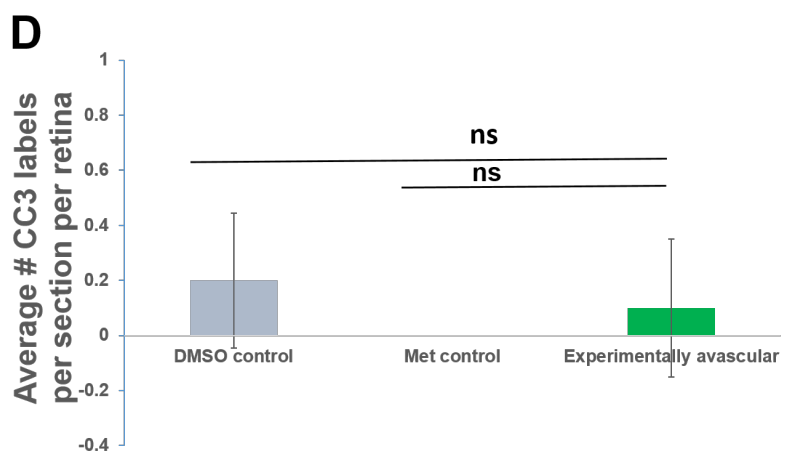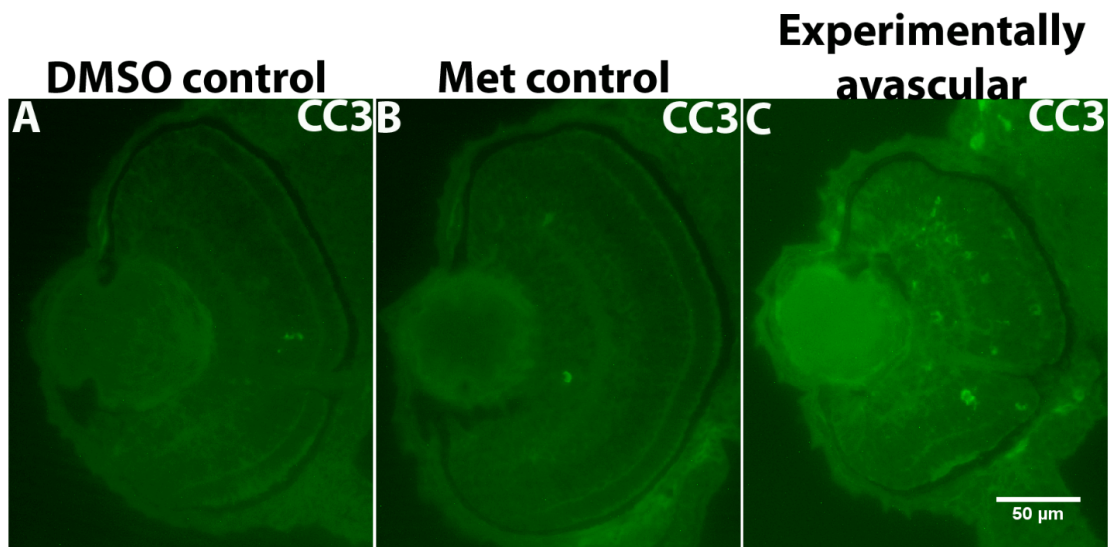
are present under the lens in DMSO control embryos at 48 hpf (A). Nasal retinal

vessels (nrv), dorsal retinal vessels (drv) and ventral retinal vessels form a part of

superficial ring surrounding the lens by 48 hpf in DMSO control embryos (A). In

contrast, vasculature is extremely reduced and present in patches in experimentally

avascular embryos (B). Some evidence of nrv is present in experimentally avascular

whereas hv is absent (B). Vasculature is disrupted over a range of time between 36

hpf and 48 hpf and circulation is absent in experimentally avascular embryos by 48

hpf (C). Screenshot of images showing circulating materials in ring vessels

surrounding the lens at 48 hpf (D). Arrows point to the circulating materials in the ring

vessels around the lens (Scale bar in A & B = 10µm).

Figure 3.2. Microphthalmia at 72 hpf in experimentally avascular embryos. Lens and eye diameters of controls and experimentally avascular embryos at 48 hpf (A) and 72 hpf (B). At 48 hpf, there was no difference in the lens and eye diameter (A). At 72hpf, there was significant difference between DMSO and Met controls and experimentally avascular embryos ($p<0.01$ (lens), $p<0.0001$ (eyes), ANOVA, Tukey test).

DMSO control   **Met control**   **Experimentally avascular**

A   PH3   CGZ   B   PH3   C   PH3   50 µm

D

#PH3 positive cells per section
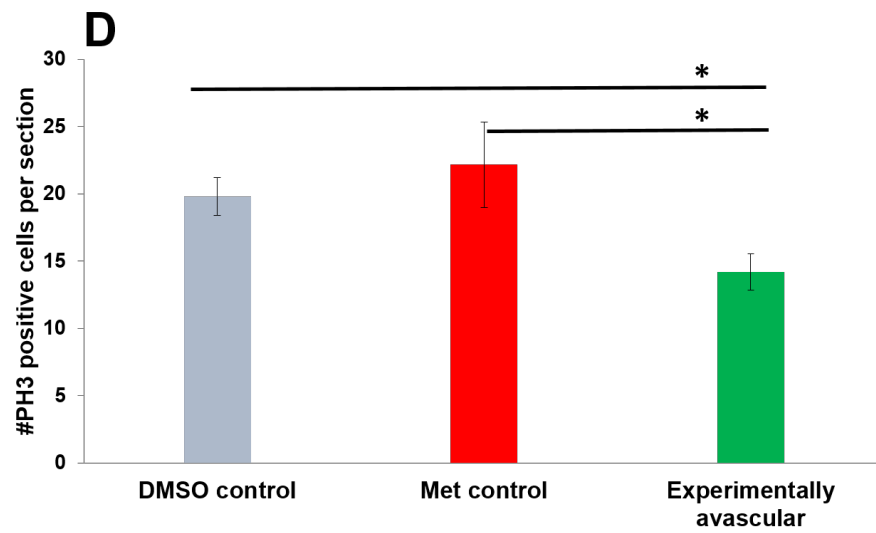
Figure 3.3. Reduced cell proliferation in experimentally avascular embryos (A.-C.). Immunofluorescence images of embryonic retina labeling the proliferating cells at M phase with anti PH3 antibody. Proliferating cells marked by PH3 labels are present throughout the developing ONL and CGZ in DMSO controls (A) and Met controls (B). In experimentally avascular embryos, fewer PH3+ cells are present in the developing OPL and the number of PH3+ cells in the CGZ is extremely reduced (C). Average number of PH3+ cells per retina is significantly reduced ($p < 0.05$, ANOVA, Tukey test) in experimentally avascular embryos at 48hpf (D).

DMSO control

Met control

Experimentally avascular

A CC3
B CC3
C CC3

50 µm

D

Average # CC3 labels per section per retina

ns

ns

DMSO control   Met control   Experimentally avascular

E

Average #CC3 labels per section per retina

**

**

DMSO control   Met control   Experimentally avascular

Figure 3.4. Increased cell death in experimentally avascular embryos (A.-C).

Immunofluorescence images of cells undergoing apoptosis labeled with CC3

antibody. At 72 hpf, very few cells are undergoing apoptosis in DMSO controls (A)

and Met controls (B). Numerous CC3+ labels present in the retina of experimentally

avascular embryos at 72 hpf (C). The number of CC3+ labels in not different in

significantly different in experimentally avascular embryos at 48 hpf (D) but is

significantly higher at 72 hpf compared to the controls (E) (p<0.01, ANOVA, Tukey

test).
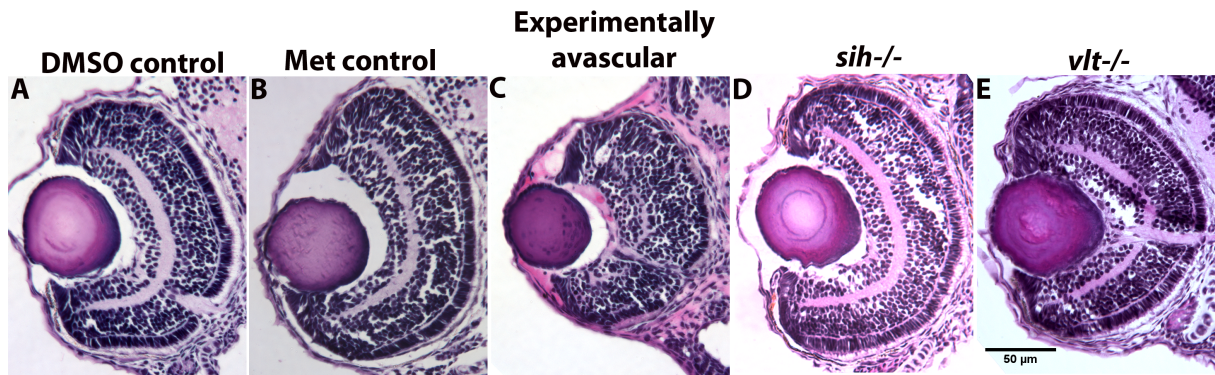
Figure 3.5. Abnormal retinal lamination in experimentally avascular embryos.

A.-E. Immunofluorescence images of DMSO control, Met controls, experimentally avascular embryos, *sih-/- and vlt-/-.* Retina develops normally with distinct nuclear and synaptic layers in DMSO (A) and Met control (B) embryos. Retinal lamination is highly disrupted with no identifiable nuclear and synaptic layers in experimentally avascular embryos (C). *Sih-/-* and *vlt-/-* embryos have normal retinal lamination (D, E).

| | DMSO control | Met control | Experimentally avascular | *sih-/-* | *vlt-/-* |
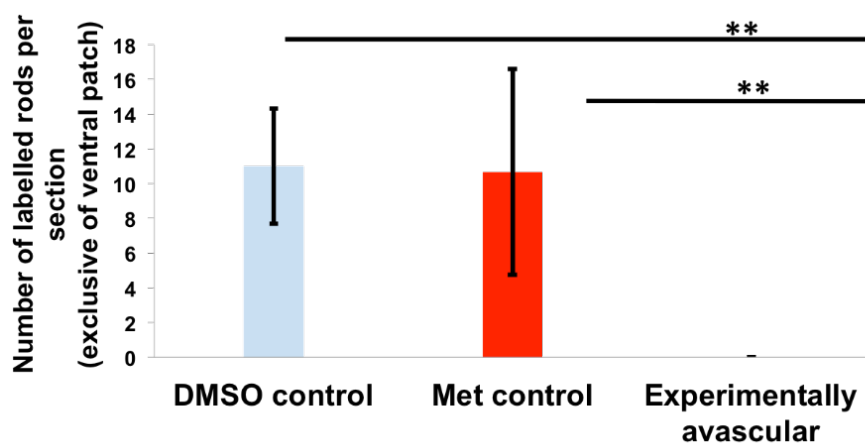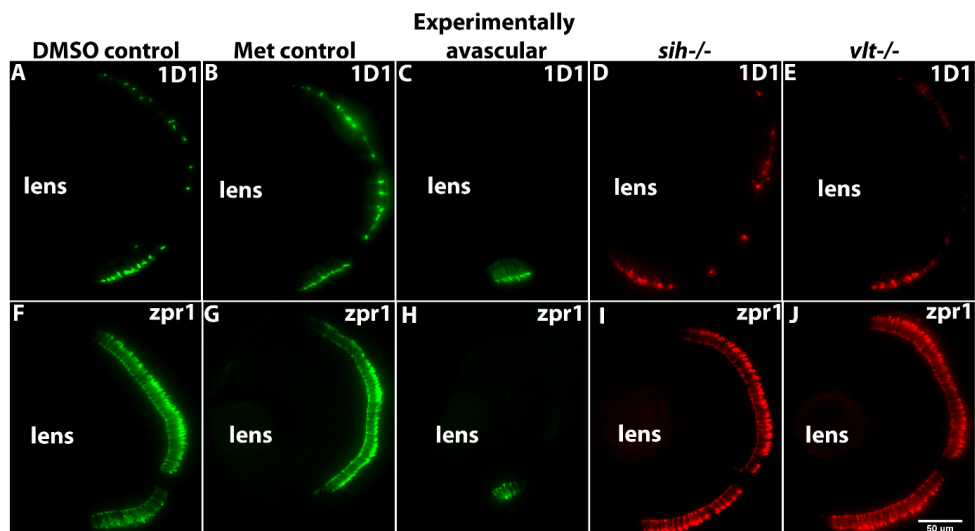
Figure 3.6. Defects in photoreceptor differentiation in experimentally avascular embryos. A.-J. Immunofluorescence image of rods (A-E) and cones (F-J) photoreceptors at 72hpf. Rod photoreceptors are present throughout the ONL in DMSO controls (A), Met controls (B), *sih-/-* (D) and *vlt-/-* (E). In experimentally avascular embryos, rod photoreceptors fail to differentiate properly and are present as a patch of cells in the ventral retina (C). Average number of 1D1 labeled rod photoreceptors is significantly smaller in experimentally avascular embryos (K) ($p<0.01$, ANOVA, Tukey test). Red-green sensitive double cone photoreceptors are present throughout the ONL in DMSO and Met controls (F, G), *sih-/-* (I) and *vlt-/-* (J). Cone photoreceptors are limited to the ventral retina as a patch in experimentally avascular embryos (H).

DMSO control

Met control

Experimentally avascular

50 μm
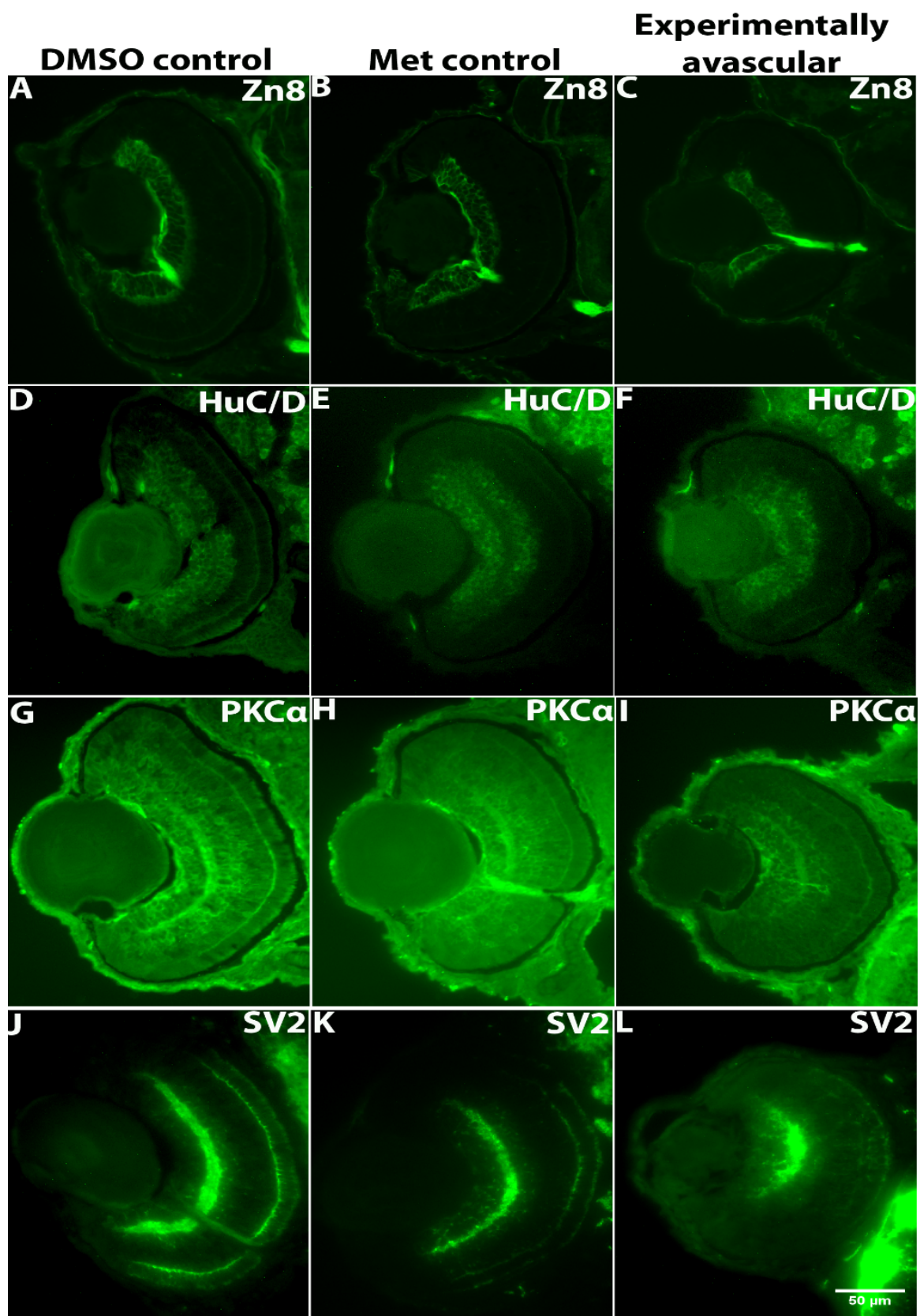
Figure 3.7. Neurons and synapse development in experimentally avascular embryos. Differentiation of RGCs (A-C), amacrine cells (D-F), rod bipolar cells (G-I) and formation of synaptic layers (J-L) at 72 hpf. A distinct GCL labeled with ZN8 antibody is present in DMSO and Met controls (A, B). Smaller GCL is seen in experimentally avascular embryos (C). HuC/D labeled amacrine cells are present in the inner INL in both control (D, E) and experimentally avascular embryos (F). Rod bipolar cells are present in the outer INL in DMSO and Met controls (G, H) whereas they are extremely reduced in experimentally avascular embryos (I). Distinct IPL and OPL are present in DMSO control (J) and Met control (K). IPL is diffused and smaller and OPL is absent in experimentally avascular embryos indicating problems with synapse formation in absence of vasculature (L).

DMSO control   **Met control**   **Experimentally avascular**

A zrf1   B zrf1   C zrf1

D L-plastin   E L-plastin   F L-plastin

50 µm

G

Average # of labeled microglia per section per retina

ns

ns

DMSO control   Met control   Experimentally avascular
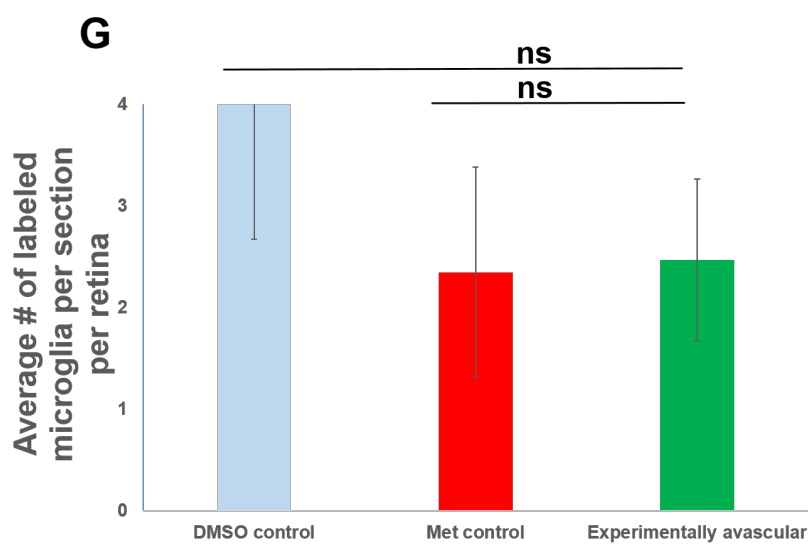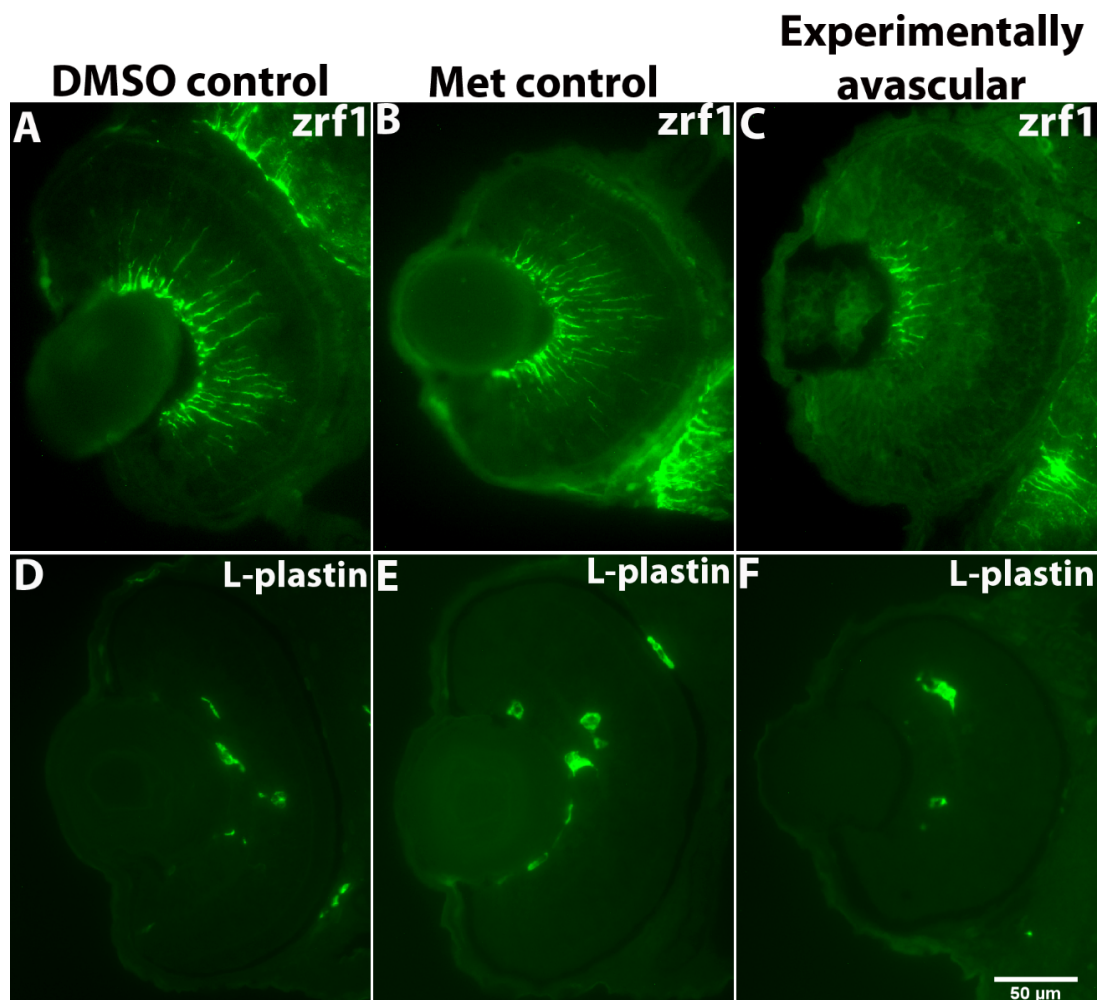
Figure 3.8. Glial differentiation in experimentally avascular embryos (A -F).

Immunofluorescence images of differentiated Müller glia (A-C) and microglia (D-F).

Differentiated Müller glia and their endfeet are present in DMSO and Met controls (A,

B). Müller glia fail to extend their endfeet in Met treated in experimentally avascular

embryos (C). Differentiated microglia are present randomly in the retinas of control

(D, E) and experimentally avascular embryos (F). There is no difference in average

number of microglia present in control and experimentally avascular embryos

(ANOVA) (G).

DMSO control   **Met control**   **Experimentally avascular**

A pax6   B pax6   C pax6

D NeuroD   E NeuroD   F NeuroD

G crx   H crx   I crx

50 µm
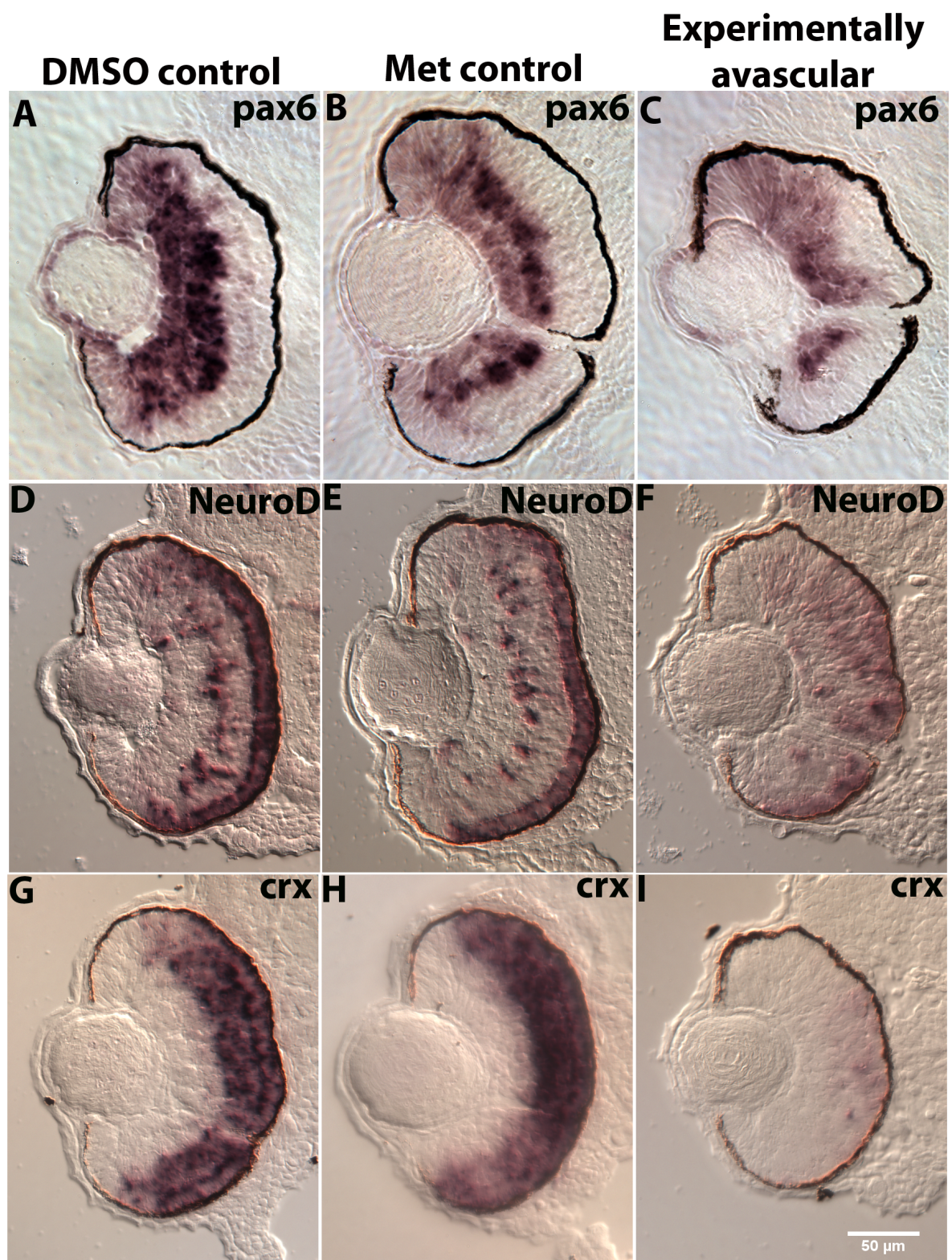
Figure 3.9. Reduced expression of retinal transcription factors in experimentally avascular embryos (A.-I.). *Pax6a* is present throughout the GCL and CGZ in DMSO and Met control embryos at 60 hpf (A,B). In experimentally avascular embryos, there is reduced *pax6a* expression in the GCL and no expression in the CGZ (C). *NeuroD* is expressed in the ONL and INL of DMSO and Met controls at 60 hpf (D,E). In experimentally avascular embryos, NeuroD expression is extremely reduced in both ONL and INL (F). Similarly, *crx* gene is expressed throughout the ONL and outer INL in DMSO and Met control embryos (G, H) whereas crx expression is very low to none existent in experimentally avascular embryos (I).
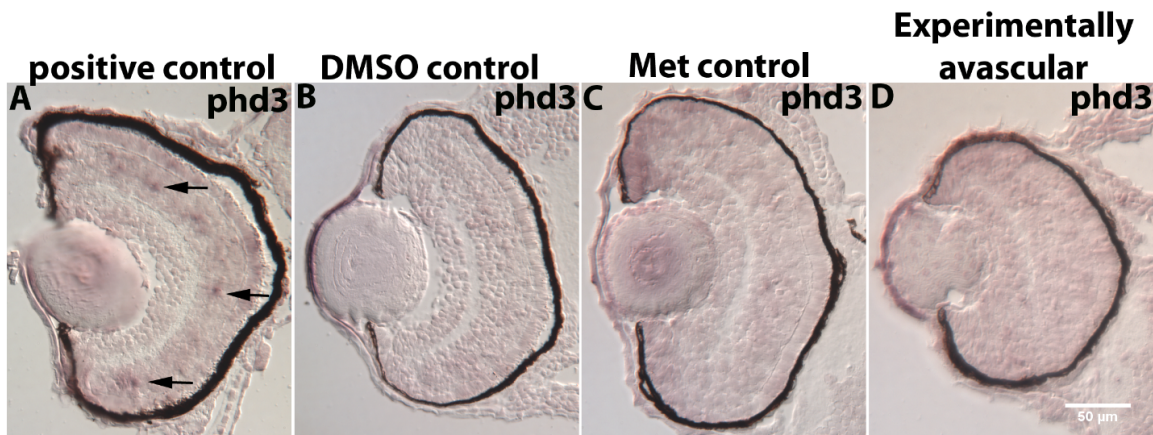
Figure 3.10. No evidence of hypoxia in experimentally avascular embryos (A.-

D.). Expression of hypoxic marker *phd3* mRNA in hypoxic zebrafish retina (A), DMSO

controls (B), Met controls (C) and, experimentally avascular embryos (D). Hypoxic

gene, *phd3*, is expressed at random locations in hypoxic retina (arrows) whereas no

evidence of phd3 expression is observed in DMSO controls, Met controls and

experimentally avascular embryos indicating that retinal tissue is not hypoxic when

blood vessels are ablated.

References

Barthel, L.K. & Raymond, P. a, 1990. Improved method for obtaining 3-microns cryosections for immunocytochemistry. *The journal of histochemistry and cytochemistry : official journal of the Histochemistry Society*, 38, pp.1383–1388.

Breviario, F. et al., 1995. Functional Properties of Human Vascular Endothelial Cadherin (7B4/Cadherin-5), an Endothelium-Specific Cadherin. *Arteriosclerosis, Thrombosis, and Vascular Biology* , 15 (8), pp.1229–1239. Available at: http://atvb.ahajournals.org/content/15/8/1229.abstract.

Cleaver, O. & Melton, D. a, 2003. Endothelial signaling during development. *Nature medicine*, 9(6), pp.661–668.

Cole, L.K. & Ross, L.S., 2001. Apoptosis in the developing zebrafish embryo. *Developmental biology*, 240, pp.123–142.

Connaughton, V.P., 2011. Bipolar cells in the zebrafish retina. *Visual neuroscience*, 28, pp.77–93.

Curado, S. et al., 2007. Conditional targeted cell ablation in zebrafish: A new tool for regeneration studies. *Developmental Dynamics*, 236(February), pp.1025–1035.

Curado, S., Stainier, D.Y. & Anderson, R.M., 2008. Nitroreductase-mediated cell/tissue ablation in zebrafish: a spatially and temporally controlled ablation method with applications in development and regenration studies. *Nature Protocols*, 3(6), pp.948–954.

D'Angelo, G. et al., 2003. Hypoxia up-regulates prolyl hydroxylase activity. A feedback mechansim that limits HIF-1 responses during reoxygenation. *Journal of Biological Chemistry*, 278, pp.38183–38187.

Dhakal, S. et al., 2015. Abnormal retinal development in cloche mutant zebrafish. *Developmental Dynamics*, pp.1–33.

Fadool, J.M., 2003. Development of a rod photoreceptor mosaic revealed in transgenic zebrafish. *Developmental Biology*, 258, pp.277–290.

Hartsock, A. et al., 2014. In vivo analysis of hyaloid vasculature morphogenesis in zebrafish: A role for the lens in maturation and maintenance of the hyaloid. *Developmental Biology*, 394(2), pp.327–339. Available at: http://linkinghub.elsevier.com/retrieve/pii/S0012160614003765.

Herbomel, P., Thisse, B. & Thisse, C., 2001. Zebrafish early macrophages colonize cephalic mesenchyme and developing brain, retina, and epidermis through a M-

CSF receptor-dependent invasive process. *Developmental biology*, 238(2), pp.274–88. Available at: http://www.sciencedirect.com/science/article/pii/S0012160601903938 [Accessed May 3, 2015].

Hochmann, S. et al., 2012. Fgf signaling is required for photoreceptor maintenance in the adult zebrafish retina. *PLoS ONE*, 7(1), pp.1–12.

Hu, M. & Easter, S.S., 1999. Retinal neurogenesis: the formation of the initial central patch of postmitotic cells. *Developmental biology*, 207, pp.309–321.

Huang, T. et al., 2012. The role of microglia in the neurogenesis of zebrafish retina. *Biochemical and Biophysical Research Communications*, 421, pp.214–220.

Jacob, E. et al., 2002. Influence of hypoxia and of hypoxemia on the development of cardiac activity in zebrafish larvae. *American journal of physiology. Regulatory, integrative and comparative physiology*, 283(4), pp.R911–R917.

Kitambi, S.S. et al., 2009. Small molecule screen for compounds that affect vascular development in the zebrafish retina. *Mechanisms of Development*, 126(5-6), pp.464–477. Available at: http://dx.doi.org/10.1016/j.mod.2009.01.002.

Lampugnani, M.G. et al., 1992. A novel endothelial-specific membrane protein is a marker of cell-cell contacts. *The Journal of cell biology*, 118(6), pp.1511–22. Available at: http://www.pubmedcentral.nih.gov/articlerender.fcgi?artid=2289607&tool=pmcentrez&rendertype=abstract [Accessed May 29, 2015].

Larison, K.D. & Bremiller, R., 1990. Early onset of phenotype and cell patterning in the embryonic zebrafish retina. *Development (Cambridge, England)*, 109, pp.567–576.

Lyons, S.E. et al., 2002. A nonsense mutation in zebrafish gata1 causes the bloodless phenotype in vlad tepes. *Proceedings of the National Academy of Sciences of the United States of America*, 99, pp.5454–5459.

Macdonald, R. et al., 1995. Midline signalling is required for Pax gene regulation and patterning of the eyes. *Development (Cambridge, England)*, 121(10), pp.3267–3278.

Marcus, R.C. & Easter, S.S., 1995. Expression of glial fibrillary acidic protein and its relation to tract formation in embryonic zebrafish (Danio rerio). *The Journal of comparative neurology*, 359(3), pp.365–81. Available at: http://www.ncbi.nlm.nih.gov/pubmed/7499535 [Accessed May 26, 2015].

Morrow, E.M. et al., 1999. NeuroD regulates multiple functions in the developing neural retina in rodent. *Development (Cambridge, England)*, 126, pp.23–36.

Nakahashi, T. et al., 2000. Vascular endothelial cells synthesize and secrete brain-derived neurotrophic factor. *FEBS Letters*, 470(2), pp.113–117. Available at: http://www.sciencedirect.com/science/article/pii/S0014579300013028 [Accessed May 21, 2015].

Newman, E. & Reichenbach, A., 1996. The Muller cell: A functional element of the retina. *Trends in Neurosciences*, 19(8), pp.307–312.

Nornes, S. et al., 1998. Zebrafish contains two Pax6 genes involved in eye development. *Mechanisms of Development*, 77(2), pp.185–196.

Palmer, T.D., Willhoite, A.R. & Gage, F.H., 2000. Vascular niche for adult hippocampal neurogenesis. *Journal of Comparative Neurology*, 425(July), pp.479–494.

Parameswaran, S. et al., 2014. Hmga2 regulates self-renewal of retinal progenitors. *Development (Cambridge, England)*, 141(21), pp.4087–97. Available at: http://www.ncbi.nlm.nih.gov/pubmed/25336737 [Accessed July 18, 2015].

Pelster, B. & Burggren, W.W., 1996. Disruption of hemoglobin oxygen transport does not impact oxygen-dependent physiological processes in developing embryos of zebra fish (Danio rerio). *Circulation research*, 79, pp.358–362.

Pisharath, H. et al., 2008. Targeted ablation of beta cellls in the embryonic zebrafish pancreas using E.coli nitroreductase. , 124(3), pp.218–229.

Raymond, P.A., Barthel, L.K. & Curran, G.A., 1995. Developmental patterning of rod and cone photoreceptors in embryonic zebrafish. *The Journal of comparative neurology*, 359(4), pp.537–50. Available at: http://www.ncbi.nlm.nih.gov/pubmed/7499546 [Accessed April 26, 2015].

Rutland, C.S. et al., 2007. Microphthalmia, persistent hyperplastic hyaloid vasculature and lens anomalies following overexpression of VEGF-A188 from the alphaA-crystallin promoter. *Molecular vision*, 13, pp.47–56. Available at: http://www.pubmedcentral.nih.gov/articlerender.fcgi?artid=2503360&tool=pmcentrez&rendertype=abstract [Accessed May 29, 2015].

Schmitt, E.A. & Dowling, J.E., 1999. Early retinal development in the zebrafish, Danio rerio: light and electron microscopic analyses. *The Journal of comparative neurology*, 404(4), pp.515–36. Available at: http://www.ncbi.nlm.nih.gov/pubmed/9987995 [Accessed June 3, 2015].

Sehnert, A.J. et al., 2002. Cardiac troponin T is essential in sarcomere assembly and cardiac contractility. *Nature genetics*, 31(April), pp.106–110.

Shen, Q. et al., 2009. Adult SVZ stem cells lie in a vascular niche: A quantitative analysis of niche cell-cell interactions. *Cell*, 3(3), pp.289–300.

Shen, Q. et al., 2004. Endothelial cells stimulate self-renewal and expand neurogenesis of neural stem cells. *Science (New York, N.Y.)*, 304(2004), pp.1338–1340.

Shen, Y.C. & Raymond, P. a., 2004. Zebrafish cone-rod (crx) homeobox gene promotes retinogenesis. *Developmental Biology*, 269, pp.237–251.

Stenkamp, D.L., 2007. Neurogenesis in the fish retina. *International review of cytology*, 259, pp.173–224. Available at: http://www.pubmedcentral.nih.gov/articlerender.fcgi?artid=2897061&tool=pmcen trez&rendertype=abstract [Accessed June 2, 2015].

Stevens, C.B., Cameron, D. a & Stenkamp, D.L., 2011. Plasticity of photoreceptor-generating retinal progenitors revealed by prolonged retinoic acid exposure. *BMC Developmental Biology*, 11(1), p.51. Available at: http://www.biomedcentral.com/1471-213X/11/51.

Tucker, N.R. et al., 2011. HSF1 is essential for the resistance of zebrafish eye and brain tissues to hypoxia/reperfusion injury. *PLoS ONE*, 6(7).

Wang, J. et al., 2013. Insulin-like growth factor-1 secreted by brain microvascular endothelial cells attenuates neuron injury upon ischemia. *The FEBS journal*, 280(15), pp.3658–68. Available at: http://www.ncbi.nlm.nih.gov/pubmed/23721666 [Accessed June 5, 2015].

Weiss, O. et al., 2012. Abnormal vasculature interferes with optic fissure closure in lmo2 mutant zebrafish embryos. *Developmental Biology*, 369(2), pp.191–198. Available at: http://dx.doi.org/10.1016/j.ydbio.2012.06.029.

Westerfield, M., 2007. *The Zebrafish Book: A Guide for the Laboratory Use of Zebrafish (Danio Rerio)*, M. Westerfield. Available at: https://books.google.com/books/about/The_Zebrafish_Book.html?id=Rud1mgEA CAAJ&pgis=1 [Accessed May 26, 2015].

Willbold, E., 1998. Muller glia cells and their possible roles during retina differentiation in vivo and in vitro. *Histology and Histopathology*, 13, pp.531–552.

Zhang, J., Fuhrmann, S. & Vetter, M.L., 2008. A nonautonomous role for retinal frizzled-5 in regulating hyaloid vitreous vasculature development. *Investigative Ophthalmology and Visual Science*, 49, pp.5561–5567.

Chapter 4: Discussion

Key findings:

The main goals of our studies were to identify the potential regulatory relationship between the vascular endothelial cells and retinal progenitor cells and to identify the potential roles of circulation and specific circulatory factors such as red blood cells during embryonic retinal development. First, we evaluated the retinal phenotypes of *cloche* mutant zebrafish embryos, which lack most of the endothelial, endocardial and hematopoietic cells. We discovered that *cloche* mutant zebrafish have microphthalmic eyes as early as 30 hpf and their retina are extremely disorganized by the time neurogenesis is complete. *Cloche* mutants also have defects with differentiation of both neuronal and non-neuronal cells in the retina along with defects in expression of transcription factors required for normal retinal cell differentiation. In addition, *cloche* mutants also have defects in cell proliferation and increased cell death during the period of retinal neurogenesis. We also discovered that increased cell death in *cloche* mutants was not solely responsible for abnormal retinal phenotype at 72 hpf (Dhakal et al. 2015, under revision).

Based on our results, abnormal phenotype of the *cloche* mutants could be attributed to lack of vasculature or circulation or combination of both. Therefore, in order to identify the specific roles of vasculature and circulation during retinal neurogenesis, we analyzed the retinal phenotypes of zebrafish embryos that lacked vascular endothelial cells, circulation and circulating red blood cells. We discovered that retinal neurogenesis is affected after the vascular endothelial cells are selectively disrupted. Our results also indicate that in absence of vascular endothelial cells, the

eyes become microphthalmic and have abnormal lamination at 72 hpf. Cell differentiation and transcription factors expression specific to the retina are also affected in absence of vascular endothelial cells. We also noticed decreased cell proliferation and cell survival in zebrafish embryos lacking vascular endothelial cells. In contrast, we discovered that retinal neurogenesis proceeds normally in absence of circulation or circulating red blood cells suggesting that retinal progenitor cells do not require signals derived from circulating factors in zebrafish embryos during embryonic retinal development.

Our results are consistent with the findings that vasculature provides different signals to the neural stem and progenitor cell niches in vertebrates which are involved mostly in the maintenance and regeneration and a regulatory relationship is likely to exist between the vascular endothelial cells and neural stem cells (Putnam 2014; Goldberg & Hirschi 2009).

Retinal stem cell niche and vasculature:

A stem cell is an undifferentiated cell, which has the ability to generate multiple different types of cells in an organism and is able to replace itself. In contrast, a progenitor cell is a sub-type of a stem cell that is developmentally committed to a specific cell line and is either multipotent or unipotent and cannot replace itself. Vasculature is very closely associated with the stem cells in different organs in adult vertebrates (Gómez-Gaviro et al. 2012). Here, for the first time, we have shown that ocular vasculature regulates retinal neurogenesis *in vivo* using zebrafish embryos. It is likely that vasculature regulates neuronal progenitor cells in the retina in multiple

ways. Vasculature may directly secrete different factors in the stem cell microenvironment to stimulate cell division and cell proliferation (Sun et al. 2010). Conversely, it is also possible that vasculature maintains the neural progenitor cells in retina in undifferentiated state by inhibiting them from entering the cell cycle as seen mouse brain (Ottone et al. 2014). Vasculature might also regulate retinal progenitor cells by secreting cell survival factors. Our results indicate that it is likely that vascular endothelial cells secrete diffusible factors that promote proliferation, differentiation and survival of retinal progenitor cells in zebrafish embryos. Circulating materials from vasculature are also likely to enter the retinal stem cell niche and help regulate neurogenesis as seen in the mouse brain (Tavazoie et al. 2008). Based on results from *silent heart* mutants, it is unlikely that circulation is involved in regulation of retinal progenitor cells by vascular endothelial cells.

Therefore, vascular endothelial cells regulate retinal progenitor cells during retinal neurogenesis, cell differentiation and development in zebrafish. It is very important to identify the specific nature of factors involved and mechanisms behind the regulation of retinal progenitor cells in order to develop new treatment methods to treat retinal pathologies.

Cloche as animal model and its limitations:

Cloche has served as an animal model for studies focusing on cardio-vascular system for years. Here, we show for the first time, that *cloche* mutant embryos have microphthalmia, abnormal retinal phenotype and defects with retinal cell differentiation and cell survival. Our findings from studying the retinal phenotype of

cloche mutants suggest that absence of vascular endothelial cells in the developing retina is likely to cause abnormal retinal development. These findings are consistent with other studies that have shown the existence of relationship between the vascular endothelial cells and neural stem cells in mammalian brain (Ottone et al. 2014; Goldberg & Hirschi 2009; Palmer et al. 2000).

One of the limitations of working with *cloche* mutants is the unknown molecular nature of mutation causing such extreme phenotypes in *cloche*. *Cloche* has been linked with mutation in lycat gene in located in telomere region of chromosome 13 in zebrafish (Xiong et al. 2008). Lycat gene is associated with expression of membrane protein, cardiolipin, which is involved in maintaining permeability and potential of cell membranes (Wang et al. 2010). Besides the absence of most of the endothelial cells, *cloche* mutants also lack endocardial cells, circulation and most of the cells of hematopoietic lineage. Rescue experiment with microinjection of lycat mRNA in *cloche* mutants is only able to rescue hematopoietic cells (Xiong et al. 2008) indicating that *cloche* mutation likely affects genes upstream of lycat gene that results in multiple cardiovascular defects. It is also very likely that *cloche* mutation affects the progenitor cells that are involved in generation of cells of both hematopoietic and endothelial lineage as supported by presence of reduced number of microglia in *cloche* mutants at 72 hpf (Dhakal et al. 2015, under revision).

Changes in blood flow have been shown to affect vascular stem cell behavior leading to different vascular disease (Zhang et al. 2013). Therefore, it is also possible that retinal progenitor cells require some factors delivered to them through circulation in order to develop properly. While our findings from *cloche* mutant retinal

development are consistent with findings from other studies about regulatory relationship between vascular endothelial cells and neural stem cells, it also leaves open possibilities for potential roles of blood flow and circulating factors for abnormal retinal phenotype. However, normal retinal development in *silent heart* mutants is an strong indicator that abnormal retinal phenotype in *cloche* mutants is likely due to absence of vascular endothelial cells instead of circulation or blood flow.

Another limitation of *cloche* as an experimental animal model is the lack of available genetic tools to identify heterozygous adults carrying the *cloche* mutation. As a result, it is very time consuming and tedious task to identify heterozygous *cloche* adults. Besides, the survival rate of heterozygous *cloche* adults is also very poor and they tend to die earlier than other strains of adult zebrafish (personal observations).

Selective ablation of vascular endothelial cells and its limitations:

In order to confirm that vascular endothelial cells interact with retinal progenitor cells during retinal neurogenesis and to rule out any other potential factors causing abnormal retinal phenotype in *cloche* mutants, we selectively destroyed vascular endothelial cells in zebrafish. Selective destruction of vascular endothelial cells resulted in microphthalmic eyes, disrupted lamination, and defective cell differentiation and reduced expression of retinal transcription factors in zebrafish embryos. In addition, we also observed defects in cell proliferation and increased cell death in the retina upon selective disruption of vasculature. Therefore, our results indicate that regulatory relationship exists between vascular endothelial cells and retinal progenitor cells.

Through this study, we presented that vascular endothelial cells are critical for normal development of the retina in zebrafish embryos from regulatory point of view. Normal retinal development of *silent heart* mutant zebrafish retina further supports our result that retinal progenitor cells in zebrafish are not dependent upon active oxygen transport via blood circulation to fulfill their metabolic needs. Therefore, vasculature is likely secreting factors required by the retinal progenitor cells in its local microenvironment rather than circulating factors

Ideally, in this study, our goal was to selectively ablate all the vascular endothelial cells as early as possible. Instead, we observed delayed ablation of circulation and incomplete ablation of vascular endothelial cells. Our results suggest that significant amount of vascular endothelial cell destruction was achieved by 48 hpf despite treating the embryos with the prodrug from 12 hpf. Neurogenesis of RGCs is complete by 48 hpf in zebrafish. Coincidentally RGCs were one of the least affected cell types as seen in our results. Cells that complete neurogenesis after 48 hpf were mainly affected in our studies. As *cloche* mutants lacked most of the endothelial cells from the very early stage, abnormal retinal phenotype was evident as early as 48 hpf. Based on these results, it is extremely likely that vascular endothelial cells secrete factors required for neurogenesis of RGCs between 30 - 48 hpf.

Normal retinal phenotype at 48 hpf retina in this study could also be due to the residual effect of non-ablated blood vessels that did not express the transgenes and signals from the remaining vessels might have been enough for developing retina. Gal4 transgenes have been shown to have mosaic expression (Asakawa &

Kawakami 2008) and UAS enhancers have higher tendency to get methylated (Goll et al. 2009). As a result, significant number of vascular endothelial cells might not express the transgene leading to no effect of Met in those cells. In such cases, Met would require longer time to cause significant disruption of vasculature and circulation in doubly transgenic embryos leading to normal retinal phenotype at 48 hpf.

Another limitation of this approach is the fact that treatment of prodrug, Met, killed vascular endothelial cells throughout the body of the zebrafish embryos. As a result the retinal phenotype we observed could also be partly contributed by epistatic effect of loss of vasculature in other parts of the embryo besides the eye. One of the potential ways to address this problem is to selectively ablate the ocular vasculature in zebrafish embryo. Although all the endothelial cells share numerous common properties, vertebrates have heterogenic group of endothelial cells and each group of endothelial cells express certain markers specific to their location in the body (Aird 2007; Garlanda & Dejana 1997). Manipulation of such ocular vasculature specific markers can potentially allow us to selectively manipulate vasculature limited to the eye. Unfortunately, to the best of our knowledge, we are not aware of any marker specific to ocular vascular endothelial cells currently.

Accumulation of metabolic waste products could also be a factor to cause abnormal retinal phenotype in developing zebrafish embryo with ablated vasculature. It is very unlikely that accumulation of waste products could be causing abnormal retinal phenotype in zebrafish embryo mainly because of two reasons: i) zebrafish retina is not extremely metabolically active until 72 hpf when they complete initial

retinal neurogenesis (Agathocleous et al. 2013) and ii) most of the waste is excreted in the form of urea in zebrafish embryos and this takes place only after the embryo is out of the chorion at 72 hpf (Braun et al. 2009). Therefore, it is very unlikely that excess metabolic waste would play any role to cause abnormal retinal phenotype in absence of vascular endothelial cells. Additionally, normal retinal neurogenesis in *silent heart* embryos also aids in ruling out accumulation of waste products as a potential cause of abnormal retinal development in zebrafish embryos without vasculature.

Roles of circulation and circulating materials:

Development of normal retina in *silent heart* mutants in our study suggests that circulation and circulating materials through the blood vessels may not be critically important during initial retinal neurogenesis. However, they are extremely likely to be required to maintain the vasculature and hematopoietic stem cells. Blood flow through vasculature has been shown to be required for maintaining the blood vessels and absence of blood flow results in remodeling of the blood vessel (Hartsock et al. 2014). Circulation and beating heart has been shown to be required for maintaining the hematopoietic stem cells and generation of blood cells at proper time to ensure that developing embryo keeps up with its metabolic requirement (North et al. 2009). Circulating blood is also likely required at later stages to keep up with high metabolic demands of the retina once initial retinal neurogenesis is completed at 72 hpf. Normal retinal development in *silent heart* could also mean that diffusion is able to compensate for absence of circulation to transport any factors that

are needed by the developing retina between 48 hpf to 72 hpf from other parts of the zebrafish.

Neurovascular interactions in the retina and implications for human retinal disorders:

We demonstrated that vascular endothelial cells interact with developing neuronal progenitor cells during the process of retinal neurogenesis through our studies. Vascular endothelial cells are likely to regulate the developing neurons via paracrine signaling by secreting different factors. Identification of such factors is critical to understand the relationship between the early ocular vasculature and developing structures of the eye. Information about such factors could provide valuable insights regarding cellular and molecular mechanisms underlying retinal abnormalities caused by abnormal ocular vasculature. Ultimately, this can lead to novel treatment therapies for blindness in humans.

References

Agathocleous, M. et al., 2013. Europe PMC Funders Group Metabolic differentiation in retinal cells. *Nature Reviews Molecular Cell Biology*, 14(8), pp.859–864.

Aird, W.C., 2007. Phenotypic heterogeneity of the endothelium: I. Structure, function, and mechanisms. *Circulation research*, 100(2), pp.158–73. Available at: http://circres.ahajournals.org/content/100/2/158 [Accessed July 11, 2014].

Asakawa, K. & Kawakami, K., 2008. Targeted gene expression by the Gal4-UAS system in zebrafish. *Development Growth and Differentiation*, 50(6), pp.391–399.

Braun, M.H. et al., 2009. Nitrogen excretion in developing zebrafish (Danio rerio): a role for Rh proteins and urea transporters. *American journal of physiology. Renal physiology*, 296(5), pp.F994–F1005. Available at: http://www.ncbi.nlm.nih.gov/pubmed/19279128 [Accessed June 6, 2015].

Dhakal, S. et al., 2015. Abnormal retinal development in cloche mutant zebrafish. *Developmental Dynamics*, pp.1–33.

Garlanda, C. & Dejana, E., 1997. Heterogeneity of Endothelial Cells : Specific Markers. *Arteriosclerosis, Thrombosis, and Vascular Biology*, 17(7), pp.1193–1202. Available at: http://atvb.ahajournals.org/content/17/7/1193.long [Accessed May 28, 2015].

Goldberg, J.S. & Hirschi, K.K., 2009. Diverse roles of the vasculature within the neural stem cell niche. *Regenerative medicine*, 4(6), pp.879–97. Available at: http://www.pubmedcentral.nih.gov/articlerender.fcgi?artid=2836203&tool=pmcentrez&rendertype=abstract [Accessed June 1, 2015].

Goll, M.G. et al., 2009. Transcriptional silencing and reactivation in transgenic zebrafish. *Genetics*, 182, pp.747–755.

Gómez-Gaviro, M.V. et al., 2012. The vascular stem cell niche. *Journal of cardiovascular translational research*, 5(5), pp.618–30. Available at: http://www.ncbi.nlm.nih.gov/pubmed/22644724 [Accessed June 6, 2015].

Hartsock, A. et al., 2014. In vivo analysis of hyaloid vasculature morphogenesis in zebrafish: A role for the lens in maturation and maintenance of the hyaloid. *Developmental Biology*, 394(2), pp.327–339. Available at: http://linkinghub.elsevier.com/retrieve/pii/S0012160614003765.

North, T.E. et al., 2009. Hematopoietic Stem Cell Development Is Dependent on Blood Flow. *Cell*, 137(4), pp.736–748. Available at: http://dx.doi.org/10.1016/j.cell.2009.04.023.

Ottone, C. et al., 2014. Direct cell-cell contact with the vascular niche maintains quiescent neural stem cells. *Nature cell biology*, 16(11), pp.1045–56. Available at: http://www.pubmedcentral.nih.gov/articlerender.fcgi?artid=4298702&tool=pmcentrez&rendertype=abstract [Accessed October 7, 2014].

Palmer, T.D., Willhoite, A.R. & Gage, F.H., 2000. Vascular niche for adult hippocampal neurogenesis. *Journal of Comparative Neurology*, 425(July), pp.479–494.

Putnam, A.J., 2014. The Instructive Role of the Vasculature in Stem Cell Niches. *Biomaterials science*, 2(11), pp.1562–1573. Available at: http://pubs.rsc.org/en/content/articlehtml/2014/bm/c4bm00200h [Accessed July 20, 2015].

Sun, J. et al., 2010. Endothelial cells promote neural stem cell proliferation and differentiation associated with VEGF activated Notch and Pten signaling. *Developmental dynamics : an official publication of the American Association of Anatomists*, 239(9), pp.2345–53. Available at: http://www.ncbi.nlm.nih.gov/pubmed/20730910 [Accessed June 5, 2015].

Tavazoie, M. et al., 2008. A specialized vascular niche for adult neural stem cells. *Cell stem cell*, 3(3), pp.279–88. Available at: http://www.ncbi.nlm.nih.gov/pubmed/18786415 [Accessed May 30, 2015].

Wang, W. et al., 2010. Expression of the Lycat gene in the mouse cardiovascular and female reproductive systems. *Developmental Dynamics*, 239(April), pp.1827–1837.

Xiong, J.-W. et al., 2008. An Acyltransferase Controls the Generation of Hematopoietic and Endothelial Lineages in Zebrafish. *Circulation Research*, 102(9), pp.1057–1064.

Zhang, C. et al., 2013. Blood flow and stem cells in vascular disease. *Cardiovascular research*, 99(2), pp.251–9. Available at: http://www.ncbi.nlm.nih.gov/pubmed/23519267 [Accessed June 5, 2015].